Aus der Kinderklinik und Kinderpoliklinik im

Dr. von Haunerschen Kinderspital,

Klinikum der Ludwig-Maximilians-Universität München

Vorstand: Prof. Dr. Dr. Christoph Klein

Generation and Characterization of CD19 CAR T Cells with PD-1_CD28 Fusion Receptor

Dissertation

zum Erwerb des Doktorgrades der Medizin

an der Medizinischen Fakultät der

Ludwig-Maximilians-Universität zu München

vorgelegt von

Antonia Josefine Apfelbeck

aus Würzburg

2022

Mit Genehmigung der Medizinischen Fakultät

der Ludwig-Maximilians-Universität München

Berichterstatter:	Prof. Dr. Tobias Feuchtinger
Mitberichterstatter:	Prof. Dr. Marion Subklewe Prof. Dr. Andreas Humpe Prof. Dr. Stefan Endres Prof. Dr. Anne Krug
Mitbetreuung durch die promovierte Mitarbeiterin:	Dr. Franziska Blaeschke
Dekan:	Prof. Dr. Thomas Gudermann
Tag der mündlichen Prüfung:	07.12.2022

“Ihre Linderung ist eine tägliche Aufgabe,
ihre Heilung eine glühende Hoffnung.“

– William Castle, über die Leukämie in 1950

Table of contents

Zusammenfassung

Die akute lymphatische Leukämie (ALL) ist die häufigste Krebserkrankung bei Kindern. Heutzutage können 80 bis 90% der erkrankten Kinder mit Hilfe von Chemotherapie und Stammzelltransplantation geheilt werden. Die Prognose für primär refraktäre oder mehrfach rezidivierende ALL ist jedoch weiterhin schlecht. Einen vielversprechenden Therapieansatz bei fortgeschrittener B-ALL stellt die Infusion von gegen CD19 gerichteten T-Zellen mit chimärem Antigenrezeptor (CAR) dar. In klinischen Studien konnte gezeigt werden, dass bis zu 90% der größtenteils schwer vorbehandelten Patienten nach CAR-T-Zell-Gabe eine komplette Remission erlangen. Trotz dieser zeitweiligen Remission erleidet jedoch etwa die Hälfte der Patienten, die mit einem konventionellen anti-CD19 CAR behandelt werden, ein Rezidiv der Grunderkrankung. Eine weitere Erforschung und Optimierung des Therapieansatzes mit CAR-T-Zellen ist somit notwendig.

Vorarbeiten unserer Arbeitsgruppe legen nahe, dass ko-inhibitorische Immuncheckpointmoleküle auf der Oberfläche von Leukämiezellen eine erfolgreiche T-Zell-Antwort beeinträchtigen können. Daraufhin entwickelten wir CAR-T-Zellen mit einem zusätzlichen PD-1_CD28 Checkpointfusionsrezeptor. Dieser Rezeptor besteht aus einer inhibitorischen extrazellulären PD-1 und einer stimulatorischen intrazellulären CD28 Domäne. Dadurch kann ein ursprünglich inhibitorisches Signal der Leukämiezelle vermittelt über die PD-1/PD-L1-Achse in ein CD28 vermitteltes stimulatorisches Signal für die T-Zelle umgewandelt werden.

In diesem Projekt konnten wir CAR-T-Zellen der ersten und zweiten Generation mit und ohne PD-1_CD28 Fusionsrezeptor mittels retroviraler Transduktion erfolgreich herstellen. Die CAR-T-Zellen besaßen eine gute Expansionsfähigkeit, eine hohe Viabilität und den vorteilhaften Phänotyp einer zentralen Gedächtnis- oder Effektor-Gedächtnis-T-Zelle. Die Funktionalitätstests zeigten ein starkes Aktivierungs-, Killing-, und Proliferations-Vermögen der anti-CD19-CAR-T-Zellen nach Erkennung der Zielzellen. Übereinstimmend mit bisherigen Veröffentlichungen setzten Zweit-Generationen-CAR-T-Zellen verglichen zu Erst-Generationen-CAR-T-Zellen höhere Zytokinmengen frei, obwohl das ko-inhibitorische Checkpointprofil der T-Zellen gleich war.

Der Fusionsrezeptor beeinträchtigte die Killing-Rate der CAR-T-Zellen nicht und vermittelte keine unspezifische, CD19-unabhängige Aktivierung. Das Killing-Vermögen der CAR-T-Zellen mit und ohne Fusionsrezeptor zeigte keine signifikanten Unterschiede. Gemessen an der Zytokinausschüttung waren die CAR-T-Zellen mit Fusionsrezeptor in Anwesenheit von PD-L1

den konventionellen Erst- und Zweit-Generationen-CAR-T-Zellen überlegen. Weitere Versuche werden *in vivo* durchgeführt, um diese Ergebnisse validieren zu können. CAR-T-Zellen mit PD-1_CD28 Fusionsrezeptor könnten ein vielversprechendes Verfahren sein, um die CAR-T-Zell-Funktionalität bei Behandlung von fortgeschrittener pädiatrischen Leukämie in einem Patienten-individualisierten Rahmen zu verbessern.

Abstract

Acute lymphoblastic leukemia (ALL) is the most common malignancy in children. 80 to 90% of the children with standard risk can be cured with chemotherapy and stem cell transplantation. Nevertheless, the prognosis for primary refractory or relapsed ALL is still dismal. As a promising treatment strategy for B-ALL, adoptive T-cell transfer of CD19 targeting T cells with chimeric antigen receptor (CAR) has emerged. Clinical studies show remission rates of heavily pretreated patients of up to 90% upon CAR T-cell infusion. Despite temporary remission, around 50% of patients treated with a conventional anti-CD19 CAR suffer from a relapse. Therefore, CAR T-cell treatment needs to be further optimized.

Preliminary data of our group suggested that co-inhibitory checkpoint molecules on the surface of leukemic blasts could prevent T cells from sufficient anti-leukemic response. Here, we designed CAR T cells with a fully human PD-1_CD28 checkpoint fusion receptor. This receptor contains an inhibitory extracellular PD-1 and a stimulatory intracellular CD28 domain. Thus, it is able to reverse the inhibitory PD-1/PD-L1 signal of the leukemic cell into a CD28-based stimulatory signal for the T cell.

In this study, we successfully generated first and second generation CAR T cells with and without PD-1_CD28 fusion receptor by retroviral transduction. CAR T cells showed good expansion/ viability and a favourable central/ effector memory phenotype. Functionality assays revealed strong activation, killing and proliferation capacity of anti-CD19 CAR T cells upon target-cell recognition. In line with previous publications, second generation CAR T cells showed improved cytokine release compared to first generation CAR T cells. PD-L1 expression on the target cells significantly decreased cytokine release of CAR T cells, although the T cells' co-inhibitory checkpoint profile was not altered.

Inclusion of the PD-1_CD28 fusion receptor did not impair the killing capacity of the CAR and induced no unspecific CD19-independent activation. The killing capacity of CAR T cells with and without fusion receptor showed no significant differences. However, in presence of PD-L1, CAR T cells with fusion receptor could outcompete conventional first and second generation CAR T cells in terms of cytokine release. Further *in vivo* analyses will be performed to validate these findings. CAR T cells with PD-1_CD28 fusion receptor could be a useful tool to improve CAR T-cell functionality for treatment of advanced pediatric leukemia.

List of Figures

Abbreviations

Abbreviation	Description
19_3z	First generation CAR T cells
19_3z_PD-1_28	First generation CAR T cells with fusion receptor
19_BB_3z	Second generation CAR T cells
19_BB_3z_PD-1_28	Second generation CAR T cells with fusion receptor
19t	Truncated CAR T cells, control CAR T cells
ALL	Acute lymphoblastic leukemia
APC	Allophycocyanin
BB	Brilliant blue
BiTE	Bispecific T-cell engager
Bp	Base pairs
BTLA	B and T lymphocyte attenuator
BUV	Brilliant ultraviolet
BV	Brilliant violet
CAR	Chimeric antigen receptor
CD	Cluster of differentiation
CEACAM1	Carcinoembryonic antigen-related cell adhesion molecule 1
CNS	Central nervous system
CRES	CAR T cell related encephalopathy syndrome

CRISPR	Clustered Regularly Interspaced Short Palindromic Repeats
CRS	Cytokine release sydrome
CTLA-4	Cytotoxic T-lymphocyte-associated protein 4
DMSO	Dimethyl sulfoxide
DNA	Deoxyribonucleic acid
E:T	Effector : target
EC	Extracellular
EFS	Event-free survival
F2A	Foot-and-mouth-disease-virus 2A peptide
FACS	Fluorescence-activated cell sorting
Fc	Fragment, crystallizable
FDA	Food and Drug Administration
FITC	Fluorescein isothiocyanate
FSB	Fetal bovine serum
GAL-9	Galectin 9
GITR	Glucocorticoid-induced tumor necrosis factor receptor-related protein
GITRL	Glucocorticoid-induced tumor necrosis factor receptor-related protein ligand
GMP	Good manufacturing practice
HEPES	Hydroxyethyl piperazineethanesulfonic acid
HSA	Human serum albumin
HVEM	Herpes virus entry mediator

IC	Intracellular
ICS	Intracellular cytokine stain
IFN-γ	Interferon gamma
IntReALL	International study for treatment of childhood relapsed ALL
LAG-3	Lymphocyte-activation gene 3
MFI	Median fluorescent intensity
MHC	Major histocompatibility complex
MLV	Murine leukemia virus
MRD	Minimal residual disease
n	Number of independent experiments
NSSM	Nonsynonymous somatic mutation
OS	Overall survival
PBMC	Peripheral blood mononuclear cell
PBS	Phosphate buffer saline
PCR	Polymerase chain reaction
PD-1	Programmed cell death 1
PD-L1	Programmed cell death 1 ligand 1
PE	Phycoerythrin
QQ plot	Quantile-Quantile plot
RPMI	Roswell Park Memorial Institute
ScFv	Single chain variable fragment

SEB	Staphylococcus enterotoxin B
SSC	Side scatter
STR	Short tandem repeat
T_{CM}	Central memory T cells
TCR	T-cell receptor
T_{EFF}	Effector T cells
T_{EM}	Effector memory T cells
TIGIT	T-cell immunoreceptor with Ig and ITIM domains
TIM-3	T-cell immunoglobulin and mucin domain 3
TM	Transmembrane
T_N	Naïve T cells
TNF-α	Tumor necrosis factor alpha
T_{SCM}	Stem cell-like memory T cells
WBC	White blood cell
WT	Wildtype

1 Introduction

1.1 Acute lymphoblastic leukemia

Introduction

The most common malignancy in children is acute lymphoblastic leukemia (ALL) (Hunger and Mullighan 2015). ALL is a malignant transformation of lymphoid progenitor cells with mutations and/or chromosomal abnormalities affecting differentiation and proliferation (Terwilliger and Abdul-Hay 2017). The lymphoid cells can be of B-cell (85%) or T-cell lineage origin (15%). Patients with ALL can suffer from thrombocytopenia, anemia and neutropenia and present with symptoms like bruising or bleeding, pallor and fatigue, and infections. In the United States the incidence is about 30 ALL cases per million persons under 20 years with a peak between three and five years of age (Hunger and Mullighan 2015). From the 1960s until today the overall survival rate has steadily increased from less than 10% up to 90% (Figure 1). This is mostly due to adjustments in chemotherapy and the improved stratification of treatment intensity (Hunger and Mullighan 2015). While most of the children can be cured from ALL, patients with relapsed or primary refractory disease still suffer from dismal prognosis (long-term overall survival 15-50%) (Nguyen et al. 2008; Gomez-Gomez et al. 2012).

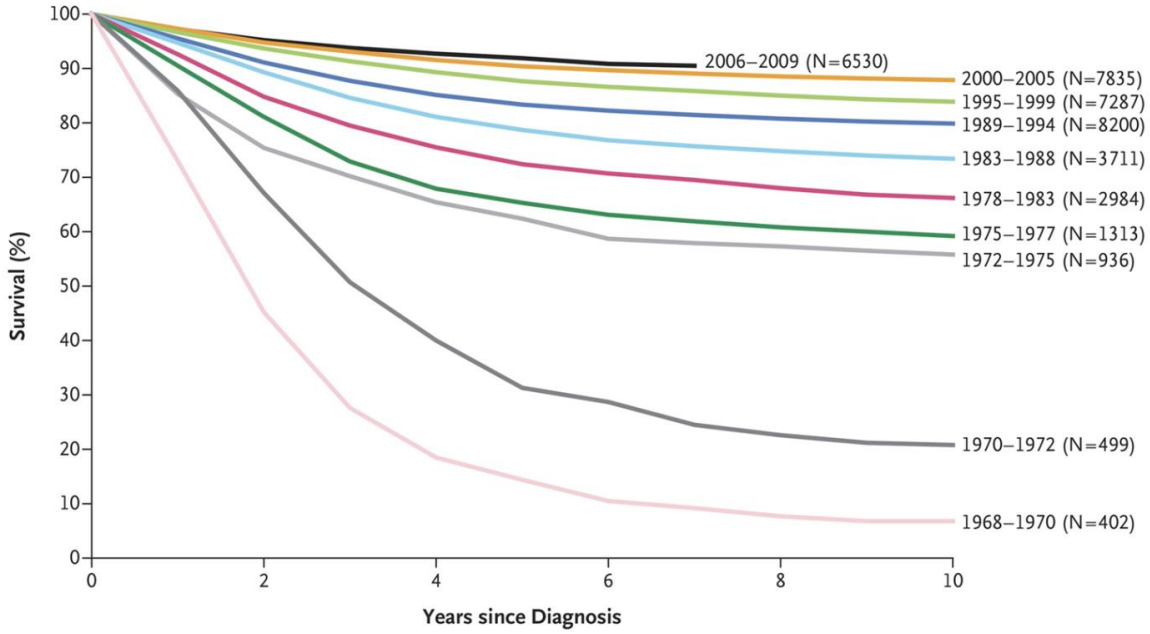

Figure 1: Survival rates of patients with pediatric acute lymphoblastic leukemia.
Since the 1960's the survival rate of childhood ALL has steadily increased from less than 10% up to 90% (Figure adapted from Hunger and Mullighan 2015). ALL: acute lymphoblastic leukemia

Risk stratification

For children with acute lymphoblastic leukemia, risk groups have been defined according to white blood cell (WBC) count and age. Due to risk stratification, patients with a lower risk of relapse can be prevented from more aggressive treatment while children in high-risk groups can be provided with an intensified therapy. According to a conference of the Cancer Therapy Evaluation Program of the National Cancer Institute are children from the age of one to nine years and WBC count at diagnosis lower than 50,000/µl included in the standard-risk category. The high-risk group contains patients either 10 years or older, with a WBC count higher than 50,000/µl or with both risk factors (Smith et al. 1996). Infants that are younger than one year are categorized in a special subgroup with worse prognosis (Hunger and Mullighan 2015). About 3% of children present with a central nervous system (CNS) involvement at time of ALL diagnosis and approximately 2% of boys demonstrate testicular involvement. Both conditions lead to classification into the high-risk group (Cooper and Brown 2015).

The minimal residual disease (MRD) at the end of induction therapy is the most powerful independent prediction factor of relapse (Borowitz et al. 2008). Borowitz et al. showed that MRD negative patients have the best clinical outcome (5-year event-free survival 88%), while patients even with a very low MRD level of 0.01-0.1% measured in flow cytometry are more likely to relapse (Figure 2).

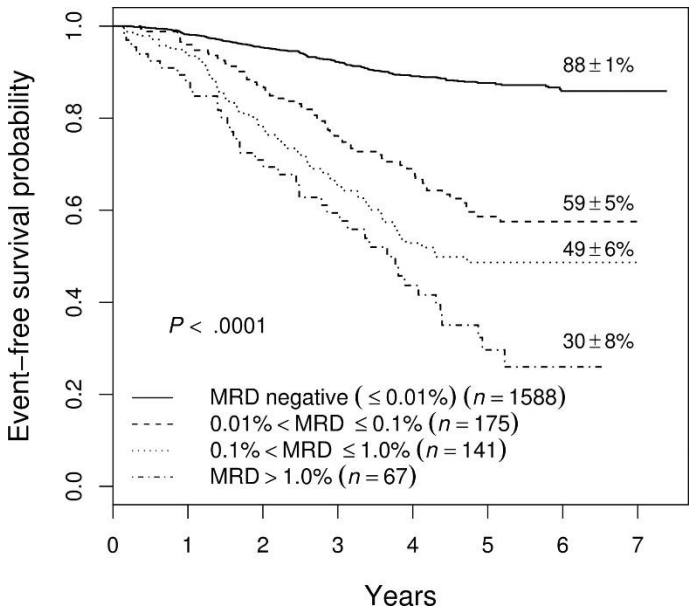

Figure 2: Minimal residual disease serves as prognostic factor for event-free survival.
Event-free survival of 1971 pediatric patients with acute lymphoblastic leukemia is shown according to minimal residual disease level at the end of induction therapy (Figure adapted from Borowitz et al. 2008). MRD: minimal residual disease

Treatment of childhood ALL

Treatment guidelines of childhood ALL are typically divided into induction, consolidation, re-induction and maintenance. Induction therapy lasting four to six weeks aims to induce complete remission (Cooper and Brown 2015). Approximately 95% of the patients achieve this aim (Cooper and Brown 2015), whereas induction treatment failure results in a decreased 10-year survival of only 32% (Schrappe et al. 2012). Those patients are then considered as high-risk patients and usually evaluated for allogeneic stem-cell transplantation and/or experimental therapy strategies (Eapen 2017). Agents included in induction chemotherapy are vincristine, corticosteroids (prednisone or dexamethasone), asparaginase and anthracycline (optional, daunorubicin or doxorubicin). Induction therapy is followed by a consolidation phase of nine to fourteen weeks (Escherich, Schrappe, and Creutzig 2016). In this period chemotherapeutic agents, which have not been used during induction therapy, are given to avoid drug resistance (Cooper and Brown 2015). Four to nine weeks of re-induction therapy follow. In this phase high dose chemotherapy is administered. Re-induction therapy is followed by maintenance chemotherapy treatment until two years after diagnosis (Escherich, Schrappe, and Creutzig 2016). It consists of an antimetabolite therapy with oral methotrexate and mercaptopurine (Hunger and Mullighan 2015). ALL treatment aims to eradicate the disease from the CNS by intrathecal chemotherapy, systemic chemotherapy that penetrates the blood-brain barrier or cranial radiation. As irradiation showed an association with increased numbers of secondary CNS tumors, delayed growth, endocrinopathies and neurocognitive effects progressively less patients were treated with it over time. By now at least 80% of children with newly diagnosed ALL are treated without cranial irradiation (Hunger and Mullighan 2015).

1.2 Immunotherapy for acute lymphoblastic leukemia

Immunotherapy has emerged as a promising strategy for treating cancer patients. Common principle of current immunotherapeutic approaches is to intervene in the response of the immune system rather than targeting the malignancy itself (Majzner, Heitzeneder, and Mackall 2017). Cancer immunotherapies can be divided into two subgroups: Immunomodulatory agents that amplify the natural anti-tumor immune response and synthetic immunotherapies that initiate new immune responses (Majzner, Heitzeneder, and Mackall 2017).

Bispecific antibody Blinatumomab

In December 2014 Blinatumomab was approved by the U.S. Food and Drug Administration (FDA) as the first immunotherapeutic agent for treatment of relapsed/refractory B-precursor ALL. Blinatumomab is an anti-CD3/anti-CD19 bi-specific T-cell engager (BiTE) connecting CD3 on physiologic T cells with CD19 on B(-precursor) cells. Hence, T cells are directed to kill the leukemic cells by bringing them into close proximity (Majzner, Heitzeneder, and Mackall 2017). In a phase I/II clinical trial, 38.6% of pediatric ALL patients achieved complete remission within the first two cycles of Blinatumomab treatment. Patients with <50% bone marrow blasts at baseline showed a complete remission rate of 55.6% (von Stackelberg et al. 2016). Blinatumomab was included into standard relapse protocols (IntreReALL) for treatment of advanced pediatric ALL in Germany.

Role of immune checkpoints in acute lymphoblastic leukemia

For T-cell activation, major histocompatibility complex (MHC)-dependent antigen recognition of the T-cell receptor (TCR) is required. Co-inhibitory and stimulatory signals regulate the amplitude and quality of T-cell activation (Pardoll 2012). Those signals are provided by the interaction of surface molecules that are often referred to as immune checkpoints. Figure 3 provides an overview of a number of checkpoint molecules which are involved in regulating cell cycle progression, proliferation, survival, effector function, cytokine production and memory formation of T cells (Lesokhin et al. 2015). The physiological purpose of co-inhibitory immune checkpoints is to maintain self-tolerance in order to prevent autoimmunity. Malignant tumors can use this mechanism to perform an immune escape by inhibiting anti-tumor T-cell responses (Pardoll 2012).

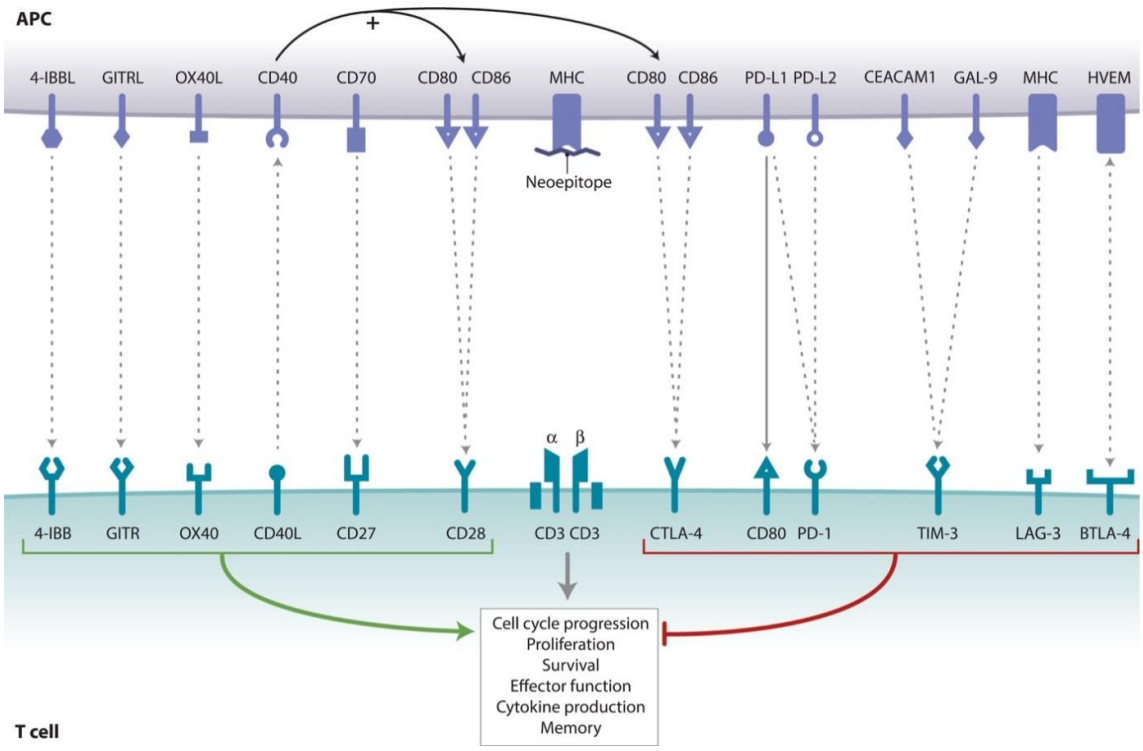

Figure 3: Checkpoint molecules regulate the interaction between antigen presenting cell and T cell.
Immune checkpoint molecules can regulate the MHC-dependent T-cell response initiated by the T-cell receptor. Immune checkpoints can have a stimulatory or inhibitory impact on T-cell activation (Figure adapted from Lesokhin et al. 2015).
APC: antigen presenting cell, GITR: glucocorticoid-induced tumor necrosis factor receptor-related protein, GITRL: glucocorticoid-induced tumor necrosis factor receptor-related protein ligand, MHC: major histocompatibility complex, CTLA-4: cytotoxic T-lymphocyte associated protein 4, PD-1: programmed cell death 1, PD-L1: programmed cell death 1 ligand 1, TIM-3: T-cell immunoglobulin and mucin domain 3, CEACAM1: carcinoembryonic antigen-related cell adhesion molecule 1, GAL-9: galectin-9, LAG-3: lymphocyte-activation gene 3, BTLA-4: B and T lymphocyte attenuator 4, HVEM: herpes virus entry mediator

Great anti-tumor effects could be reached by blocking inhibitory checkpoint molecules on the T-cell or tumor-cell surface in metastatic melanoma (Postow et al. 2015; Robert et al. 2015), non-small-cell lung cancer (Brahmer et al. 2015), Hodgkin's lymphoma (Ansell et al. 2015), bladder carcinoma (Powles et al. 2014), and head and neck cancer (Topalian, Drake, and Pardoll 2015). In those trials adult patients were treated with the checkpoint inhibitors Ipilimumab (anti-CTLA-4 antibody), Nivolumab, Pembrolizumab (both anti-PD-1 antibodies) or MPDL3280A (anti-PD-L1 antibody). For childhood cancer, there has been only one trial with checkpoint blockade so far: 33 patients with melanoma, sarcoma or other refractory solid tumors were treated with Ipilimumab but showed no objective anti-tumor activity (Merchant et al. 2016). Since high numbers of non-synonymous somatic mutations (NSSMs) are associated with a better response to checkpoint inhibitors, therapy failure of checkpoint inhibitors in pediatric tumors is attributed to low mutational load of pediatric cancer (Majzner,

Heitzeneder, and Mackall 2017; Snyder et al. 2014). Genomes of children with acute lymphoblastic leukemia bear 10 to 20 non-silent coding mutations at time of diagnosis (Hunger and Mullighan 2015). So far, it has not been shown that pediatric ALL patients benefit from the single treatment with checkpoint inhibitors.

Nevertheless, previous work of our group has reported that checkpoint molecules do play a role in acute lymphoblastic leukemia in children (Feucht et al. 2016). The surface expression of several co-inhibitory and stimulatory checkpoint molecules differs significantly between ALL blasts and B-precursor cells of healthy controls. On bone marrow T cells, inhibitory checkpoint molecules like programmed cell death 1 (PD-1) are higher expressed in ALL patients compared to healthy controls (Figure 4A). When treated with T_{H1} cytokines *in vitro*, leukemic blasts are able to up-regulate co-inhibitory checkpoint molecules such as programmed cell death 1 ligand 1 (PD-L1) hinting at an interaction between bone marrow T cells and leukemic cells via the co-inhibitory PD-L1/PD-1 axis (Figure 4B). Administration of PD-1 blocking antibody increased *in vitro* T-cell responses against leukemic blasts mediated by Blinatumomab.

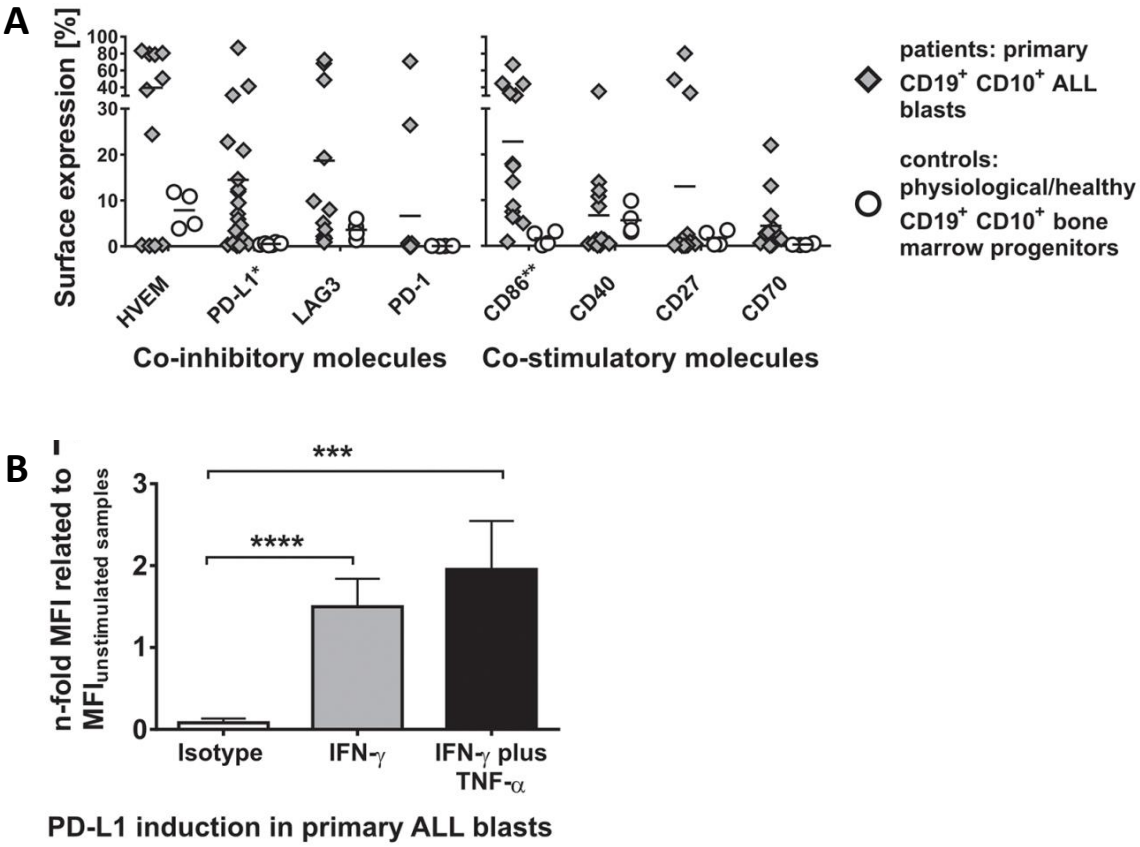

Figure 4: PD-L1 surface expression of primary pediatric ALL blasts and PD-L1 induction through cytokines.

(A) ALL blasts showed an inter-individual expression profile of co-inhibitory and co-stimulatory molecules. PD-L1 expression was significantly increased on blasts of ALL patients compared to control individuals (without malignancies). **(B)** Inflammatory T_{H1} cytokines (IFN-γ, TNF-α) induced up-regulation of PD-L1 on primary pediatric ALL blasts *in vitro* (Figures adapted from Feucht et al. 2016). HVEM: herpes virus entry mediator, PD-L1: programmed cell death 1 ligand 1, LAG-3: lymphocyte-activation gene 3, PD-1: programmed cell death 1, MFI: mean fluorescence intensity, IFN-γ: interferon gamma, TNF-α: tumor necrosis factor alpha

1.3 CAR T-cell therapy

Structure of CAR T cells

Treatment with T cells transduced with a chimeric antigen receptor (CAR) is a very promising immunotherapeutic approach. CARs consist of an antibody-derived single chain variable fragment (scFv), a spacer and a transmembrane domain that is linked to a CD3ζ chain as part of the T-cell receptor complex (Figure 5). Consequently, a redirected T-cell specificity in a major histocompatibility complex (MHC)-independent way can be obtained. By varying the scFv, different tumor surface antigens can be targeted (Sadelain, Brentjens, and Riviere 2013). In case of B-precursor ALL, CD19 represents a suitable target as it is a B-cell lineage specific antigen but not present in any healthy tissue other than that (Maude et al. 2015; Sadelain, Brentjens, and Riviere 2013).

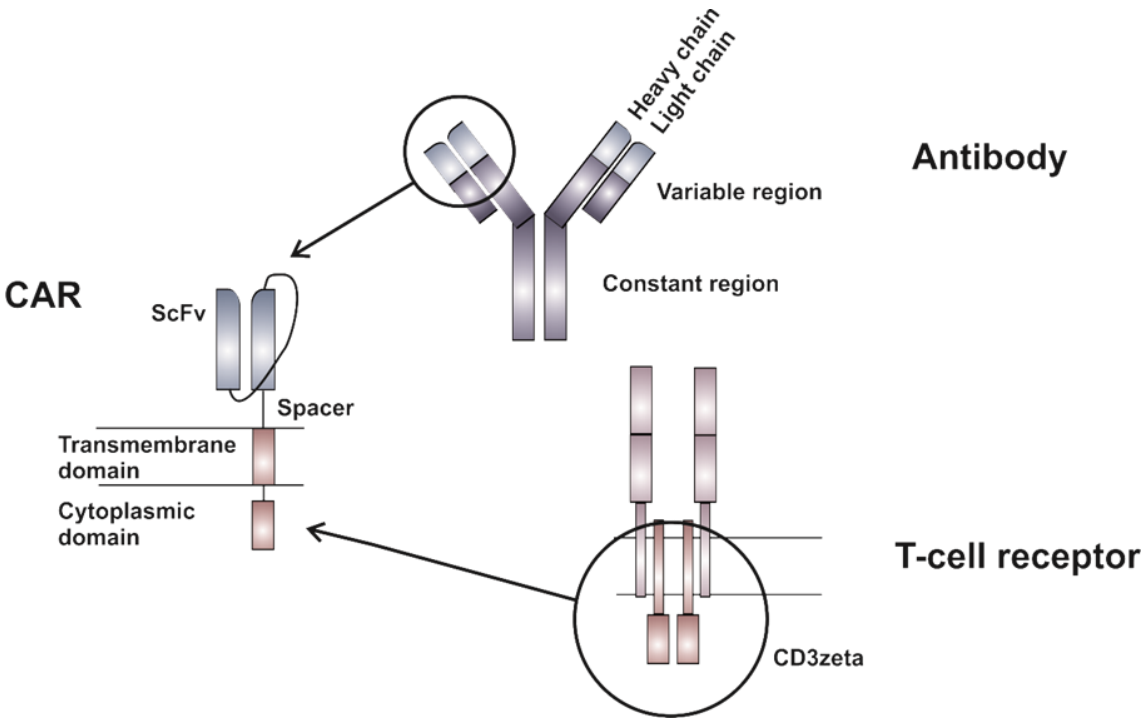

Figure 5: CAR structure.
The CAR is built of an antibody derived single chain variable fragment (scFv). The spacer and transmembrane domain links the scFv to a CD3ζ chain which is part of the T-cell receptor complex. A CAR thus combines antibody-mediated recognition with T-cell receptor-based signaling (Figure provided by F. Blaeschke and T. Feuchtinger). CAR: chimeric antigen receptor, ScFv: single chain variable fragment

In 1989, Zelig Eshhar first described immunoglobulin-T-cell receptor chimeric molecules (Gross, Waks, and Eshhar 1989). Since then, CAR T cells have been further improved and different generations of CAR T cells have emerged (Figure 6). First generation CAR T cells contain ScFv,

spacer and transmembrane domains linked to a CD3ζ signaling sequence. For second generation CARs one additional co-stimulatory domain such as 4-1BB or CD28 is included between the transmembrane domain and the CD3ζ chain. In third generation CARs, two co-stimulatory domains are combined (Maus et al. 2014).

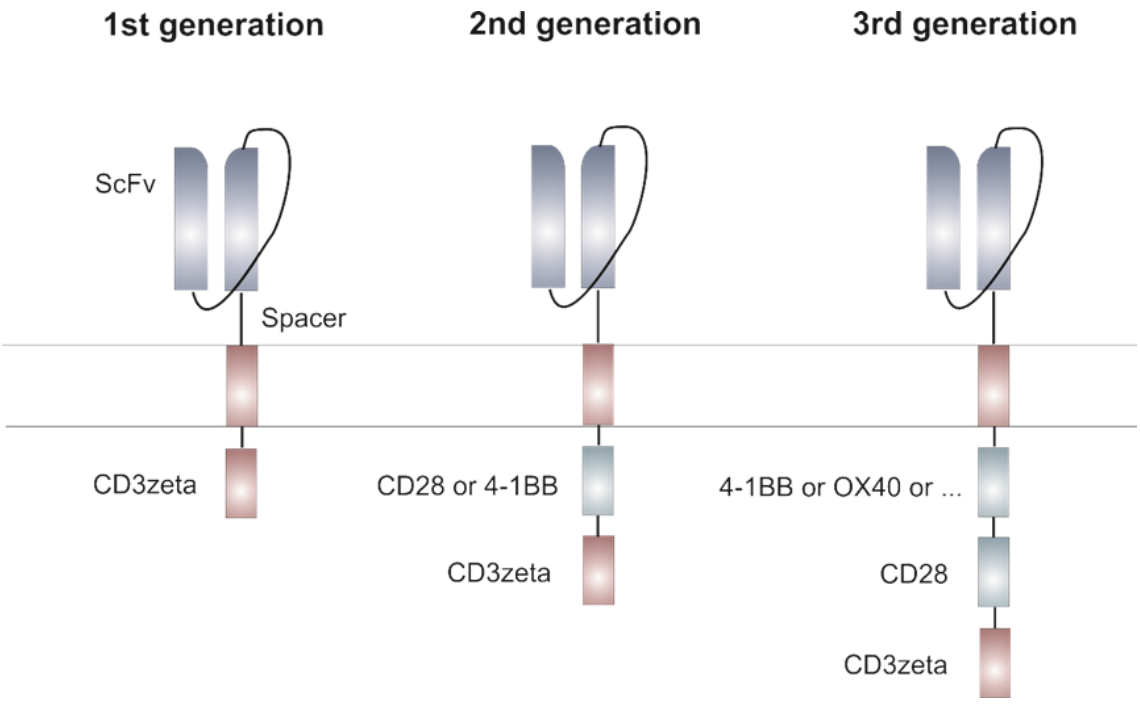

Figure 6: CAR T-cell generations.
Intracellularly the first generation CAR contains only a CD3ζ chain, whereas the second generation CAR has one additional costimulatory domain like 4-1BB or CD28. The third generation CAR combines two costimulatory domains (Figure provided by F. Blaeschke and T. Feuchtinger). ScFv: single chain variable fragment

Efficacy of CD19 CAR T-cell therapy in acute lymphoblastic leukemia

The majority of CAR T-cell protocols use patient-derived autologous T cells which are collected and *ex vivo* lenti- or retrovirally transduced with the CAR. After *in vitro* expansion, the CAR T cells are reinfused into the patient (Figure 7) (Klebanoff, Yamamoto, and Restifo 2014). Before CAR infusion, the patients receive a lymphodepleting chemotherapy typically containing fludarabine and cyclophosphamide. Lymphodepletion is important to limit T-cell responses against the murine ScFv, which is used in most CAR T-cell trials (Cao et al. 2018), and to provide access to the homeostatic cytokines.

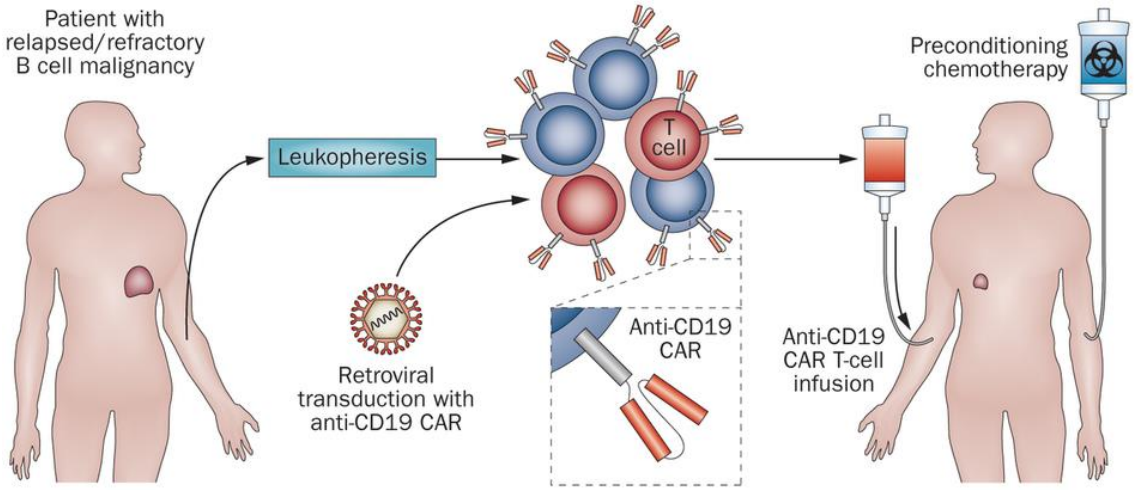

Figure 7: Therapy with CAR T cells.
T cells derived from patients with B-cell malignancies are lenti- or retrovirally transduced with an anti-CD19 CAR. The CAR T cells are expanded *in vitro* and reinfused into the patient (Figure adapted from Klebanoff, Yamamoto, and Restifo 2014).

Clinical trials testing first generation CARs have shown that the approach was safe but there was limited T-cell persistence and proliferation in the patients, which seems crucial for successful CAR therapy (Barrett et al. 2014). Second generation CAR T cells showed great results in terms of initial response rates. A complete early remission of 81-90% has been reported in heavily pretreated patients with relapsed/refractory B-precursor ALL (Park et al. 2018; Zhang, Song, and Liu 2018; Maude et al. 2018). In August 2017, the FDA approved tisagenlecleucel, a second generation CD19-CAR, for the treatment of pediatric and young adult B-precursor ALL (U.S. Food & Drug Administration 2017). Despite those promising results, long-term follow-up studies report a median event-free survival (EFS) of 6.1 months and a median overall survival (OS) of 12.9 months (Park et al. 2018). In another study, Gardner et al. showed a 12-month OS of 65.9% and a 12-month EFS of 50.3% (Gardner et al. 2017). Within 40 patients with MRD^- complete remission after CAR insfusion 18 patients relapsed. Relapses after anti-CD19 CAR T-cell therapy can be grouped into $CD19^+$ and $CD19^-$ relapses. $CD19^+$ relapses occure after loss of functional CAR T cells (Gardner et al. 2017). CD19 antigen-loss can be due to CD19 splice variants. Orlando et al. revealed that mutations of $CD19^-$ relapsed B-ALL cells were found throughout exons important for membrane anghorage (Orlando et al. 2018). Also there have been cases reported where a lineage switch of the leukemic cells occurred. Patients treated with CD19-CAR T cells developed an acute myeloid leukemia that was clonally related to their B-precursor ALL (Gardner et al. 2016). In one case report a relapse caused by the CAR transduction of a leukemic B cell was published. By masking the CD19 with the CAR, the CAR transduced leukemic cells could escape the CAR T cells (Ruella et al. 2018).

CAR T-cell treatment related toxicities

Similar treatment related toxicities have been reported for all trials investigating CD19-CAR T-cell therapy. Especially cytokine release sydrom (CRS) and neurotoxicities have been limiting factors for broading the adoption of CAR T-cell treatment (Gardner et al. 2017). CRS is characterized by elevated serum cytokines accompanied with symptoms like fever, hypotension and respiratory insufficiency (Giavridis et al. 2018). If an uncontrolled systematic inflammatory response occurs, life threatening conditions with circulatory shock, vascular leakage, disseminated intravascular coagulation and multi-organ system failure can be developed (Shimabukuro-Vornhagen et al. 2018). The severity of CRS correlates with a high initial disease burden (Park, Geyer, and Brentjens 2016) and its mean onset is around day 4 after CAR T-cell infusion (Lee et al. 2015). A common treatment for CRS has been interleukine blockade with or without corticosteroids administration. When approving tisagenlecleucel the FDA additionally approved the treatment of CAR related CRS with Tocilizumab, an antibody blocking the interleukin-6 receptor (U.S. Food & Drug Administration 2017).

The second most comon adverse effect after CAR T-cell infusion is neurotoxicity, called “CAR T cell related encephalopathy syndrome” (CRES) (Neelapu et al. 2018). The severity of neurologic symptoms differs from mild confusion with difficulties in finding words, headaches and hallucinations to serious conditions with hemiparesis, cranial nerve palsies, seizures and somnolence (Shimabukuro-Vornhagen et al. 2018). The most severe neurotoxicity reported was fatal cerebral edema. Due to fatal cerebral edema, an anti-CD19 CAR-T cell trial was terminated (Torre et al. 2018). For the vast majority of anti-CD19 constructs no such fatal clinical courses occurred and mostly all neurological symptoms were reversible (Lee et al. 2015; Maude et al. 2015; Maus et al. 2014).

Due to CD19-specific on-target off-tumor reactivity 83% of the anti-CD19 CAR treated patients had sustained B-cell aplasia 6 months after infusion (Maude et al. 2018). Resulting hypogammaglobulinemia can be treated with immunoglobulin replacement.

2 Aims and objectives of this study

CAR T cells have emerged as promising treatment strategy and remission in up to 90% of pediatric B-precursor ALL patients was achieved after CAR T-cell infusion. Unfortunately, about 50% of patients treated with a conventional anti-CD19 CAR suffer from a relapse. A major reason for treatment failure of CAR T cells is an insufficient sustained activation and expansion *in vivo*.

We hypothesize that secondary inhibition through co-inhibitory molecules are involved in this lack of persistence. Sustained activation of the initial response is likely to improve CAR T-cell therapy.

The aim of this study is to develop new therapeutic concepts for treatment of advanced pediatric ALL by disrupting inhibitory checkpoint axes.

In this study we want to generate CAR T cells that are less susceptible to checkpoint inhibition. By expressing a PD-1_CD28 fusion receptor on the cell surface they can break the inhibitory PD-1/PD-L1 axis. The receptor can turn an inhibitory signal of the leukemic cell via PD-1/PD-L1 interaction into a stimulatory signal via the intracellular CD28 domain of the fusion receptor.

In a first step production feasibility of different CAR T-cell constructs with and without fusion receptor via retroviral transduction will have to be ensured. After an expansion period of 14 days the cell products will have to be characterized by flow cytometry regarding transduction rate and phenotype of the cells. We will test the functionality after antigen contact and will compare the results of the different constructs with each other.

Collecting *in vitro* functionality data of CAR T cells with fusion receptor will build the basis for *in vivo* experiments performed with a patient-derived xenograft mouse model.

3 Materials

3.1 Equipment and software

Equipment/software	Name, Manufacturer
Autoclaves	VX-55, VX-150, DX-65, Systec, Linden, Germany
Cell counting auxiliaries	Cell Counting Chamber Neubauer, Chamber Depth 0.1 mm, Paul Marienfeld, Lauda-Königshofen, Germany
Centrifuges	Multifuge X3R and Mini Centrifuge Fresco 17, Heraeus, Hanau, Germany
Cleaner Box	UVC/T-M-AR, DNA-/RNA UV-cleaner box, Biosan, Riga, Latvia
Cooling units	Cooler (4 °C) Comfort No Frost, Liebherr, Biberach an der Riß, Germany
	Cryogenic Freezer MVE 600 Series, Chart, Luxemburg
	Freezer (-20 °C) Premium No Frost, Liebherr, Biberach an der Riß, Germany
	Freezer (-86 °C) HERAfreeze HFC Series, Heraeus, Hanau, Germany
	Freezer (-86 °C) HERAfreeze HFU T Series, Heraeus, Hanau, Germany
	Thermo Scientific Cryo 200 liquid nitrogen dewar, Thermo Fisher Scientific, Waltham, Massachusetts, USA
Flow cytometer	BD FACSAria III, BD, Franklin Lakes, New Jersey, USA
	BD LSRFortessa Cell Analyzer, BD, Franklin Lakes, New Jersey, USA
	MACSQuant Analyzer 10, Miltenyi Biotec, Bergisch Gladbach, Germany
Freezing container	Nalgene Mr. Frosty, Thermo Fisher Scientific, Waltham, Massachusetts, USA

Gel Imager	Gel iX20 Imager, Intas Science Imaging, Göttingen, Germany
Heat block	Eppendorf ThermoMixer comfort, Eppendorf, Hamburg, Germany
Incubator	HERAcell 240, 150i CO_2 Incubator, Thermo Fisher, Waltham, Massachusetts, USA
Laminar flow hood	HERAsafe, Thermo Fisher, Waltham, Massachusetts, USA
	Uniflow KR130, Uniequip, Planegg, Germany
Magnetic cell separator	MACS MultiStand, Miltenyi Biotec, Bergisch Gladbach, Germany
	MidiMACS Separator, Miltenyi Biotec, Bergisch Gladbach, Germany
	QuadroMACS Separator, Miltenyi Biotec, Bergisch Gladbach, Germany
Microscope	Axiovert 25, Carls Zeiss Microscopy, Jena, Germany
	Leica DM IL, Leica Microsysteme, Wetzlar, Germany
Spectrophotometer	Nanodrop ND-1000 spectrophotometer, Nanodrop Technologies, Wilmington, Delaware, USA
Pipettes (electrical)	Easypet 3, Eppendorf, Hamburg, Germany
Pipettes (manual)	2.5 µl, 20 µl, 200 µl, 1000 µl Eppendorf Research, Eppendorf, Hamburg, Germany
Power Supply	Biorad Power Pac 200, Biorad, Hercules, California, USA
Scale	R 200 D, Sartorius AG, Göttingen, Germany
Software	BD FACSDiva 8.0.1, BD Biosciences, Franklin Lakes, New Jersey, USA
	CorelDRAW Graphics Suite, Corel Corporation, Ottawa, Kanada
	FlowJo 10.0.7r2, Ashland, Oregon, USA
	Gel iX20 Imager Windows Version, Intas Science Imaging, Göttingen, Germany

	GraphPad PRISM 7.0, La Jolla, California, USA
	MACSQuantify, Miltenyi Biotec, Bergisch Gladbach, Germany
	Microsoft Office 2010, Redmond, Washington, USA
Thermocycler	peqSTAR 96 Universal Gradient, Isogen, Utrecht, Netherlands
Vacuum pump	Vakuumsytem BVC 21 NT, Vacuubrand, Wertheim, Germany
Water bath	LAUDA Aqualine AL 18, LAUDA-Brinkmann, Delran, New Jersey, USA

3.2 Solutions, media and sera for cell culture

Solution/ Medium/Serum	**Order number**	**Manufacturer**
100 bp DNA Ladder Ready to Load	01-11-00050	Solis BioDyne, Tartu, Estonia
Agarose	50004	Seakem Le Agarose, DMA, Rockland, Maine, USA
Albiomin 5 % infusion solution human albumin (HSA)	623 050	Biotest, Dreieich, Germany
Biocoll separating solution	L6115	Biochrom, Berlin, Germany
Brefeldin A	5936	Sigma-Aldrich, Steinheim, Germany
CellTrace Violet Proliferation Kit	C34557	Invitrogen, Thermo Fisher Scientific, Life Technologies Cooperation, Eugene, Oregon, USA
Compensation beads	552843	BD Biosciences, San Diego, California, USA
	130-097-900, 130-104-693	MACS Comp Bead Kit anti mouse/anti REA, Miltenyi Biotec, Bergisch Gladbach, Germany

Dimethylsulfoxid	D5879	Honeywell, Seelze, Germany
	4720.4	Carl Roth, Karlsruhe, Germany
DMEM	FG1445	Biochrom, Berlin, Germany
DNA Clean & Conentrator -5	D4014	Zymo Research, Irvine, California, USA
DNA Gel Loading Dye (6X)	R0611	Thermo Fisher Scientific, Waltham, Massachusetts, USA
Dulbeccos phosphate buffer saline (PBS)	14190-250	Gibco, Life Technologies, Darmstadt, Germany
Ethidium bromide	2218.1	Roth, Karlsruhe, Germany
FcR Blocking Reagent	130-059-901	Miltenyi Biotec, Bergisch Gladbach, Germany
Fetal Bovine Serum	F0804	Sigma-Aldrich CHEMIE, Steinheim, Germany
Fix & Perm Cell Permeabilization Kit	GAS004	Life Technologies, Frederick, Maryland, USA
Heparin sodium 25,000 I.U./5ml		Ratiopharm, Ulm, Germany
HEPES-Buffer (1M)	L 1613	Biochrom, Berlin, Germany
Human AB serum		Human AB serum was kindly provided by Prof. R. Lotfi, University Hospital Ulm, Institute for Transfusion Medicine and German Red Cross Blood Services Baden-Württemberg—Hessen, Institute for Clinical Transfusion Medicine and Immunogenetics, both from Ulm, Germany
IL-7, IL-15 (human, premium grade)	130-95-363, 130-095-764	Miltenyi Biotec, Bergisch Gladbach, Germany
L-Glutamine 200 mM	K 0283	Biochrom, Berlin, Germany

MicroBeads (CD4, CD8, CD56)	130-045-101, 130-045-201, 130-050-401	Miltenyi Biotec, Bergisch Gladbach, Germany
Non-Essential Amino Acids	11140-035	Gibco, Life Technologies, Darmstadt, Germany
Penicillin/Streptomycin	15140-122	Gibco, Life Technologies, Darmstadt, Germany
Protamine sulfate	P3369	Sigma-Aldrich CHEMIE, Steinheim, Germany
Q5 High-Fidelity DNA Polymerase	M0491S	New England BioLabs, Frankfurt am Main, Germany
QIAamp DNA Mini Kit	51306	QIAGEN, Hilden, Germany
RetroNectin Reagent	T100A	Takara, Saint-Germain-en-Laye, France
Sodium pyruvate	11360-039	Gibco, Life Technologies, Darmstadt, Germany
Stapyhlococcal enterotoxin B	4881	Sigma-Aldrich CHEMIE, Steinheim, Germany
TAE Buffer	A4686	TAE buffer (50x), Applichem, Darmstadt, Germany
TexMACS GMP Medium	170-076-307	Miltenyi Biotec, Bergisch Gladbach, Germany
T Cell TransAct, human	130-111-160	Miltenyi Biotec, Bergisch Gladbach, Germany
TransIT-293 Transfection Reagent	Mirumir2704	Mirus Bio LLC, Madison, Wisconsin, USA
Trypan blue	15250-061	Gibco, Life Technologies, Darmstadt, Germany
Tween 20	9127.1	Carl Roth, Karlsruhe, Germany
VLE RPMI 1640 Medium	F1415	Biochrom, Berlin, Germany

3.3 Consumables

Consumable	Order number	Name, Manufacturer
Cannula	851.638.235	Safety-Multifly-Needle, Sarstedt, Nümbrecht, Germany
Cell culture dish	664 160	Cellstar Greiner Labortechnik, Kremsmünster, Austria
Cell culture flasks with ventilation caps	83.3910.002, 83.3911.002, 83.3912.002	T25, T75, T175, Sarstedt, Nümbrecht, Germany
Cell culture multiwell plates, 6 well	657160	Cellstar Greiner Labortechnik, Kremsmünster, Austria
Cell culture multiwell plates, 24 well	3524	Costar Corning Incorporated, Corning, New York, USA
Cell culture multiwell plates, 48 well	3548	Costar Corning Incorporated, Corning, New York, USA
Cell culture multiwell plates, 96 well	163320	Nunclon Delta Surface, Thermo Fisher Scientific, Waltham, Massachusetts, USA
Compresses	18507	Gauze Compresses 10 x 10 cm, Nobamed Paul Danz, Wetter, Germany
Cover slips	C10143263NR1	Menzel-Gläser 20 x 20 mm, Gerhard Menzel, Braunschweig, Germany
FACS buffers and solutions	130-092-747, 130-092-748, 130-092-749	Running Buffer, Storage Solution, Washing Solution, Miltenyi Biotec, Bergisch Gladbach, Germany
	340345,	FACS clean/rinse/flow, Becton, Dickinson and Company (BD), Franklin Lakes, New

	340346, 342003	Jersey, USA
Freezing tubes	72.379	Cryo Pure Gefäß 1.8 ml, Sarstedt, Nümbrecht, Germany
Magnetic separation columns	130-042-401, 130-042-901	LS Columns, LD Columns, Miltenyi Biotec, Bergisch Gladbach, Germany
Pasteur pipettes	747720	Glass Pasteur Pipettes 230 mm, Brand, Wertheim, Germany
Pipette tips	70.1130.217, 70.760.213, 70.760.212, 70.762.211	0.1-2.5 µl, 10 µl, 20 µl, 100 µl, 2-200 µl, 1000 µl, Sarstedt, Nümbrecht, Germany
Reaction vessels	62.554.502	15 ml, Sarstedt, Nümbrecht, Germany
	4440100	50 ml, Orange Scientific, Braine-l'Alleud, Belgium
	72.690.550	1.5 ml, Sarstedt, Nümbrecht, Germany
Round bottom tubes with cell strainer snap cap	352235	5 ml Polystyrene Round Bottom Tube, Falcon, Corning Science, Taumaulipas, Mexico
Safety gloves	9209817	Vaso Nitril Blue, B. Braun Melsungen, Melsungen, Germany
Serological pipettes	86.1685.001, 86.1253.001, 86.1254.001	5 ml, 10 ml, 25ml Serological Pipette, Sarstedt, Nümbrecht, Germany
Skin disinfectant	975512, 306650	Sterilium Classic Pure, Sterilium Virugard, Hartmann, Heidenheim, Germany

Sterile filters	SE2M229104, SE2M230104	0.2µm, 0.45µm, Carl Roth, Karlsruhe, Germany
Surface disinfectant	CLN-1006.5000	Ethanol 80 % MEK/Bitrex, CLN, Niederhummel, Germany
Syringe	309658	3ml, Becton, Dickinson and Company (BD), Franklin Lakes, New Jersey, USA
	4606728V	10ml, B. Braun Melsungen, Melsungen, Germany
	4617509F	50ml, Omnifix, B. Braun Melsungen, Melsungen, Germany

3.4 Antibodies

Fluoro-chrome	**Antigen**	**Clone**	**Order number**	**Manufacturer**
7AAD	Viability dye		420404	Biolegend, San Diego, California, USA
APC	CD137	4B4-1	130-094-821	Miltenyi Biotec, Bergisch Gladbach, Germany
APC	CD14	TÜK4	130-115-559	Miltenyi Biotec, Bergisch Gladbach, Germany
APC	2B4	C1.7	329512	Biolegend, San Diego, California, USA
APC	CD28	CD28.2	559770	Becton, Dickinson and Company (BD), Franklin Lakes, New Jersey, USA
APC	CD56	NCAM16.2	341027	Becton, Dickinson and Company (BD), Franklin Lakes, New Jersey, USA
APC	CD95	DX2	130-092-417	Miltenyi Biotec, Bergisch Gladbach,

				Germany
APC	VISTA	730804	FAB71261A	R&D Systems, Minneapolis, Minnesota, USA
APC/Cy7	CD62L	DREG-56	304814	Biolegend, San Diego, California, USA
APC-Vio 770	CD8	BW135/80	130-096-561	Miltenyi Biotec, Bergisch Gladbach, Germany
BB515	CD19	HIB19	564456	Becton, Dickinson and Company (BD), Franklin Lakes, New Jersey, USA
BUV395	CD3	SK7	564001	Becton, Dickinson and Company (BD), Franklin Lakes, New Jersey, USA
BUV496	CD8	RPA-T8	564804	Becton, Dickinson and Company (BD), Franklin Lakes, New Jersey, USA
BUV737	CD56	NCAM16.2	564447	Becton, Dickinson and Company (BD), Franklin Lakes, New Jersey, USA
BV421	CD137	4B4-1	309820	Biolegend, San Diego, California, USA
BV421	CTLA-4	BNI3	369606	Biolegend, San Diego, California, USA
BV421	CD154	TRAP1	563886	Becton, Dickinson and Company (BD), Franklin Lakes, New Jersey, USA
BV421	PD-L1	29E.2A3	329714	Biolegend, San Diego, California, USA
BV421	PD-1	EH12.2H7	329920	Biolegend, San Diego, California, USA
BV421	TIM3	F38-2E2	345007	Biolegend, San Diego, California, USA
BV421	CD56	HCD56	318328	Biolegend, San Diego, California, USA
BV650	BTLA	J168-540	564803	Biolegend, San Diego, California, USA
BV650	PD-1	EH12.2H7	329950	Biolegend, San Diego, California, USA

BV650	CD69	FN50	563835	Becton, Dickinson and Company (BD), Franklin Lakes, New Jersey, USA
BV785	CD95	DX2	305646	Biolegend, San Diego, California, USA
FITC	Anti-c-myc	14D3	130-092-472	Miltenyi Biotec, Bergisch Gladbach, Germany
Pacific Blue	TNF-α	MAb11	502920	Biolegend, San Diego, California, USA
PE	CD19	LT19	130-113-169	Miltenyi Biotec, Bergisch Gladbach, Germany
PE	CD25	REA570	130-091-024	Miltenyi Biotec, Bergisch Gladbach, Germany
PE	CD45RO	UCHL1	304206	Biolegend, San Diego, California, USA
PE	CD56	REA196	170-078-057	Miltenyi Biotec, Bergisch Gladbach, Germany
PE	IFN-γ	25723.11	340452	Becton, Dickinson and Company (BD), Franklin Lakes, New Jersey, USA
PE	TIGIT	MBSA44	12-9500-41	eBioscience/ Thermo Fisher Scientific, Waltham, Massachusetts, USA
PE	LAG3	11C3C65	369305	Biolegend, San Diego, California, USA
PE	OX40	Ber-ACT35	350003	Biolegend, San Diego, California, USA
PE-Vio 770	CD3	REA613	130-109-463	Miltenyi Biotec, Bergisch Gladbach, Germany
PE-Vio 770	CD19	LT19	130-096-641	Miltenyi Biotec, Bergisch Gladbach, Germany
PE-Vio 770	CD45RO	REA611	130-096-739	Miltenyi Biotec, Bergisch Gladbach, Germany

PE-Vio 770	CD69	FN50	130-099-750	Miltenyi Biotec, Bergisch Gladbach, Germany
VioBlue	CD62L	145/15	130-098-699	Miltenyi Biotec, Bergisch Gladbach, Germany
VioGreen	CD4	REA623	130-113-230	Miltenyi Biotec, Bergisch Gladbach, Germany
VioGreen	CD62L	145/15	130-113-623	Miltenyi Biotec, Bergisch Gladbach, Germany

4 Methods

4.1 CAR T-cell generation

4.1.1 PBMC isolation and T-cell activation

Cells were derived from 100 ml peripheral blood of healthy donors. All donors gave written informed consent before venous puncture for heparin blood collection. Peripheral blood mononuclear cells (PBMCs) were generated *via* density gradient centrifugation. Therefore heparin blood was diluted 1:2 with PBS and carefully layered on 15 ml Biocoll. After centrifugation at 800 g for 30 minutes without brake PBMCs were aspirated. T cells were isolated by CD4 MicroBeads and CD8 MicroBeads which was performed according to the manufacturer's information. T cells were cultured in TexMACS GMP medium supplemented with 2.5% human AB serum and 12.5 ng/ml interleukins 7 and 15. Isolated T cells were activated with T Cell TransAct, human as suggested in the supplier's information and washed two days after activation.

4.1.2 Virus generation

Producer cells (293Vec-RD114 cells) were previously generated for all constructs according to published literature (Ghani et al. 2007; Ghani et al. 2009). Untransduced producer cells were kindly provided by Manuel Caruso, BioVec Pharma, Québec, Canada.

Virus was harvested by aspirating supernatant of 293VEC-RD114 cells. Supernatant was filtered with a 0.45µm filter, frozen and stored at -80 °C.

For verification of the constructs a PCR followed by Sanger sequencing was performed. Therefore, genomic DNA of transduced producer cells was isolated with the QIAamp DNA Mini Kit according to the manufacturer's information. For PCR, isolated genomic DNA was amplified using Q5 High-Fidelity DNA Polymerase according to the supplier's information. The thermocycler setting consisted of initial denaturation at 98 °C for 30 seconds, 35 cycles of 98 °C for 10 seconds, 60 °C for 20 seconds and 72 °C for 60 seconds, and a final elongation step of 72 °C for 2 minutes. For electrophoresis, gel was loaded with DNA Gel Loading Dye (6X) according to the supplier's information. Bands were extracted from the gel using Gel iX20 Imager, purified with DNA Clean and Concentrator kit according to the supplier's information and sent

for Sanger sequencing (Eurofins genomics). Electrophoresis analysis (see page 88), primer (see page 79) and CAR sequences (see page 79) are shown in the supplements.

4.1.3 Retroviral CAR T-cell transduction

Transduction process was performed two days after T-cell isolation. 24-well plates were coated with 2.5 µg RetroNectin Reagent per well either overnight at 4 °C or for 2 hours at 37 °C. Plates were blocked with 2% Albumin Fraction V in PBS for 30 minutes and afterwards washed with a 1:40 dilution of HEPES 1M in PBS. 1 ml of thawed virus supernatant was centrifuged on coated wells at 3000 g for 90 minutes at 32 °C. Supernatants were discarded and $1x10^6$ T cells in 1ml TexMACS GMP medium/2.5% human AB serum + 12.5 ng/ml interleukins 7 and 15 were added per well. For untransduced control same amount of T cells was added in untreated wells. Plates were centrifuged at 450 g for 10 minutes at 32 °C and on day 2 after transduction T cells were washed to remove virus.

T cells were cultured in TexMACS GMP medium/2.5% human AB serum + 12.5 ng/ml interleukins 7 and 15 throughout the expansion process. Every two to three days, new medium was added to the cell culture. Expansion rate and viability was assessed every two or three days under light microscope after diluting the cells 1:2 with trypan blue. On day 12 after transduction, cells were harvested and frozen as described in 4.4.

For characterization of the final product, cellular composition and transduction rate was analysed by flow cytometry on day 12 after transduction by staining for CD3, CD4, CD8, CD56, c-myc, CD14, CD19 or for CD3, CD4, CD8, CD56, c-myc, PD-1. The phenotype of the T cells was evaluated on day 13 after transduction by flow cytometric stain for CD62L, CD45RO and CD95.

4.2 Functionality assays

4.2.1 Checkpoint expression assay

Before CAR T cells were frozen, checkpoint surface expression was evaluated by flow cytometry. T cells were stained for LAG-3, 2B4, PD-1, TIM-3, OX40, CD28, CD69, 4-1BB, TIGIT, VISTA, BTLA and CTLA-4. All panels included CD3, CD8, CD56, CD62L, CD45RO, CD95 and c-myc to identify T-cell subsets. Cells were co-cultured with $CD19^+$ K562 cells and $CD19^+$/$PD\text{-}L1^+$ K562

cells for 24 and 48 hours at an effector to target ratio of 5:1. Effector count was calculated on the total T-cell count. For evaluation of the initial surface expression of the checkpoints, T cells without co-culture were stained.

4.2.2 Cytotoxicity assay

CAR T cells were thawed and rested overnight in TexMACS GMP medium/2.5% human AB serum + 12.5 ng/ml interleukin 7 and 15. On day 1 after thawing, NK(T) cells were depleted with CD56 MicroBeads according to the supplier's information. In a FITC c-myc single stain the transduction rate was reevaluated and all conditions were adjusted to the lowest transduction rate within the donor by adding untransduced cells. K562 cells were used as target cells, labeled according to CellTrace Violet Cell Proliferation Kit and co-cultured with CAR T cells at different effector to target ratios. Effector count was calculated on the number of CAR^+ T cells. Cells were co-cultured for 48 hours. Absolute cell count of CellTrace Violet positive cells was measured and killing rate was calculated with following formula: 100-(100/effectors only*effectors left in co-culture). "Effectors only" describes effector cell lines without co-cultured target cells and were used as reference. Experiments were performed in technical duplicates and measured on a MACSQuant Analyzer 10.

4.2.3 Intracellular cytokine stain (ICS)

For ICS, thawed T cells were used. On day 3 after thawing, a FITC c-myc single stain for transduction rate reevaluation was performed and all conditions were adjusted to the lowest transduction rate within the donor by adding untransduced cells. T cells were co-cultured with target cells at a 5:1 ratio for 24 hours. Effector to target ratio was calculated on the total T-cell count. For positive control, T cells were stimulated with 10 µg/ml staphylococcus enterotoxin B (SEB). 2 hours after stimulation, 10 µg/ml Brefeldin A was added. Stimulation was stopped with cold PBS after 4 hours and T cells were washed. Intracellular stain for IFN-γ and TNF-α was performed with FIX & PERM cell Fixation & Permeabilization Kit according to the supplier's information. T cells were stained for CD3, CD4, CD8, CD56 and c-myc to identify T-cell subsets.

4.2.4 Proliferation assay

For proliferation assay, thawed T cells and K562 cells were used. The transduction rate was adjusted as described before (4.2.3). On day 4 after thawing, T cells were labeled according to CellTrace Violet Cell Proliferation Kit and co-cultured with target cells at a 5:1 ratio for 72 hours. Effector to target ratio was calculated on the total T-cell count. An SEB positive control with 10 µg/ml was performed. T cells cultured without target cells were used as negative control. Additional to CellTrace Violet, cells were stained for CD19, CD8, CD62L, CD45RO, CD95 and c-myc.

4.3 Transduction of cell lines

CD19_pMP71/ PD-L1_pMP71 and helper plasmids MLV env (pALF-10A1-env) and MLV gag/pol (pcDNA3.1-MLV-g/p) were transfected into HEK 293T cells using TransIT-293 Transfection Reagent according to the supplier's information. Helper plasmids were kindly provided by Sebastian Kobold, Department of Clinical Pharmacology, Ludwig-Maximilian-University of Munich. Vector map of pcDNA3.1-MLV-g/p is shown in the supplements (see page 90) and pALF-10A1 is described in Stitz et al. (Stitz et al. 2000). Vector pMP71 was kindly provided by Christopher Baum, Department of Experimental Hematology, Hannover Medical School, and a vector map is shown in the supplements (see page 89). After 48 hours, viral supernatant was harvested and used for transduction of K562 cells. 24-well plates were coated with 2.5 µg RetroNectin Reagent overnight at 4 °C. Plates were blocked with 2% Albumin Fraction V in PBS for 30 minutes and washed with a 1:40 dilution of HEPES 1M in PBS. Virus supernatant was centrifuged at 500 g for 5 minutes at 32 °C and filtered with a 0.45 µm filter. 1 ml of virus supernatant was centrifuged on coated wells at 3000 g for 90 minutes at 32 °C. Supernatant was discarded and $1x10^6$ K562 cells in RPMI + 10% fetal bovine serum (FBS) + 1% penicillin streptomycin + 1% L-glutamine were added per well. 4 µg of protamine sulfate and 1% HEPES 1M were added. On day 2 after transduction, cells were washed to remove virus. Cells were sorted for $CD19^+$/$PD\text{-}L1^+$ K562 cells at a FACSAria III and cultured in RPMI + 10% fetal bovine serum (FBS) + 1% penicillin/streptomycin + 1% L-glutamine.

4.4 General cell culture

Cells were cultured at 37 °C with 5% CO_2.

Cell lines were cultured in RPMI + 10% fetal bovine serum (FBS) + 1% penicillin/streptomycin + 1% L-glutamine and splitted at least every five days in a 1:10 ratio. Identity of cell lines was verified by STR analysis regularly.

Cell lines were frozen in RPMI + 20% fetal bovine serum (FBS) + 1% penicillin/streptomycin + 1% L-glutamine containing 10% dimethyl sulfoxide (DMSO). Primary T cells were frozen in 5% human serum albumin (HSA) containing 10% DMSO. After cells were frozen in a freezing container at -80 °C, they were transferred to liquid nitrogen (-179° C) for preservation.

For thawing, cells were rapidly warmed in the water bath, transferred to prewarmed RMPI medium and washed in TexMACS GMP medium.

4.5 Flow cytometry

Antibodies for flow cytometry staining were titrated prior to use. PBS + 1% fetal bovine serum (FBS) was used as staining buffer. Cells were stained for 10 minutes at 4 °C and washed once with buffer. For stains with K562 cells, Fc receptor block was used according to the manufacturer's information. Except for the checkpoint expression assay, all measurements were performed at a MACSQuant Analyzer 10. Checkpoint expression assay was measured at BD LSRFortessa Cell Analyzer.

4.6 Computer programs

Flow cytometry data was analysed using FlowJo 10.

Schematic illustrations in Figure 5, Figure 6 and part A of Figure 8, Figure 11, Figure 12 and Figure 17 were created with CorelDRAW and kindly provided by Franziska Blaeschke.

Graphs were created with GraphPad Prism 7.

4.7 Statistical analysis

Statistics were performed with GraphPad Prism 7. For intracellular cytokine stain and cytotoxicity assays it was shown exemplary that results are normally distributed using Shapiro-Wilk test for sample sizes n ≥ 10. Quantile-Quantile Plots are shown in the supplements (see page 91). Therefore, statistical differences between experimental conditions were examined using paired Student's t test also for smaller sample sizes. A p value of <0.05 indicates significant (*), <0.01 very significant (**) and <0.001 extremely significant (***) differences.

5 Results

Parts of following results, data and figures have been published in the article “Augmenting anti-CD19 and anti-CD22 CAR T-cell function using PD-1-CD28 checkpoint fusion proteins” in the Blood Cancer Journal in 2021 (Blaeschke et al. 2021). The relevant data has been marked and cited accordingly.

5.1 Generation of CD19 CAR T cells with high expansion rate and viability

T cells were successfully transduced with different CAR constructs two days after activation. A schematic overview of the constructs is given below (Figure 8A). All CAR constructs were designed in collaboration with Sebastian Kobold and Felicitas Rataj, Department of Clinical Pharmacology, Ludwig-Maximilian-University of Munich. The first generation CAR 19_3z was built of an anti-CD19 single chain variable fragment, a c-myc tag for detection in flow cytometry, an extracellular CD8 spacer domain, a CD8 transmembrane domain and an intracellular CD3ζ chain. The DNA sequence included the restriction sites for NotI and EcoRI as well as a Kozak sequence to increase expression levels. 19t served as control as it contained the extracellular and transmembrane part of the CAR but lacked the intracellular CD3ζ chain. Therefore, the 19t CAR could not provide an activating signal to the T cell. Twelve days after transduction, a mean transduction rate of 69.0% for 19_3z (range 52.1-87.5%) and of 46.9% for 19t (range 33.4-70.7%) was reached (Figure 8B). Transduction efficacy showed donor-dependent inter-individual differences.

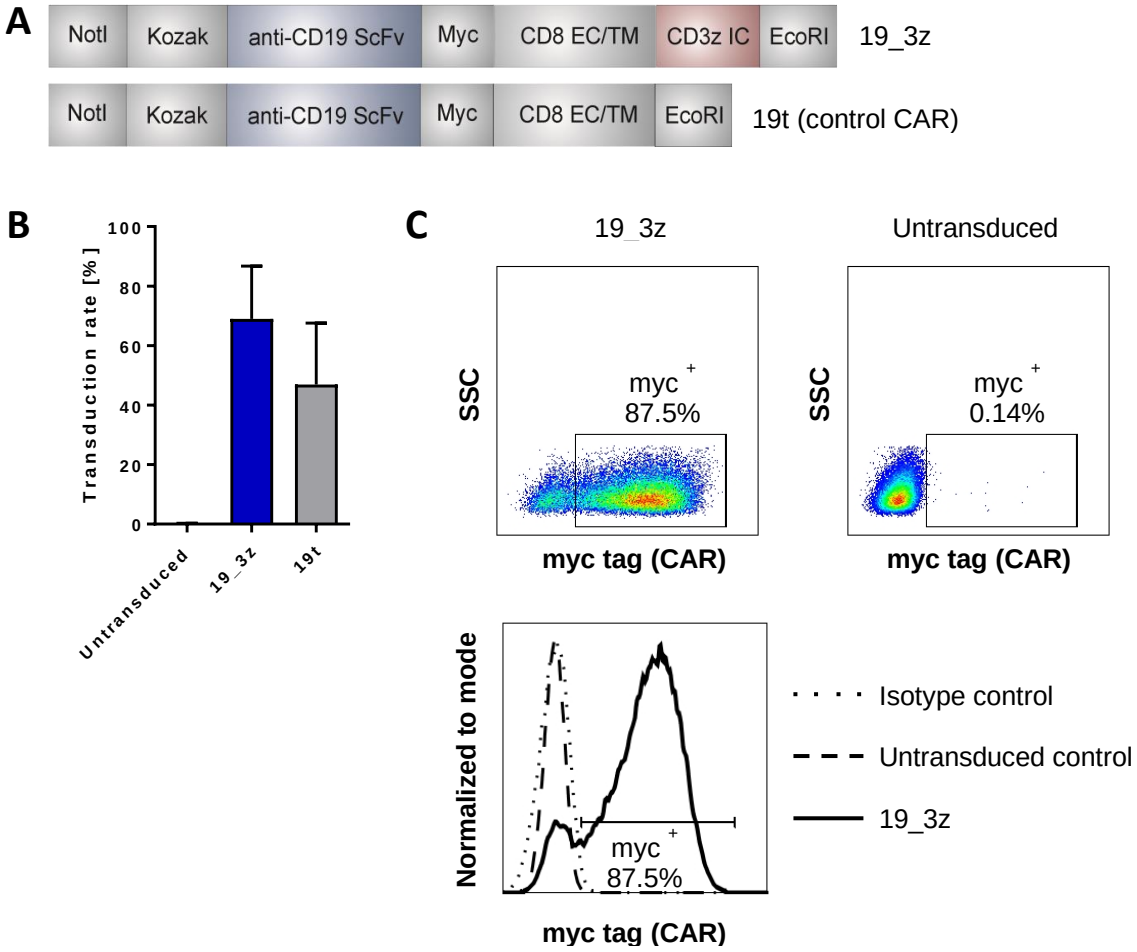

Figure 8: Retroviral T-cell transduction of first generation CD19 CAR (19_3z) and control CAR (19t) is feasible.
(A) The first generation CAR (19_3z) consisted of an anti-CD19 single chain variable fragment, a c-myc tag for detection in flow cytometry, an extracellular CD8 spacer domain, a CD8 transmembrane domain and an intracellular CD3ζ chain. The control CAR (19t) served as control since it lacked the CD3ζ chain and could not provide a signal to the T cell (Figure provided by F. Blaeschke and T. Feuchtinger). **(B)** The transduction rate of the first generation (19_3z) and control CAR (19t) was detected 12 days after transduction by a c-myc tag in flow cytometry. Untransduced T cells served as control (n ≥ 3 individual donors). **(C)** The dot plots and the histogram show gating strategy for CAR T cells in a representative experiment. ScFv: single chain variable fragment, Myc: c-myc tag EC: extracellular, TM: transmembrane, IC: intracellular, SSC: side scatter

T cells were cultured and expanded for 14 days in total. On day 12 after transduction, an expansion of over 100 fold was reached (Figure 9A, Data and figure published in an adapted version by Blaeschke et al. 2021). Throughout the expansion process the viability for the first generation CAR was within a range of 89.2-100% (Figure 9B). 13 days after transduction, the T-cell product of the first generation CAR showed a mainly central memory like (mean 59.4%, range 37.7-76.2%) and effector memory like (mean 37.5%, range 18.7-59.7%) phenotype (Figure 9C). The transduction process had no influence on the T-cell phenotype since the cell

product of the first generation CAR and the untreated control did not show significant differences in the distribution of T-cell subpopulations.

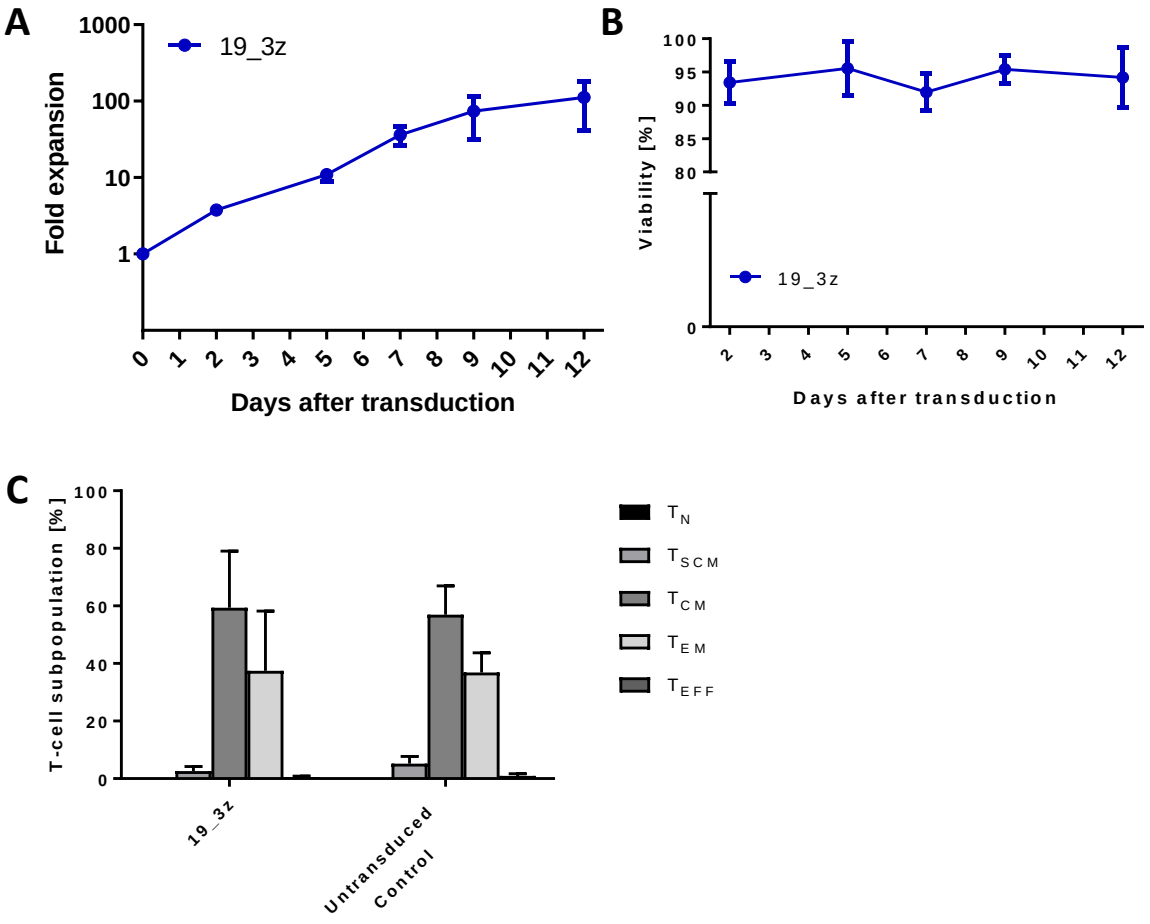

Figure 9: Expansion, viability and phenotype of 19_3z CAR T cells.
(A) First generation CAR T cells (19_3z) showed an expansion rate of over 100 fold within twelve days after transduction (n ≥ 3; Data and figure published in an adapted version by Blaeschke et al. 2021). **(B)** The viability throughout the generation process was >89% for first generation CAR T cells (n ≥ 3). **(C)** 13 days after transduction, CAR T-cell products (19_3z) and untransduced cells had a mainly central memory and effector memory like phenotype. The two conditions did not significantly differ from each other. The subsets were evaluated by flow cytometric analysis of CD62L, CD45RO and CD95 expression (n ≥ 3). Two-tailed paired t test was performed to determine statistical significance.
T_N: $CD62L^+$, $CD45RO^-$, $CD95^-$; T_{SCM}: $CD62L^+$, $CD45RO^-$, $CD95^+$; T_{CM}: $CD62L^+$, $CD45RO^+$, $CD95^+$; T_{EM}: $CD62L^-$, $CD45RO^+$, $CD95^+$; T_{EFF}: $CD62L^-$, $CD45RO^-$, $CD95^+$.
T_N: naïve T cells, T_{SCM}: stem cell-like memory T cells, T_{CM}: central memory T cells, T_{EM}: effector memory T cells, T_{EFF}: Effector T cells

5.2 First generation CAR T cells show high CD19-specific functionality *in vitro*

To test the functionality, CAR T cells were analysed for their killing capacity, cytokine release, proliferative potential and expression of activation markers after co-culture with $CD19^+$ K562 cells. When co-cultured for 48h, CAR T cells showed an effector to target ratio-dependent cytotoxicity (Figure 10A). In the co-culture with 1:1 E:T ratio, a mean of 79.7% (range 65.6-94.1%) of the target cells were killed. The target-cell killing was antigen dependent since the co-culture of CAR T cells with $CD19^-$ target cells (K562 WT cells) showed a killing of less than 7% (E:T 1:1, p=0.0032).

High proliferative potential of anti-CD19 CAR T cells after antigen recognition was detectable (Figure 10B). The number of cell divisions was identified by the cell trace violet intensity of labelled T cells. 72h after begin of the co-culture with $CD19^+$ K562 cells, 95.5% of T cells within the 19_3z population proliferated for at least one generation. This was CAR specific as gating on all proliferating T cells revealed that a mean of 88.4% were CAR^+ T cells and 11.6% CAR^- T cells.

CAR T cells were able to produce cytokines after antigen contact. A mean of 17.9% (range 15.1-19.6%) of the CAR T cells were IFN-γ positive after co-culture with $CD19^+$ K562 cells (Figure 10C). For TNF-α a mean of 13.1% (range 8.3-17.5%) positive cells was measured. For both cytokines a significant difference in the cytokine secretion between first generation CAR T cells and control CAR T cells was detected (IFN-γ p=0.0053; TNF-α p=0.0405). This effect was CAR specific as only a mean of 4.2% of CAR^- cells within the 19_3z population was IFN-γ positive (p=0.0227).

Distribution of phenotype subsets and surface expression of activation markers on first generation CAR T cells were evaluated over time (0h, 24h and 48h) (Figure 10D, E). CAR T cells showed an up-regulation of the activation markers 4-1BB (mean expression 3.5% vs. 95.8%) and CD69 (mean expression 35.0% vs. 99.0%) before vs. 24h after antigen contact.

To evaluate the T-cell phenotype of the original product (0h), CAR T cells were measured prior to co-culture. While in the original product 58.0% of T cells had a central memory and only 39.5% an effector memory phenotype, the distribution after co-culture shifted towards an effector memory phenotype for almost all CAR T cells already 24h after antigen contact (24h 98.5%, 48h 97.3%).

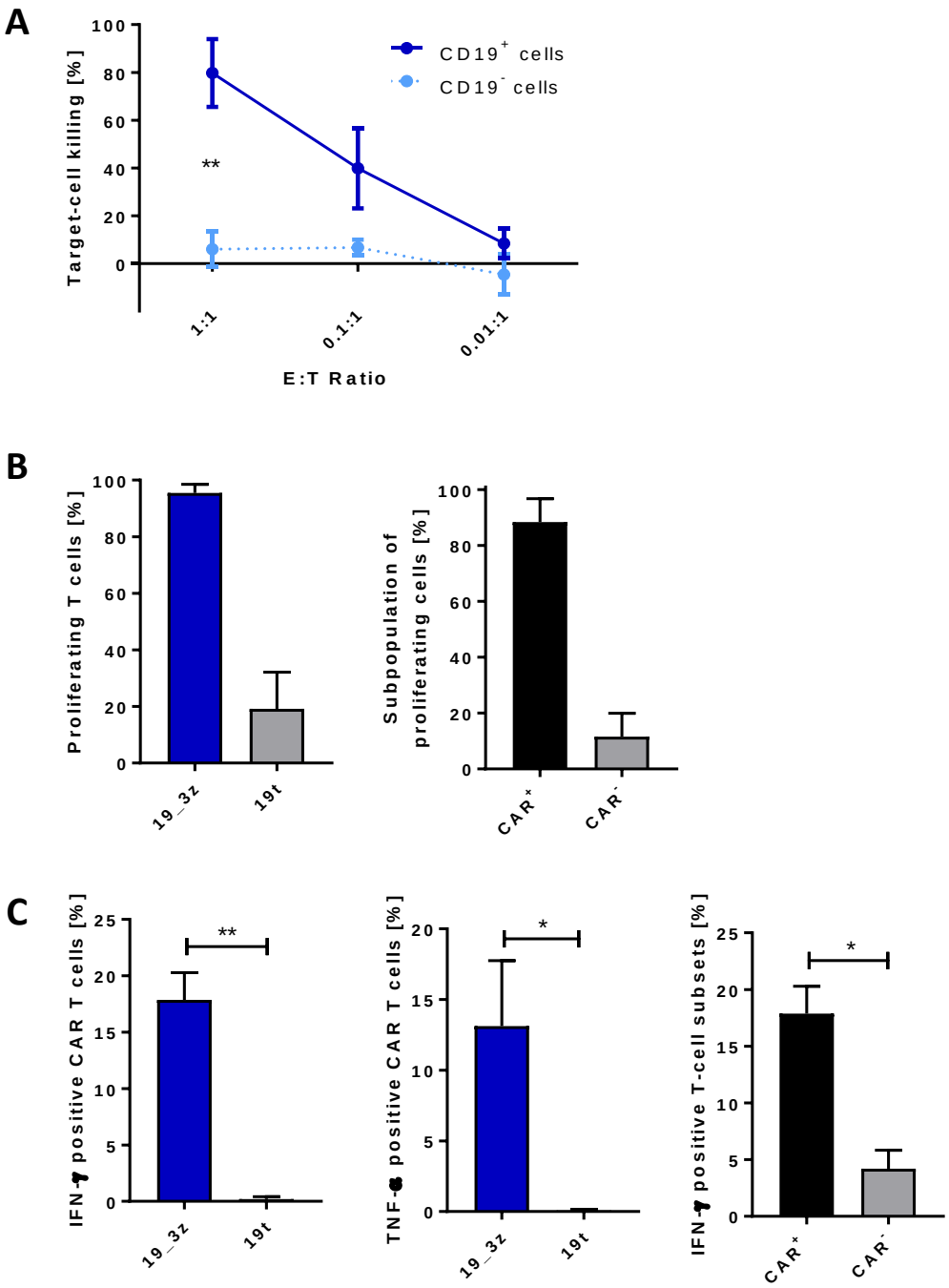

Figure 10: High functionality of first generation anti-CD19 CAR T cells (19_3z) upon target recognition.

(A) The flow cytometry based cytotoxicity assay showed an E:T ratio dependent killing efficacy after 48h (1:1 p=0.0032). The killing was antigen dependent as the co-culture of CAR T cells with $CD19^-$ cells showed less than 7% killing (n ≥ 3). **(B)** Gated on all T cells within the population of the first generation CAR, a high proliferative capacity could be detected 72h after CD19 antigen contact compared to the control CAR (left part). Gating on all proliferating cells within the 19_3z population revealed that this effect was mediated mainly by 19_3z CAR T cells and not untransduced T cells (right part) (n ≥ 3). **(C)** The first generation CAR was co-cultured with $CD19^+$ cells and a flow based intracellular stain showed CAR-dependent IFN-γ release. IFN-γ and TNF-α secretion of the 19_3z CARs were significantly higher compared to the control CAR (left and middle part; IFN-γ p=0.0053; TNF-α p=0.0405). In the right part the IFN-γ release of CAR^+ and CAR^- T cells within the 19_3z population was compared. Gating was set on the CAR^+ or the CAR^- T-cell subset and percentage of IFN-γ^+ cell was examined (p=0.0227, n ≥ 3). Two-tailed paired t test was performed to determine statistical significance. E:T Ratio: Effector to target ratio, 19t: control CAR, IFN-γ: interferon gamma, TNF-α: tumor necrosis factor alpha *(Continued)*

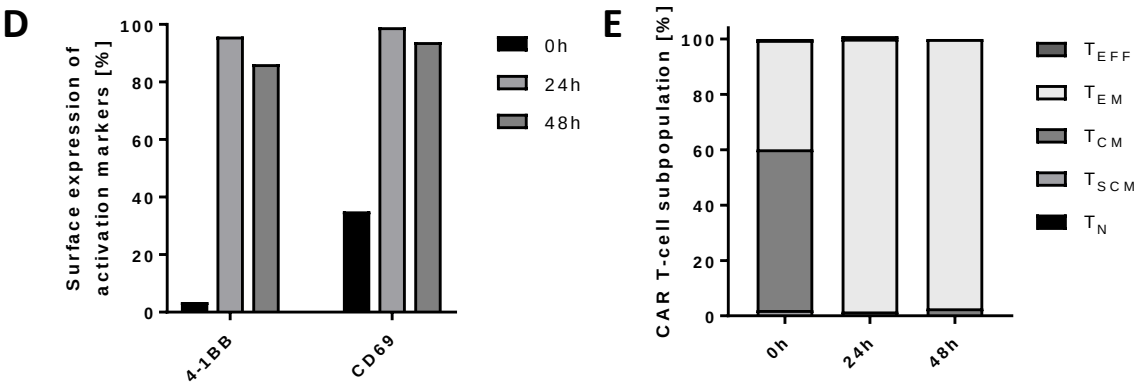

Figure 10 (Continued): High functionality of first generation anti-CD19 CAR T cells (19_3z) upon target recognition.
(D) Expression of activation markers 4-1BB and CD69 was detected without co-culture (0h) and 24h and 48h after CD19 antigen contact in flow cytometry. An up-regulation of activation markers within 24h was detectable (representative experiment). **(E)** The T-cell phenotype distribution was measured at three different time points by flow cytometry. Without co-culture (0h), CAR T cells had a mainly central memory phenotype. After co-culture with $CD19^+$ cells for 24h and 48h, this switched to effector memory phenotype. The phenotype subsets were evaluated by expression of CD62L, CD45RO and CD95 (representative experiment). Two-tailed paired t test was performed to determine statistical significance. T_N: naïve T cells, T_{SCM}: stem cell-like memory T cells, T_{CM}: central memory T cells, T_{EM}: effector memory T cells, T_{EFF}: Effector T cells
T_N: $CD62L^+$, $CD45RO^-$, $CD95^-$; T_{SCM}: $CD62L^+$, $CD45RO^-$, $CD95^+$; T_{CM}: $CD62L^+$, $CD45RO^+$, $CD95^+$; T_{EM}: $CD62L^-$, $CD45RO^+$, $CD95^+$; T_{EFF}: $CD62L^-$, $CD45RO^-$, $CD95^+$.

5.3 Second generation CAR T cells show higher cytokine secretion compared to first generation CAR T cells

The structure of the second generation CAR is similar to the first generation CAR but contains an additional 4-1BB co-stimulatory domain (Figure 11A). The mean transduction rate for the second generation CAR (19_BB_3z) was 53.4% (range 31.7-71.3%) and therefore comparable to the first generation CAR (19_3z) (mean 69.0%) (Figure 11B).

When co-cultured with $CD19^+$ K562 cells for 48h, no significant difference in terms of killing efficacy between the first generation and the second generation CAR was detectable (Figure 11C). The killing rate of 19_BB_3z for the 1:1 E:T ratio was 77.9% (range 54.3-93.7%) which was comparable to the first generation CAR 19_3z (mean 79.7%). Co-culture with $CD19^-$ target cells served as control.

The amount of IFN-γ positive cells after antigen contact ($CD19^+$ K562 cells) was significantly increased for the second generation CAR T cells compared to the first generation CAR T cells ($p=0.0010$, Figure 11D). A mean of 33.6% (range 29.8-35.7%) of second generation CAR T cells

were IFN-γ positive after co-culturing with CD19⁺ K562 cells compared to 17.9% (range 15.1-19.6%) of first generation CAR T cells.

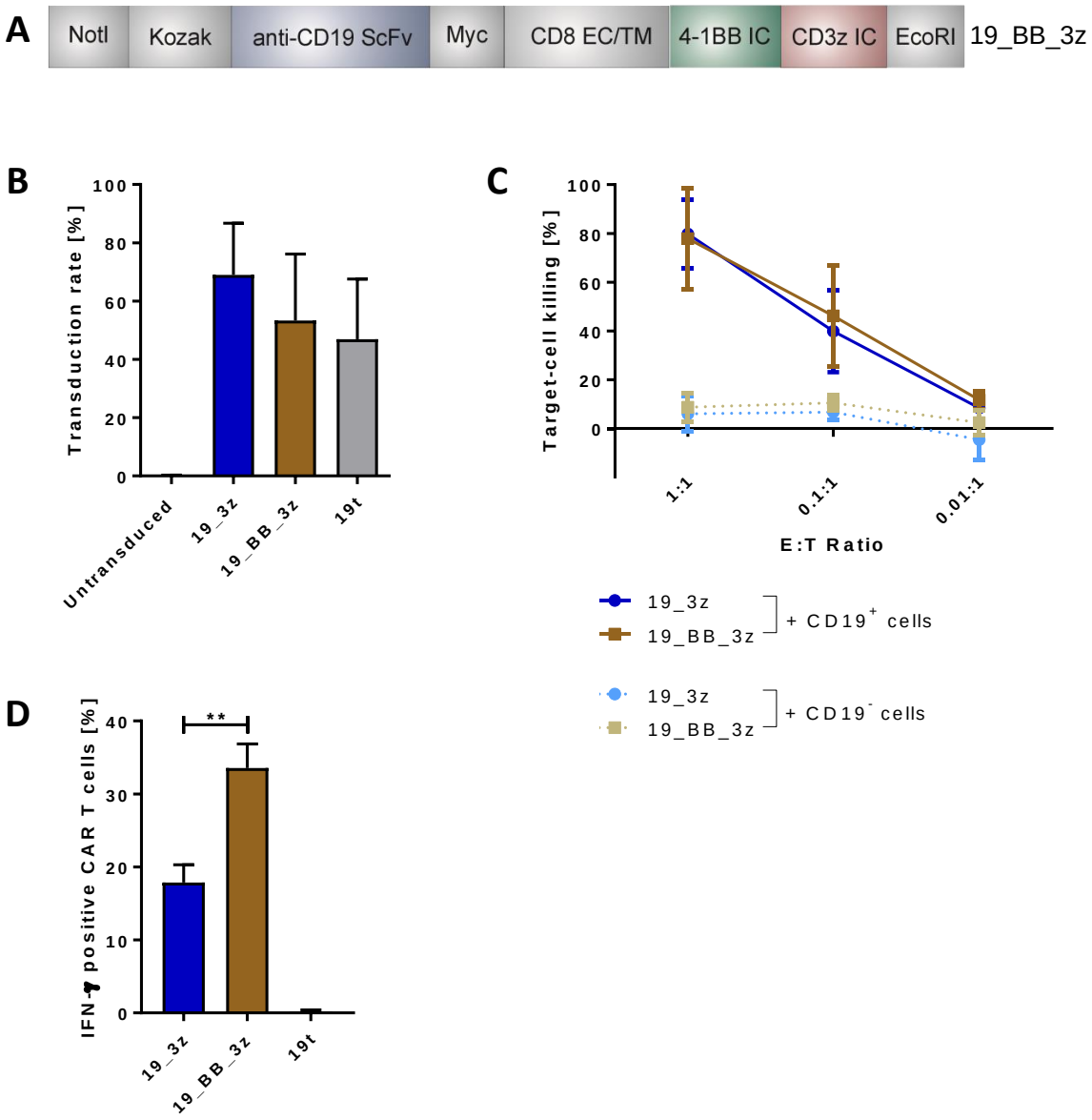

Figure 11: Second generation CAR T cells (19_BB_3z) show a higher cytokine secretion compared to first generation CAR T cells.
(A) The second generation CAR contains a co-stimulatory intracellular 4-1BB domain. The other domains are identical with the first generation CAR (Figure provided by F. Blaeschke and T. Feuchtinger). **(B)** Transduction rates were measured by flow cytometry on day 12 after transduction via a c-myc tag in the CAR. First and second generation CAR T cells showed no significant difference in transduction rates. Untransduced cells served as control (n ≥ 3). **(C)** The flow cytometry based killing assay showed no significant difference of the second generation CAR compared to the first generation CAR when co-cultured with CD19⁺ cells for 48h (n ≥ 3). **(D)** The percentage of IFN-γ positive cells of the second generation CAR T cells was significantly increased compared to the first generation CAR T cells (p=0.0010; n ≥ 3). Two-tailed paired t test was performed to determine statistical significance. ScFv: single chain variable fragment, Myc: c-myc tag, EC: extracellular, TM: transmembrane, IC: intracellular, 19t: control CAR, E:T Ratio: Effector to target ratio, IFN-γ: interferon gamma

5.4 PD-1_CD28 fusion receptor improves cytokine release of CAR T cells in presence of PD-L1

To test the functionality of an anti-CD19 CAR with a PD-1_CD28 fusion receptor, a bi-cistronic construct was designed. The construct consisted of a conventional first generation CAR (see 5.1) connected to a PD-1_CD28 fusion receptor via a F2A linker (Figure 12A). The linker mediated cleavage of the CAR and the fusion receptor during translation. The fusion receptor contained the extracellular and transmembrane PD-1 domain and the intracellular CD28 domain to turn an inhibitory PD-1 signal into CD28-mediated T-cell activation. The receptor was a complete human version of the murine receptor published by Kobold et al (Kobold et al. 2015). Despite the large size of the construct, the transduction rate of CAR T cells with fusion receptor (mean 54.8%, range 45.9-71.3%) was comparable to the first generation CAR T cells (mean 69.0%) (Figure 12B). Flow cytometry-based analysis showed that the CAR signal correlated with the PD-1 expression indicating simultaneous expression of the CAR and the fusion receptor on the cell surface (Figure 12C). Mean endogenous PD-1 expression of conventional first generation CAR T cells was 11.05% (range 2.1-22.9%).

When co-cultured with $CD19^{+}$ K562 cells, the CAR with the fusion receptor (19_3z_PD-1_28) showed no significant difference in killing capacity compared to the conventional CAR (19_3z) (Figure 12D, Data and figure published in an adapted version by Blaeschke et al. 2021) proofing that the fusion receptor did not impair CAR T-cell function.

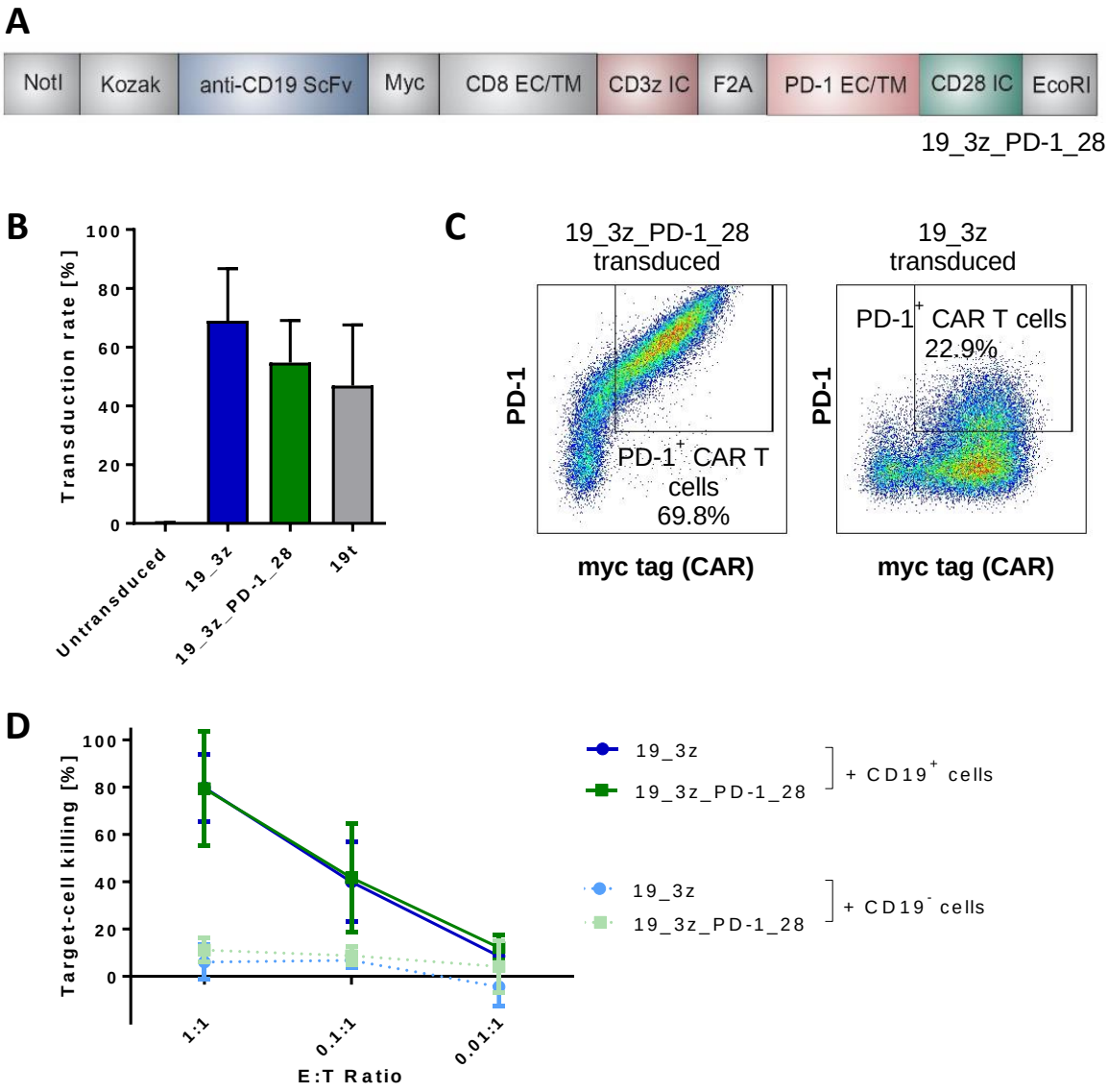

Figure 12: Generation of first generation CD19 CAR T cells with PD-1_CD28 fusion receptor (19_3z_PD-1_28).

(A) The fusion receptor contains an extracellular and transmembrane PD-1 domain and an intracellular CD28 domain. The receptor is linked to a first generation CAR via a F2A linker which mediates the cleavage of CAR and fusion receptor during translation (Figure provided by F. Blaeschke and T. Feuchtinger). **(B)** The transduction rate of the first generation CAR with fusion receptor (19_3z_PD-1_28) was comparable to the first generation CAR T cells without fusion receptor (19_3z) ($n \geq 3$). **(C)** The exemplary dot plot on the left shows simultaneous expression of the first generation CAR and the PD-1_CD28 fusion receptor. The right plot shows the endogenous PD-1 expression of the first generation CAR on day 12 after transduction. Gates are set according to isotype control. **(D)** When co-cultured with $CD19^+$ target cells for 48h, there was no significant difference in the killing capacity between CAR T cells with and without fusion receptor. The fusion receptor did not impair the killing efficacy of CAR T cells ($n \geq 3$; Data and figure published in an adapted version by Blaeschke et al. 2021). ScFv: single chain variable fragment, Myc: c-myc tag, EC: extracellular, TM: transmembrane, IC: intracellular, F2A: Foot-and-mouth-disease-virus 2A peptide, PD-1: programmed cell death 1, 19t: control CAR, E:T Ratio: Effector to target ratio

In order to detect the effect of the fusion receptor in presence of PD-L1, K562 cells were transduced with CD19 and PD-L1. After transduction and sorting, 99.9% of the cells stably expressed PD-L1 on the cell surface (Figure 13A, Data and figure published by Blaeschke et al. 2021).

Inhibitory checkpoint markers on CAR T cells were evaluated to evaluate if the presence of PD-L1 on the target cells influences the surface expression of inhibitory T-cell checkpoints (Figure 13B). Therefore, CAR T cells without fusion receptor were co-cultured with $CD19^+$ or $CD19^+/PD\text{-}L1^+$ K562 cells for 24h. No significant difference of 2B4, BTLA, CTLA-4, LAG3, PD-1, TIGIT or TIM-3 expression was detectable between the two conditions.

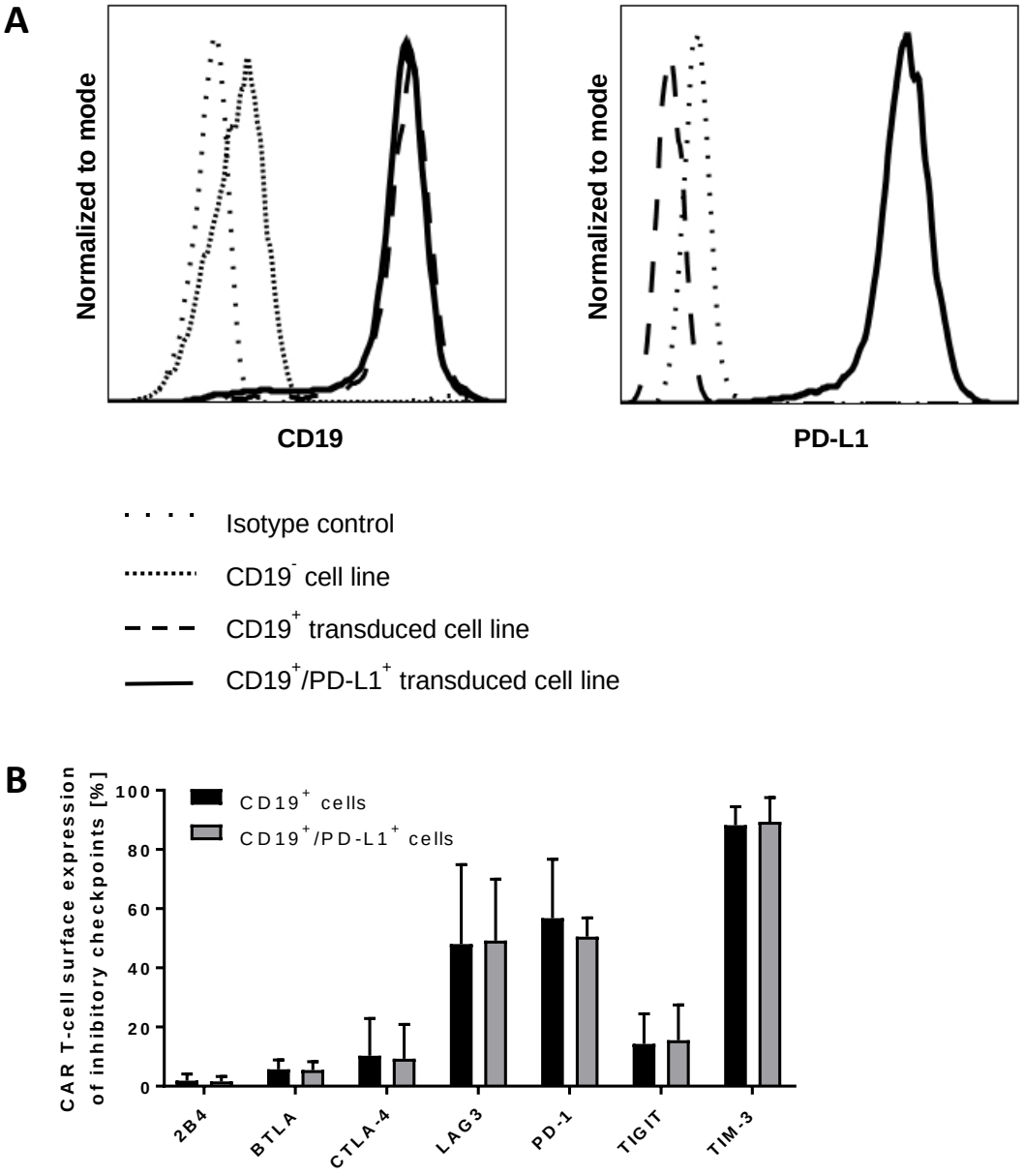

Figure 13: PD-L1 transduction of cell lines.
(A) K562 cells were transduced with CD19 or CD19 and PD-L1 and stably expressed the antigens on the cell surface (Data and figure published by Blaeschke et al. 2021). **(B)** Presence of PD-L1 on the target-cell surface did not change the checkpoint profile of anti-CD19 CAR T cells without fusion receptor after antigen contact (n ≥ 3). Two-tailed paired t test was performed to determine statistical significance. BTLA: B- and T-lymphocyte attenuator, CTLA-4: cytotoxic T-lymphocyte-associated protein 4, LAG3: lymphocyte-activation gene 3, PD-1: programmed cell death protein 1, TIGIT: T-cell immunoreceptor with Ig and ITIM domains, TIM-3: T-cell immunoglobulin and mucin domain 3

To ensure that the fusion receptor is only specifically activated in presence of the CAR signal, the first generation CAR with the fusion receptor (19_3z_PD-1_28) was co-cultured with $CD19^-$, $CD19^-/PD\text{-}L1^+$ and $CD19^+/PD\text{-}L1^+$ K562 cells (Figure 14A, Data and figure published in an adapted version by Blaeschke et al. 2021). Only in presence of CD19, the CAR T cells were producing IFN-γ (mean 44.9%, range 33.1-51.3%). In co-culture with $CD19^-/PD\text{-}L1^+$ cells, only

1.5% of the CAR T cells were IFN-γ positive (p=0.0169) precluding unspecific activation of the fusion receptor in absence of an anti-CD19 CAR signal.

When co-cultured with $CD19^+$/$PD\text{-}L1^+$ K562 cells the killing efficacy of the 19_3z and 19_3z_PD-1_28 CAR did not show significant differences (Figure 14B, Data and figure published in an adapted version by Blaeschke et al. 2021). For the 0.1:1 E:T ratio, the CAR with the fusion receptor killed 44.0% (range 23.8-57.9%) of the target cells while the CAR without the fusion receptor killed 32.7% (range 23.0-48.3%).

To evaluate the cytokine secretion, CAR T cells with and without fusion receptor were co-cultured with either $CD19^+$ or $CD19^+$/$PD\text{-}L1^+$ K562 cells for 24h (Figure 14C). The 19_3z_PD-1_28 CAR showed 26.0% IFN-γ positive CAR T cells in co-culture with $CD19^+$ targets, whereas additional presence of PD-L1 on target cells increased the percentage of IFN-γ positive CAR T cells to 51.2% (range 33.1-69.9%) (p=0.0071). After co-culture of 19_3z CAR T cells with $CD19^+$/$PD\text{-}L1^+$ target cells 19.1% (range 17.0-21.7%) CAR T cells were IFN-γ positive. In conclusion, CAR T cells with fusion receptor released a significant higher amount of IFN-γ in presence of PD-L1 compared to conventional CAR T cells (p=0.0195).

First generation CAR T cells with the fusion receptor were co-cultured with $CD19^+$ or $CD19^+$/$PD\text{-}L1^+$ K562 cells and expression of activation markers on CAR T cells was analysed by flow cytometry (Figure 14D). All activation markers were expressed on >70% of CAR T cells after target-cell contact. No significant differences in activation profile were observed after co-culture with $CD19^+$/$PD\text{-}L1^+$ compared to $CD19^+$/$PD\text{-}L1^-$ cell lines.

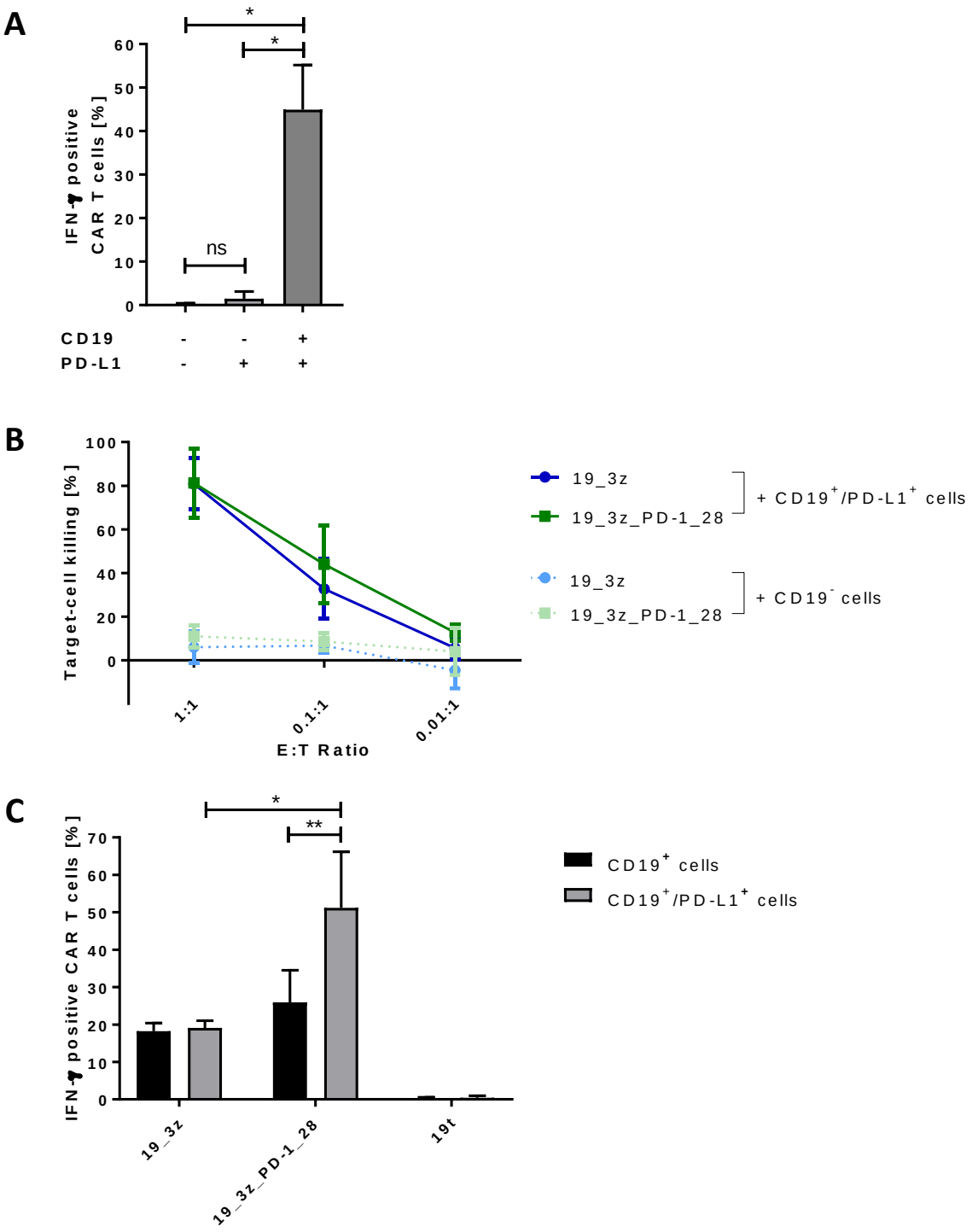

Figure 14: Functional characterization of CAR T cells with PD-1_CD28 fusion receptor (19_3z_PD-1_28). **(A)** 19_3z_PD-1_28 CAR T cells were co-cultured with a $CD19^-/PD\text{-}L1^+$ cell line in order to exclude unspecific activation mediated by the fusion receptor. The intracellular cytokine level was measured by flow cytometry. $CD19^-/PD\text{-}L1^-$ cells served as negative and $CD19^+/PD\text{-}L1^+$ cells as positive control confirming that fusion receptor-mediated activation is dependent on CD19 antigen recognition and anti-CD19 CAR signaling (n ≥ 3; Data and figure published in an adapted version by Blaeschke et al. 2021). **(B)** The killing efficacy, measured by flow cytometry, of both constructs showed no significant difference in co-culture with $CD19^+/PD\text{-}L1^+$ cells after 48h (n ≥ 3; Data and figure published in an adapted version by Blaeschke et al. 2021). **(C)** In presence of PD-L1, the CAR with the fusion receptor showed a significant increase of INF-γ positive cells (p=0.0071). When co-cultured with $CD19^+/PD\text{-}L1^+$ cells the 19_3z_PD-1_28 CAR showed a significantly higher INF-γ production compared to conventional 19_3z CAR (p=0.0195) (n ≥ 3). Two-tailed paired t test was performed to determine statistical significance. IFN-γ: interferon gamma, E:T Ratio: Effector to target ratio, 19t: control CAR *(Continued)*

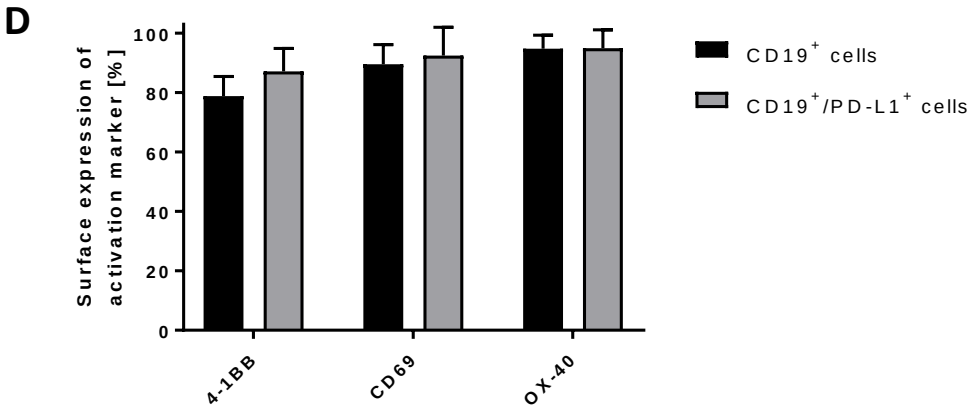

Figure 14 (Continued): Functional characterization of CAR T cells with PD-1_CD28 fusion receptor (19_3z_PD-1_28).
(D) The expression of activation markers on the cell surface of 19_3z_PD-1_28 CARs showed no significant difference when either co-cultured with $CD19^+$ or $CD19^+/PD\text{-}L1^+$ cells ($n \geq 3$). Two-tailed paired t test was performed to determine statistical significance.

To confirm the results of the intracellular cytokine stain, the assay was performed with different $CD19^+$ cell lines. In order to diminish the effect of CAR-CD19 interaction and thus strengthening the functional relevance of the PD-1_CD28 fusion receptor, target cell lines were evaluated for low CD19 median fluorescence intensity (MFI). CD19 MFI of analysed cell lines are shown in Table 1. As Daudi cells showed a significantly lower CD19 MFI compared to CD19-transduced K562, Daudi cells were chosen for further testing of the fusion receptor and were transduced with PD-L1 (Figure 15A).

Table 1: Median fluorescent intensity (MFI) of CD19$^+$ cell lines.

Cell lines were stained for PE-CD19 and analysed by their median CD19 expression. MFI represents the number of CD19 molecules on the cells' surface.

Cell line	Median fluorescent intensity
Isotype control	61.7
Daudi	5086
Nalm-6	6734
Nalm-16	9192
Raji	20630
K562 CD19 transduced	54602

First generation CAR T cells with and without fusion receptor were co-cultured with WT and PD-L1$^+$ Daudi cells to evaluate the cytokine secretion after antigen contact (Figure 15B, Data and figure published in an adapted version by Blaeschke et al. 2021). The fusion receptor induced an increase of INF-γ positive CAR T cells when PD-L1 was present compared to absence of PD-L1 ($p=0.0129$). In co-culture with PD-L1$^+$ Daudi cells, 3.0% CAR T cells without fusion receptor (range 2.1-5.37%) were IFN-γ positive while with fusion receptor there were 10.6% IFN-γ positive CAR T cells detectable (range 7.7-15.4%; $p=0.0240$).

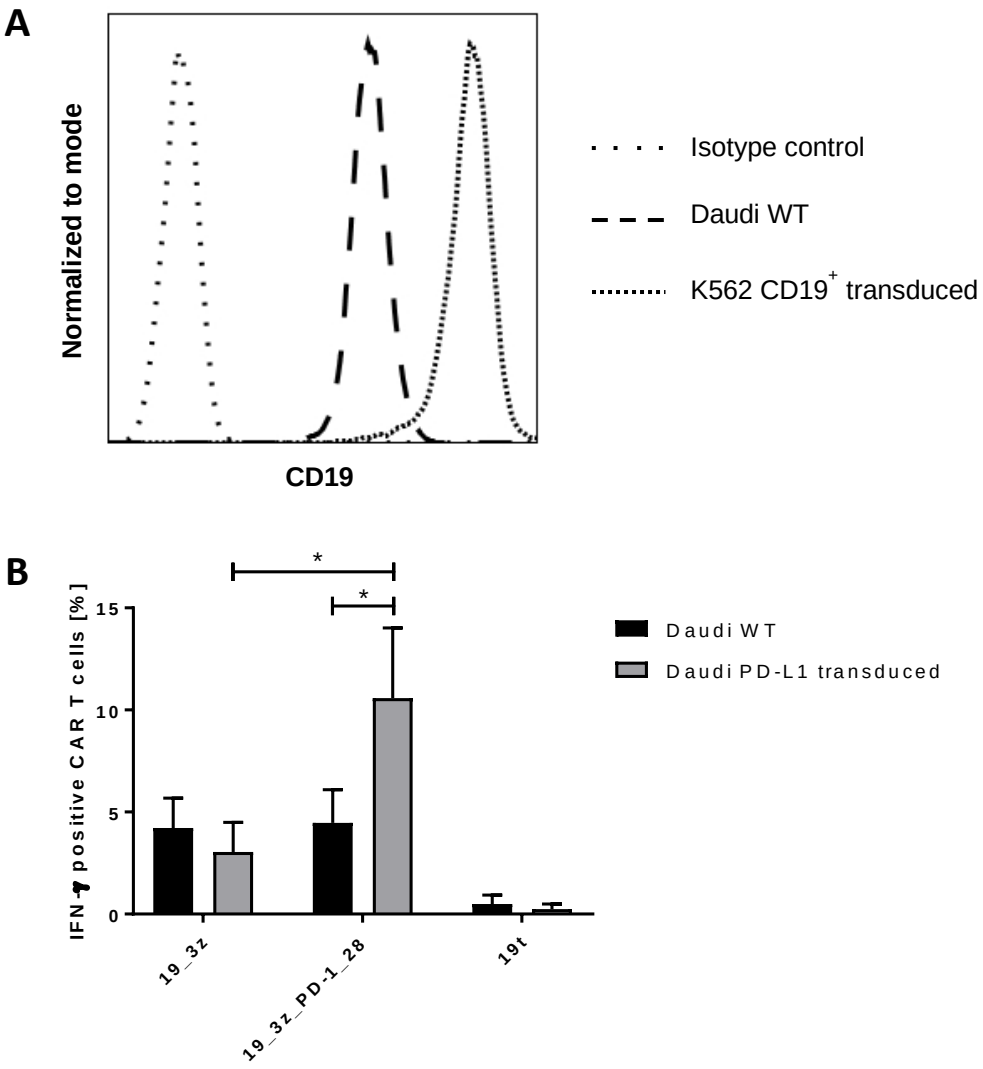

Figure 15: Confirmation of cytokine secretion assay with CD19$^+$ lymphoma cell line.
(A) Leukemic cell lines were tested for their CD19 median fluorescent intensity to identify a cell line with lower CD19 expression as transduced K562 cells. Isotype stain served as negative, CD19-transduced K562 cells served as positive control. Daudi cells were chosen for further testing of the CAR T cells with fusion receptor and transduced with PD-L1. **(B)** First generation CAR T cells with and without fusion receptor were co-cultured with WT and PD-L1$^+$ Daudi cells to evaluate the cytokine secretion after antigen contact in a flow cytometry based assay. The fusion receptor of the 19_3z_PD-1_28 CAR induced an increase of IFN-γ positive cells comparing absence and presence of PD-L1 (p=0.0129). In co-culture with PD-L1$^+$ Daudi cells, the 19_3z_PD-1_28 CAR was superior to the 19_3z CAR (p=0.0240; n ≥ 3; Data and figure published in an adapted version by Blaeschke et al. 2021). Two-tailed paired t test was performed to determine statistical significance. IFN-γ: interferon gamma, 19t: control CAR, WT: wildtype

Since conventional second generation CARs were superior to first generation CARs, assays were performed to analyze whether first generation CAR T cells with fusion receptor (19_3z_PD-1_28) can outcompete conventional second generation CAR T cells (19_BB_3z) (Figure 16, Data and figure published in an adapted version by Blaeschke et al. 2021). When CAR T cells were co-cultured with CD19$^+$ but PD-L1$^-$ Daudi cells, the 19_BB_3z CAR (mean 8.0%) showed a higher IFN-γ secretion than the 19_3z_PD-1_28 CAR (mean 4.0%). In co-culture with

CD19^{+}/PD-L1^{+} Daudi cells however, the inhibitory effect of the PD-L1 diminished the IFN-γ production of the conventional second generation CAR (mean 5.2%, p=0.0282). In contrast, IFN-γ production of the first generation CAR with the fusion receptor was increased (mean 9.8%, p=0.0120) after contact with the PD-L1^{+} cell line confirming that in presence of PD-L1 the first generation CAR with fusion receptor can outcompete conventional second generation CAR T cells in terms of IFN-γ release (p=0.0101).

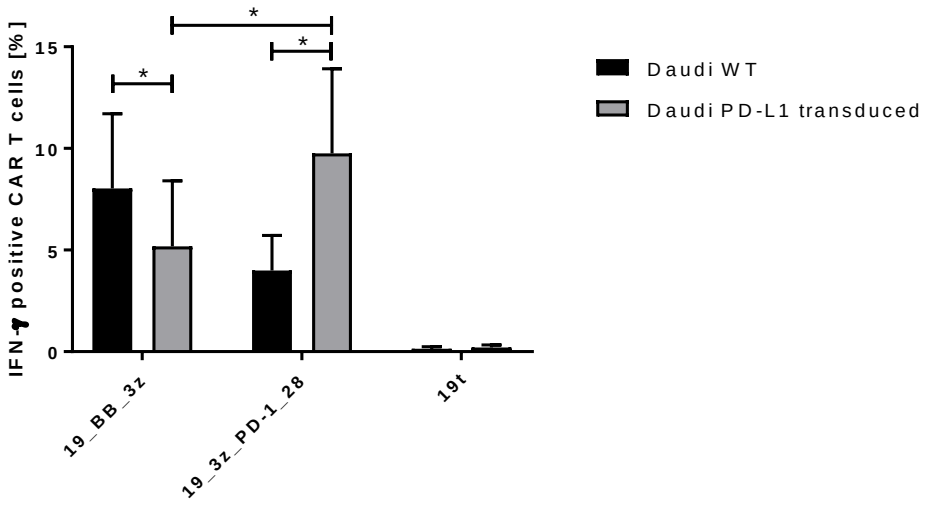

Figure 16: First generation CAR T cells with fusion receptor (19_3z_PD-1_28) outcompete conventional second generation CAR T cells (19_BB_3z) in presence of PD-L1.
Conventional second generation CAR T cells and first generation CAR T cells with fusion receptor were co-cultured with PD-L1^{-} and PD-L1^{+} Daudi cells. Percentage of IFN-γ^{+} CAR T cells was analysed 24h hours after co-culture. Presence of PD-L1 diminished the IFN-γ release of the second generation CAR (p=0.0282) and increased the release of the first generation CAR with fusion receptor (p=0.0120). In presence of PD-L1 the 19_3z_PD-1_28 CAR could outcompete the 19_BB_3z CAR (p=0.0101) (n ≥ 3; Data and figure published in an adapted version by Blaeschke et al. 2021). Two-tailed paired t test was performed to determine statistical significance. IFN-γ: interferon gamma, 19t: control CAR, WT: wildtype

5.5 Second generation CAR with fusion receptor showed enhanced T_{H1} responses compared to conventional second generation CAR

Since the second generation CAR was superior to the first generation CAR, a second generation CAR with PD-1_CD28 fusion receptor was designed. The second generation CAR and fusion receptor were built as described before (see 5.3 and 5.4). A schematic overview of the structure of the second generation CAR with fusion receptor (19_BB_3z_PD-1_28) is given below (Figure 17A). The generation of this construct was feasible and mean transduction rates of 66.4% (range 47.2-81.0%) were reached (Figure 17B, Data and figure published in an adapted version by Blaeschke et al. 2021).

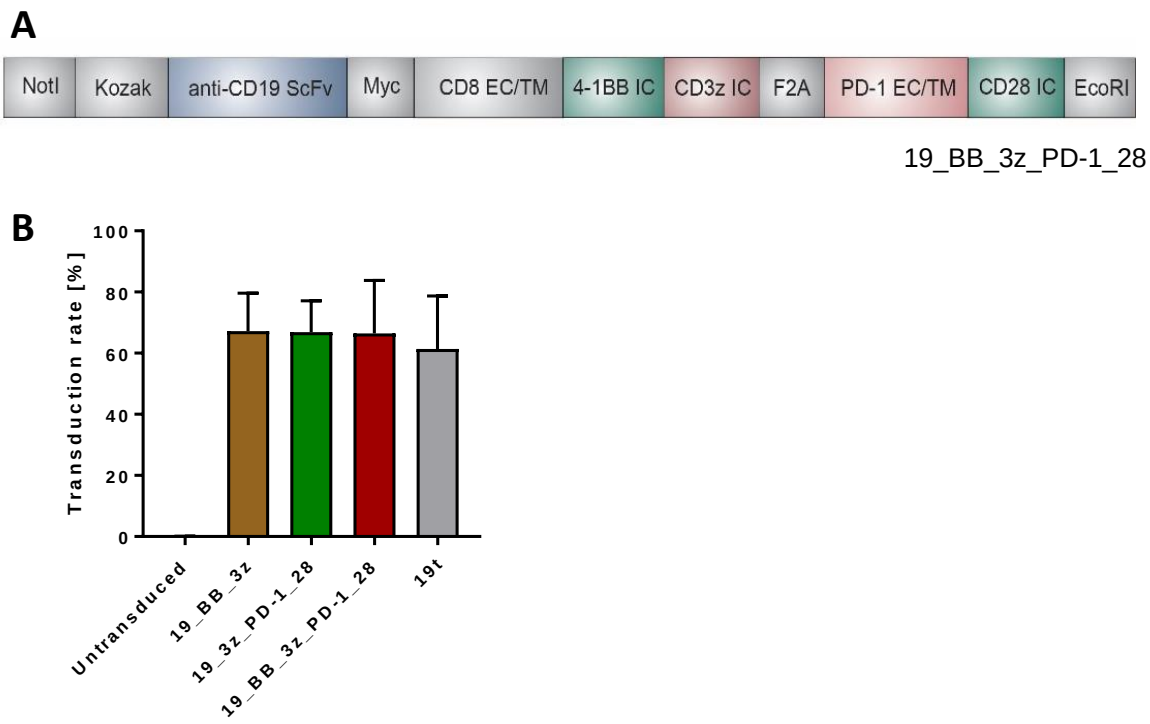

Figure 17: Generation of second generation CAR T cells with PD-1_CD28 fusion receptor (19_BB_3z_PD-1_28).
(A) The second generation CAR contains a 4-1BB co-stimulatory domain fused to CD3zeta. The fusion receptor is built of an extracellular and transmembrane PD-1 domain and an intracellular CD28 domain. Both parts are linked via a F2A linker mediating the cleavage of CAR and fusion receptor during translation (Figure provided by F. Blaeschke and T. Feuchtinger). **(B)** Transduction of second generation CAR T cells with fusion receptor (19_BB_3z_PD-1_28) was feasible. Transduction rates were comparable to the second generation CAR without fusion receptor and the first generation CAR with fusion receptor ($n \geq 3$; Data and figure published in an adapted version by Blaeschke et al. 2021). ScFv: single chain variable fragment, Myc: c-myc tag, EC: extracellular, TM: transmembrane, IC: intracellular, F2A: Foot-and-mouth-disease-virus 2A peptide, 19t: control CAR

Second generation CAR T cells with and without fusion receptor were co-cultured with $CD19^+$/$PD\text{-}L1^+$ K562 cells for 48h to assess killing capacity (Figure 18A, Data and figure published in an adapted version by Blaeschke et al. 2021). There was no significant difference detectable between the two constructs.

IFN-γ secretion of the second generation CAR with and without fusion receptor was evaluated after co-culture with two different cell lines (Figure 18B and C). When co-cultured with Daudi wildtype cells, the second generation CAR with and without fusion receptor released a comparable amount of IFN-γ (19_BB_3z: 4.8%, 19_BB_3z_PD-1_28: 5.0%). When PD-L1 was present on the Daudi target cells, 19_BB_3z CARs showed a slightly diminished IFN-γ release (mean 2.0%) while 19_BB_3z_PD-1_28 CARs increased IFN-γ release (mean 8.4%). In presence of PD-L1 on Daudi cells, the CAR with fusion receptor could outcompete the CAR without fusion receptor ($p=0.0490$).

In co-culture with $CD19^+$/$PD\text{-}L1^+$ K562 cells, the second generation CAR with PD-1_CD28 fusion receptor showed a significant higher amount of IFN-γ^+ CAR T cells (mean 49.3%) compared to the conventional second generation CAR (mean 38.0%) ($p=0.0245$).

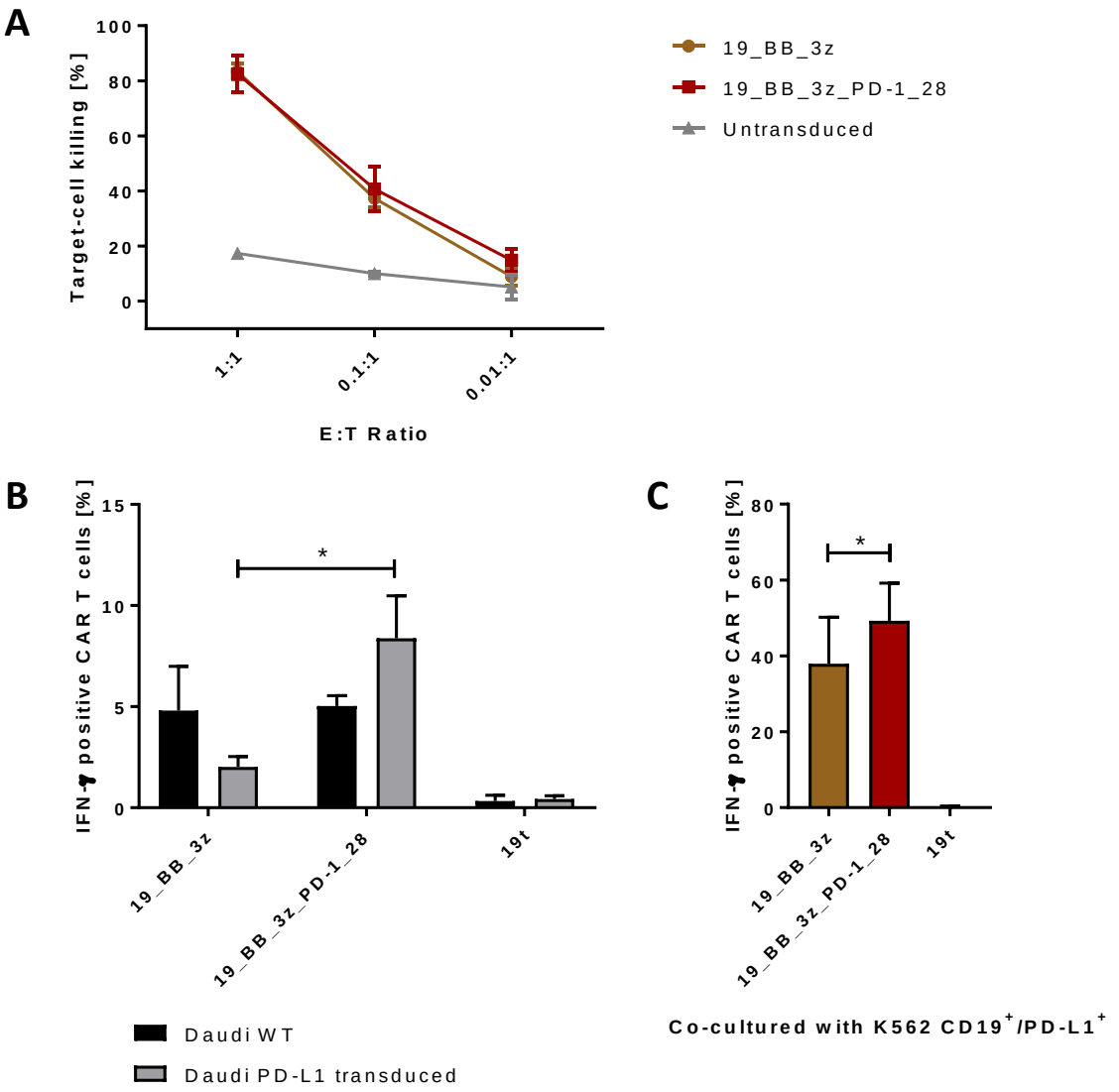

Figure 18: Second generation CAR with fusion receptor (19_BB_3z_PD-1_28) showed a higher IFN-γ release in presence of PD-L1 compared to a conventional second generation CAR (19_BB_3z).
(A) The killing capacity of 19_BB_3z and 19_BB_3z_PD-1_28 showed no significant differences when co-cultured with $CD19^+/PD\text{-}L1^+$ K562 cells for 48h. Co-culture of untransduced T cells with target cells served as control. One representative experiment in technical duplicates is shown (Data and figure published in an adapted version by Blaeschke et al. 2021). **(B)** IFN-γ secretion after co-culture of the second generation CAR with fusion receptor and Daudi WT cells (mean 5.0%) was comparable to the secretion of the conventional second generation CAR in absence of PD-L1 (mean 4.8%). Upon presence of PD-L1, the IFN-γ release of the 19_BB_3z_PD-1_28 CAR increased significantly compared to the 19_BB_3z CAR ($p= 0.0490$, $n \geq 3$). **(C)** 24h after co-culture with $CD19^+/PD\text{-}L1^+$ K562 cells, the second generation CAR with fusion receptor showed a significant higher amount of $IFN\text{-}\gamma^+$ CAR T cells compared to the second generation CAR without fusion receptor ($p=0.0245$). Two-tailed paired t test was performed to determine statistical significance. E:T Ratio: Effector to target ratio, IFN-γ: interferon gamma, 19t: control CAR, WT: wildtype

In a last step, the second generation CAR with fusion receptor was compared to the first generation CAR with fusion receptor. The target cell killing of $CD19^+$/$PD\text{-}L1^+$ K562 cells for both fusion receptor constructs did not differ significantly (Figure 19A).

IFN-γ release of the 19_3z_PD-1_28 CAR and the 19_BB_3z_PD-1_28 CAR was analysed in co-culture with two different cell lines after 24h.

In co-culture with $CD19^+$/$PD\text{-}L1^+$ K562 cells, no significant difference between the two constructs with fusion receptor could be detected (Figure 19B). The 19_3z_PD-1_28 CAR showed a mean IFN-γ release of 52.7% (range 44.1-65.8) and the 19_BB_3z_PD-1_28 CAR of 49.3% (range 38.0-56.7%).

After contact with $PD\text{-}L1^+$ Daudi cells however, 8.4% (range 6.6-10.7%) IFN-γ positive CAR T cells were measured for the second generation CAR with fusion receptor and 6.7% (range 4.7-8.67%) for the first generation CAR with fusion receptor (Figure 19C). This finding hints that, dependent on the target-cell characteristics, 19_BB_3z_PD-1_28 CAR are able to show significantly higher cytokine release as compared to the 19_3z_PD-1_28 CAR ($p=0.0341$).

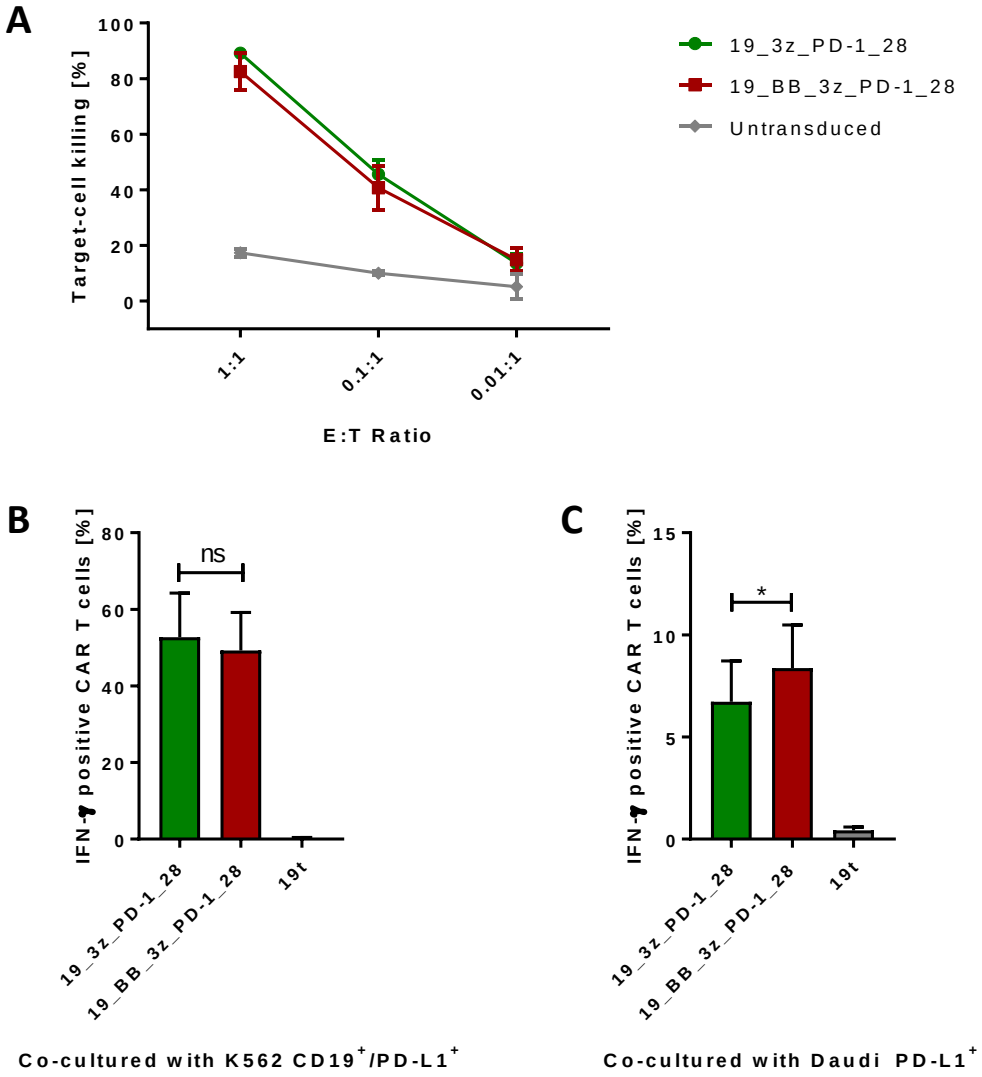

Figure 19: Benefit of second generation CARs with fusion receptor (19_BB_3z_PD-1_28) compared to first generation CARs with fusion receptor (19_3z_PD-1_28) is cell line dependent.
(A) To evaluate the killling efficacy of the 19_3z_PD-1_28 and the 19_BB_3z_PD-1_28 CAR, the cells were co-cultured with CD19$^+$/PD-L1$^+$ K562 cells for 48h. The conditions showed no significant differences (n ≥ 3). **(B+C)** IFN-γ secretion of the 19_3z_PD-1_28 and the 19_BB_3z_PD-1_28 CAR was tested in co-culture with two different CD19$^+$/PD-L1$^+$ cell lines. In the co-culture with PD_L1$^+$ Daudi cells (B) the second generation CAR with fusion receptor was superior to the first generation CAR with fusion receptor (p=0.0341). In co-culture with CD19$^+$/PD-L1$^+$ K562 cells (C) there was no significant difference between the two constructs with fusion receptor detecable (n ≥ 3). E:T Ratio: Effector to target ratio, IFN-γ: interferon gamma, 19t: control CAR

6 Discussion

CAR T-cell therapy has shown to induce initial responses of up to 90% in heavily pretreated children with B-cell precursor ALL (Park et al. 2018; Zhang, Song, and Liu 2018; Maude et al. 2018). Nevertheless, follow-up studies have shown that about 50% of pediatric patients relapse within one year after CAR T-cell infusion (Gardner et al. 2017). Hence, it is necessary to further enhance efficacy of CAR T cells to reach better long-term results for patients with advanced ALL. Sustained persistence *in vivo* is an important marker for long term response rates.

6.1 CAR T cell generation is feasible

In this study, we were able to successfully generate different CAR T-cell constructs derived from healthy donor samples. High transduction rates between 33.4 and 81.0 % were reached varying due to inter-individual differences. The CAR consisted of the scFv of the CD19 antibody clone FMC63 which has been published before (Kochenderfer et al. 2009) and has been used for CD19 CAR T cells in multiple clinical trials (Turtle et al. 2016; Kochenderfer et al. 2012). For detection in flow cytometry, a c-myc tag was included. In this study, a CD8 transmembrane domain was used. Alabanza et al. compared second generation CAR T cells with a CD28 co-stimulatory domain including either a CD8 or a CD28 transmembrane domain. They showed that CAR T cells with CD8 transmembrane domains displayed advantages such as decreased production of inflammatory cytokines and less activation-induced cell death after antigen contact while the killing efficacy was comparable (Alabanza et al. 2017). Viral gene delivery systems include retroviral and lentiviral transduction. During the past years, gene editing of T cells via CRISPR/Cas9 is emerging as a method for non-viral targeted genetic engineering. In our approach, we used a retroviral transduction with producer cell lines (293Vec-RD114 cells) to create comparable stable virus titers. Post transduction CAR T cells expanded around 100 fold within 12 days. During the expansion process the cells showed a high viability and had a mainly central memory phenotype. Central memory and stem cell-like memory T cells are known to have a good *in vivo* persistence while sustaining a functional immune response after adoptive transfer (Wang et al. 2016; Biasco et al. 2015).

6.2 High CD19 specific functionality of first generation CAR

To test the functionality of the first generation CAR T cells, they were analysed for their killing capacity, cytokine release, proliferative potential and expression of activation markers. Already low effector to target ratios showed a high killing capacity in vitro. After antigen contact, the CAR T cells started to proliferate for at least one generation. This effect was CAR T-cell specific as at least 80% of the proliferating cells were CAR^+. A small bystander effect of untransduced T cells within the co-culture was detectable. Assessed by the expression of 4-1BB and CD69, the first generation CAR T cells showed a good activation potential upon CD19 contact. Already 24 hours after antigen contact, the phenotype of the CAR T cells switched from a mainly central memory phenotype to a mainly effector memory phenotype.

6.3 Second generation CAR with superior function

When first generation CARs were tested in clinical trials it was demonstrated that the approach was safe but lack of T-cell persistence and proliferation in the patients limited therapeutic efficacy (Barrett et al. 2014). For an optimal physiological T-cell response one or more co-stimulatory signals are required additional to the signal of the T-cell receptor (Lenschow, Walunas, and Bluestone 1996). Second generation CAR T cells incorporating a co-stimulatory domain have been predominantly used for clinical therapy of pediatric B-cell ALL and approved by the FDA in 2017 (U.S. Food & Drug Administration 2017). In this research project, we included a second generation CAR with 4-1BB domain to set our experiments in a more clinical context. In current clinical studies, mainly 4-1BB and CD28 have been used so far. For leukemia treatment 4-1BB has been favored, as the peak of *in vivo* proliferation is lower and slower but provides the T cells with a longer persistence (Davis and Mackall 2016). We co-cultured the first and second generation CAR T cells with $CD19^+$ target cells to compare their killing capacity and cytokine release. Although the target cell killing did not significantly differ between first and second generation CAR T cells, we could confirm that the second generation CAR was superior to the first generation CAR in terms of cytokine release.

6.4 Breaking the inhibitory PD-1/PD-L1 axis

The interaction of immunosuppressive checkpoint molecules on the surface of T cells and tumor cells can lead to hypofunction of T cells indicated by decreased proliferative capacity, survival and effector function (Lesokhin et al. 2015). These functional characteristics are required for an efficient anti-tumor response in CAR T-cell therapy (Barrett et al. 2014). So far, the role of immune checkpoints in pediatric acute lymphoblastic leukemia has not been elucidated sufficiently. For different tumors like malignant melanoma, PD-1 and CTLA-4 have been discovered to play an important role. Therapy strategies with checkpoint inhibitors aim to intervene into those axes and have revolutionized treatment of advanced melanoma (Singh and Salama 2016). Because of its low mutational load ALL is considered a malignancy with low immunogenicity. Therefore, therapy with immune checkpoint blockade is less successful in pediatric ALL patients (Merchant et al. 2016; Majzner, Heitzeneder, and Mackall 2017; Snyder et al. 2014).

Nevertheless, it has been proven that immune checkpoints can play a role in ALL. The inhibitory interaction of PD-1 with PD-L1 – one of its ligands – can diminish the efficacy of immunotherapy. This has been shown *in vitro* for the treatment of B-ALL with the bispecific CD3/CD19 T-cell engager blinatumomab. Breaking the PD-1/PD-L1 axis by adding PD-1 blocking antibody increased the *in vitro* efficacy of blinatumomab in terms of proliferation capacity, cytokine production and cytotoxic effects of the T cells (Feucht et al. 2016). Rupp et al. demonstrated the immunosuppressive effects of PD-L1 also on CAR T cells. The CRISPR/Cas9-mediated disruption of PD-1 in CAR T cells led to a better control of a PD-L1$^+$ tumor in mice (Rupp et al. 2017). Nevertheless, manipulating the *Pdcd1* locus, which encodes for PD-1, might bear a risk for T-cell therapy: Wartewig et al. showed that *Pdcd1* also functions as a master gene, suppressing oncogenic T-cell signaling in T-cell lymphomas (Wartewig et al. 2017).

We confirmed that PD-1/PD-L1 interaction has an inhibitory effect on CAR T cells. In presence of PD-L1 on CD19$^+$ target cells, the IFN-γ release of the second generation anti-CD19 CAR was significantly reduced. To decrease susceptibility of CAR T cells to PD-1/PD-L1 mediated inhibition, we generated T cells with an anti-CD19 CAR and an additional PD-1_CD28 fusion receptor. We used a complete human version of the murine fusion receptor that was published by Kobold et al. They showed that in presence of PD-L1 on target cells the fusion receptor can mediate enhanced cytokine release, T-cell proliferation and T cell-induced lysis of target cells when transduced into primary T cells (Kobold et al. 2015). Schlenker et al. also

demonstrated the beneficial effects of a PD-1_CD28 fusion receptor in tumor infiltrating lymphocytes as the receptor upgraded the function of low-avidity T cells and restored effector functions of exhausted T cells (Schlenker et al. 2017). In contrast to PD-1_CD28 fusion receptor used in our research, the receptor used in this study consists of a CD28 transmembrane domain.

Our studies showed that the fusion receptor does not impair the function and signaling when transduced with a first generation CAR. In presence of the CAR target antigen CD19, the first generation CAR T cells with and without fusion receptor led to a comparable killing rate and cytokine release. When PD-L1 was expressed on the $CD19^+$ target cells, a co-stimulatory effect of the PD-1_CD28 fusion receptor was demonstrated. By adding the fusion receptor to a first generation CAR, the cells outcompeted a conventional first generation CAR in terms of INF-γ secretion when PD-L1 was present.

Even in comparison to a second generation CAR which is used for clinical treatment of pediatric ALL, the first generation CAR with fusion receptor released significantly higher amounts of IFN-γ when PD-L1 was present on the target cells.

To avoid on-target off-tumor activation it is important to exclude unspecific activation via the PD-1 domain of the fusion receptor. We demonstrated that the PD-1_CD28 fusion receptor is only functional in simultaneous presence of the CAR target antigen CD19 and PD-L1. Exclusive PD-L1 target cell expression did not activate the T cells.

6.5 Evaluating the most functional molecular design of CAR T cells with PD-1_CD28 fusion receptor

To initiate the best anti-leukemic response, it is crucial to evaluate the most functional molecular design of the CAR, the fusion receptor and their combination. Kobold et al. tested different fusion sites between murine PD-1 and CD28 domains. The fusion receptor with a PD-1 transmembrane domain was superior to the construct with a CD28 transmembrane domain and the construct with an extracellular CD28 segment and transmembrane domain (Kobold et al. 2015). Thus, in this study we used a completely human fusion receptor with PD-1 transmembrane domain.

As we discovered that the first generation CAR with fusion receptor is superior to a conventional second generation CAR we generated not only first generation CAR T cells with

fusion receptor but also second generation CAR T cells with fusion receptor. When comparing the second generation CAR with and without fusion receptor we saw that in presence of PD-L1 the CAR with fusion receptor released significantly higher amounts of IFN-γ.

Since the first generation and second generation CAR with fusion receptor both were superior to the conventional CARs we compared those two constructs with each other. Depending on the cell line the second generation CAR with fusion receptor trended towards higher cytokine release in presence of PD-L1.

In order to validate which molecular design is most functional against leukemic cells, CAR T cells with fusion receptor were tested in an *in vivo* mouse model. Our group could validate the *in vitro* results and showed enhanced functionality of CAR T cells with fusion receptor in presence of PD-L1. Second generation CAR T cells with fusion receptor outcompeted first generation CAR T cells with fusion receptor in terms of survival and *in vivo* persistence (Blaeschke et al. 2021).

Also Liu et al. have published *in vivo* results of 4-1BB CARs with PD-1_CD28 fusion receptor. They demonstrated the beneficial effect of the fusion receptor in NSG mice injected with a solid flank tumor expressing either human mesothelin or prostate specific cancer antigen (Liu et al. 2016). In contrast to our study they designed a fusion receptor with CD28 transmembrane domain.

6.6 Clinical potential of the PD-1_CD28 fusion receptor

Our study indicates that PD-L1 expression on leukemic target cells is crucial for enhanced efficacy of PD-1_CD28 fusion receptor approaches. In a clinical setting, it might be important to analyze the leukemic blasts of patients very precisely in order to examine if a patient could benefit from the CAR treatment with PD-1_CD28 fusion receptor. Evaluating PD-L1 levels should not only include initial expression of the leukemic blasts, but also a possible up-regulation of PD-1 after stimulation with T_{H1} cytokines as there are seen very interindividual responses (Blaeschke et al. 2021).

Due to the high functionality of both the first and the second generation CAR T cells with fusion receptor the risk of increased adverse effects might be given. Therefore, integrating a safety switch in the CAR could be considered and easily implemented if administered to patients (Straathof et al. 2005).

However, in contrast to antibody-mediated PD-1 blockade, PD-1_CD28 fusion receptors are selectively relevant in CAR T cells and do not interfere with all PD-1 interactions in the body. The great benefit of CAR T cells with fusion receptor is a disruption of the PD-1/PD-L1 axis at the tumor/target site instead of systemic disruption as seen with checkpoint blocking antibodies.

Tolerability and safety of CAR T cells with PD-1_CD28 fusion receptor administered to patients with relapsed/refractory B cell lymphoma could be demonstrated (Liang et al. 2021; Liu et al. 2021). In their clinical studies with 17 and six patients only mild cytokine release syndromes and no severe neurologic toxicities were reported. The CAR T cells with PD-1_CD28 fusion receptor showed promising efficacy in relapsed/refractory B cell lymphoma patients.

In conclusion, CAR T cells with fusion receptors could represent a great strategy to develop a more patient individualized CAR therapy and avoid escape mechanisms mediated by inhibitory checkpoint molecules.

Literature

Alabanza, L., M. Pegues, C. Geldres, V. Shi, J. J. W. Wiltzius, S. A. Sievers, S. Yang, and J. N. Kochenderfer. 2017. 'Function of Novel Anti-CD19 Chimeric Antigen Receptors with Human Variable Regions Is Affected by Hinge and Transmembrane Domains', *Mol Ther*, 25: 2452-65.

Ansell, S. M., A. M. Lesokhin, I. Borrello, A. Halwani, E. C. Scott, M. Gutierrez, S. J. Schuster, M. M. Millenson, D. Cattry, G. J. Freeman, S. J. Rodig, B. Chapuy, A. H. Ligon, L. Zhu, J. F. Grosso, S. Y. Kim, J. M. Timmerman, M. A. Shipp, and P. Armand. 2015. 'PD-1 blockade with nivolumab in relapsed or refractory Hodgkin's lymphoma', *N Engl J Med*, 372: 311-9.

Barrett, D. M., N. Singh, D. L. Porter, S. A. Grupp, and C. H. June. 2014. 'Chimeric antigen receptor therapy for cancer', *Annu Rev Med*, 65: 333-47.

Biasco, L., S. Scala, L. Basso Ricci, F. Dionisio, C. Baricordi, A. Calabria, S. Giannelli, N. Cieri, F. Barzaghi, R. Pajno, H. Al-Mousa, A. Scarselli, C. Cancrini, C. Bordignon, M. G. Roncarolo, E. Montini, C. Bonini, and A. Aiuti. 2015. 'In vivo tracking of T cells in humans unveils decade-long survival and activity of genetically modified T memory stem cells', *Sci Transl Med*, 7: 273ra13.

Blaeschke, F., D. Stenger, A. Apfelbeck, B. L. Cadilha, M. R. Benmebarek, J. Mahdawi, E. Ortner, M. Lepenies, N. Habjan, F. Rataj, S. Willier, T. Kaeuferle, R. G. Majzner, D. H. Busch, S. Kobold, and T. Feuchtinger. 2021. 'Augmenting anti-CD19 and anti-CD22 CAR T-cell function using PD-1-CD28 checkpoint fusion proteins', *Blood Cancer J*, 11: 108.

Borowitz, M. J., M. Devidas, S. P. Hunger, W. P. Bowman, A. J. Carroll, W. L. Carroll, S. Linda, P. L. Martin, D. J. Pullen, D. Viswanatha, C. L. Willman, N. Winick, and B. M. Camitta. 2008. 'Clinical significance of minimal residual disease in childhood acute lymphoblastic leukemia and its relationship to other prognostic factors: a Children's Oncology Group study', *Blood*, 111: 5477-85.

Brahmer, J., K. L. Reckamp, P. Baas, L. Crino, W. E. Eberhardt, E. Poddubskaya, S. Antonia, A. Pluzanski, E. E. Vokes, E. Holgado, D. Waterhouse, N. Ready, J. Gainor, O. Aren Frontera, L. Havel, M. Steins, M. C. Garassino, J. G. Aerts, M. Domine, L. Paz-Ares, M. Reck, C. Baudelet, C. T. Harbison, B. Lestini, and D. R. Spigel. 2015. 'Nivolumab versus Docetaxel in Advanced Squamous-Cell Non-Small-Cell Lung Cancer', *N Engl J Med*, 373: 123-35.

Cao, J., G. Wang, H. Cheng, C. Wei, K. Qi, W. Sang, L. Zhenyu, M. Shi, H. Li, J. Qiao, B. Pan, J. Zhao, Q. Wu, L. Zeng, M. Niu, G. Jing, J. Zheng, and K. Xu. 2018. 'Potent anti-leukemia activities of humanized CD19-targeted Chimeric antigen receptor T (CAR-T) cells in patients with relapsed/refractory acute lymphoblastic leukemia', *Am J Hematol*, 93: 851-58.

Cooper, S. L., and P. A. Brown. 2015. 'Treatment of pediatric acute lymphoblastic leukemia', *Pediatr Clin North Am*, 62: 61-73.

Davis, K. L., and C. L. Mackall. 2016. 'Immunotherapy for acute lymphoblastic leukemia: from famine to feast', *Blood Adv*, 1: 265-69.

Eapen, M. 2017. 'Relapsed acute lymphoblastic leukemia: Is it crucial to achieve molecular remission prior to transplant?', *Best Pract Res Clin Haematol*, 30: 317-19.

Escherich, G., M. Schrappe, and U. Creutzig. 2016. 'S1-Leitlinie 025/014: Akute lymphoblastische- (ALL) Leukämie im Kindesalter', Accessed 2018/09/18. https://www.awmf.org/uploads/tx_szleitlinien/025-014l_S1_Akute_lymphoblastische_Leukaemie_ALL_2016-04.pdf.

Feucht, J., S. Kayser, D. Gorodezki, M. Hamieh, M. Doring, F. Blaeschke, P. Schlegel, H. Bosmuller, L. Quintanilla-Fend, M. Ebinger, P. Lang, R. Handgretinger, and T. Feuchtinger. 2016. 'T-cell responses against CD19+ pediatric acute lymphoblastic leukemia mediated by bispecific T-cell engager (BiTE) are regulated contrarily by PD-L1 and CD80/CD86 on leukemic blasts', *Oncotarget*, 7: 76902-19.

Gardner, R. A., O. Finney, C. Annesley, H. Brakke, C. Summers, K. Leger, M. Bleakley, C. Brown, S. Mgebroff, K. S. Kelly-Spratt, V. Hoglund, C. Lindgren, A. P. Oron, D. Li, S. R. Riddell, J. R. Park, and M. C. Jensen. 2017. 'Intent-to-treat leukemia remission by CD19 CAR T cells of defined formulation and dose in children and young adults', *Blood*, 129: 3322-31.

Gardner, R., D. Wu, S. Cherian, M. Fang, L. A. Hanafi, O. Finney, H. Smithers, M. C. Jensen, S. R. Riddell, D. G. Maloney, and C. J. Turtle. 2016. 'Acquisition of a CD19-negative myeloid phenotype allows immune escape of MLL-rearranged B-ALL from CD19 CAR-T-cell therapy', *Blood*, 127: 2406-10.

Ghani, K., S. Cottin, A. Kamen, and M. Caruso. 2007. 'Generation of a high-titer packaging cell line for the production of retroviral vectors in suspension and serum-free media', *Gene Ther*, 14: 1705-11.

Ghani, K., X. Wang, P. O. de Campos-Lima, M. Olszewska, A. Kamen, I. Riviere, and M. Caruso. 2009. 'Efficient human hematopoietic cell transduction using RD114- and GALV-pseudotyped retroviral vectors produced in suspension and serum-free media', *Hum Gene Ther*, 20: 966-74.

Giavridis, T., S. J. C. van der Stegen, J. Eyquem, M. Hamieh, A. Piersigilli, and M. Sadelain. 2018. 'CAR T cell-induced cytokine release syndrome is mediated by macrophages and abated by IL-1 blockade', *Nat Med*, 24: 731-38.

Gomez-Gomez, Y., J. Organista-Nava, M. V. Saavedra-Herrera, A. B. Rivera-Ramirez, M. A. Teran-Porcayo, L. Del Carmen Alarcon-Romero, B. Illades-Aguiar, and M. A. Leyva-Vazquez. 2012. 'Survival and risk of relapse of acute lymphoblastic leukemia in a Mexican population is affected by dihydrofolate reductase gene polymorphisms', *Exp Ther Med*, 3: 665-72.

Gross, G., T. Waks, and Z. Eshhar. 1989. 'Expression of immunoglobulin-T-cell receptor chimeric molecules as functional receptors with antibody-type specificity', *Proc Natl Acad Sci U S A*, 86: 10024-8.

Hunger, S. P., and C. G. Mullighan. 2015. 'Acute Lymphoblastic Leukemia in Children', *N Engl J Med*, 373: 1541-52.

Klebanoff, Christopher A., Tori N. Yamamoto, and Nicholas P. Restifo. 2014. 'Treatment of aggressive lymphomas with anti-CD19 CAR T cells', *Nature Reviews Clinical Oncology*, 11: 685.

Kobold, S., S. Grassmann, M. Chaloupka, C. Lampert, S. Wenk, F. Kraus, M. Rapp, P. Duwell, Y. Zeng, J. C. Schmollinger, M. Schnurr, S. Endres, and S. Rothenfusser. 2015. 'Impact of a New Fusion Receptor on PD-1-Mediated Immunosuppression in Adoptive T Cell Therapy', *J Natl Cancer Inst*, 107.

Kochenderfer, J. N., M. E. Dudley, S. A. Feldman, W. H. Wilson, D. E. Spaner, I. Maric, M. Stetler-Stevenson, G. Q. Phan, M. S. Hughes, R. M. Sherry, J. C. Yang, U. S. Kammula, L. Devillier, R. Carpenter, D. A. Nathan, R. A. Morgan, C. Laurencot, and S. A. Rosenberg. 2012. 'B-cell depletion and remissions of malignancy along with cytokine-associated toxicity in a clinical trial of anti-CD19 chimeric-antigen-receptor-transduced T cells', *Blood*, 119: 2709-20.

Kochenderfer, J. N., S. A. Feldman, Y. Zhao, H. Xu, M. A. Black, R. A. Morgan, W. H. Wilson, and S. A. Rosenberg. 2009. 'Construction and preclinical evaluation of an anti-CD19 chimeric antigen receptor', *J Immunother*, 32: 689-702.

Lee, D. W., J. N. Kochenderfer, M. Stetler-Stevenson, Y. K. Cui, C. Delbrook, S. A. Feldman, T. J. Fry, R. Orentas, M. Sabatino, N. N. Shah, S. M. Steinberg, D. Stroncek, N. Tschernia, C. Yuan, H. Zhang, L. Zhang, S. A. Rosenberg, A. S. Wayne, and C. L. Mackall. 2015. 'T cells expressing CD19 chimeric antigen receptors for acute lymphoblastic leukaemia in children and young adults: a phase 1 dose-escalation trial', *Lancet*, 385: 517-28.

Lenschow, D. J., T. L. Walunas, and J. A. Bluestone. 1996. 'CD28/B7 system of T cell costimulation', *Annu Rev Immunol*, 14: 233-58.

Lesokhin, A. M., M. K. Callahan, M. A. Postow, and J. D. Wolchok. 2015. 'On being less tolerant: enhanced cancer immunosurveillance enabled by targeting checkpoints and agonists of T cell activation', *Sci Transl Med*, 7: 280sr1.

Liang, Y., H. Liu, Z. Lu, W. Lei, C. Zhang, P. Li, A. Liang, K. H. Young, and W. Qian. 2021. 'CD19 CAR-T expressing PD-1/CD28 chimeric switch receptor as a salvage therapy for DLBCL patients treated with different CD19-directed CAR T-cell therapies', *J Hematol Oncol*, 14: 26.

Liu, H., W. Lei, C. Zhang, C. Yang, J. Wei, Q. Guo, X. Guo, Z. Chen, Y. Lu, K. H. Young, Z. Lu, and W. Qian. 2021. 'CD19-specific CAR T Cells that Express a PD-1/CD28 Chimeric Switch-Receptor are Effective in Patients with PD-L1-positive B-Cell Lymphoma', *Clin Cancer Res*, 27: 473-84.

Liu, X., R. Ranganathan, S. Jiang, C. Fang, J. Sun, S. Kim, K. Newick, A. Lo, C. H. June, Y. Zhao, and E. K. Moon. 2016. 'A Chimeric Switch-Receptor Targeting PD1 Augments the Efficacy of Second-Generation CAR T Cells in Advanced Solid Tumors', *Cancer Res*, 76: 1578-90.

Majzner, R. G., S. Heitzeneder, and C. L. Mackall. 2017. 'Harnessing the Immunotherapy Revolution for the Treatment of Childhood Cancers', *Cancer Cell*, 31: 476-85.

Maude, S. L., T. W. Laetsch, J. Buechner, S. Rives, M. Boyer, H. Bittencourt, P. Bader, M. R. Verneris, H. E. Stefanski, G. D. Myers, M. Qayed, B. De Moerloose, H. Hiramatsu, K. Schlis, K. L. Davis, P. L. Martin, E. R. Nemecek, G. A. Yanik, C. Peters, A. Baruchel, N. Boissel, F. Mechinaud, A. Balduzzi, J. Krueger, C. H. June, B. L. Levine, P. Wood, T. Taran, M. Leung, K. T. Mueller, Y. Zhang, K. Sen, D. Lebwohl, M. A. Pulsipher, and S. A. Grupp. 2018. 'Tisagenlecleucel in Children and Young Adults with B-Cell Lymphoblastic Leukemia', *N Engl J Med*, 378: 439-48.

Maude, S. L., D. T. Teachey, D. L. Porter, and S. A. Grupp. 2015. 'CD19-targeted chimeric antigen receptor T-cell therapy for acute lymphoblastic leukemia', *Blood*, 125: 4017-23.

Maus, M. V., S. A. Grupp, D. L. Porter, and C. H. June. 2014. 'Antibody-modified T cells: CARs take the front seat for hematologic malignancies', *Blood*, 123: 2625-35.

Merchant, M. S., M. Wright, K. Baird, L. H. Wexler, C. Rodriguez-Galindo, D. Bernstein, C. Delbrook, M. Lodish, R. Bishop, J. D. Wolchok, H. Streicher, and C. L. Mackall. 2016. 'Phase I Clinical Trial of Ipilimumab in Pediatric Patients with Advanced Solid Tumors', *Clin Cancer Res*, 22: 1364-70.

Neelapu, S. S., S. Tummala, P. Kebriaei, W. Wierda, C. Gutierrez, F. L. Locke, K. V. Komanduri, Y. Lin, N. Jain, N. Daver, J. Westin, A. M. Gulbis, M. E. Loghin, J. F. de Groot, S. Adkins, S. E. Davis, K. Rezvani, P. Hwu, and E. J. Shpall. 2018. 'Chimeric antigen receptor T-cell therapy - assessment and management of toxicities', *Nat Rev Clin Oncol*, 15: 47-62.

Nguyen, K., M. Devidas, S. C. Cheng, M. La, E. A. Raetz, W. L. Carroll, N. J. Winick, S. P. Hunger, P. S. Gaynon, and M. L. Loh. 2008. 'Factors influencing survival after relapse from acute lymphoblastic leukemia: a Children's Oncology Group study', *Leukemia*, 22: 2142-50.

Orlando, Elena J., Xia Han, Catherine Tribouley, Patricia A. Wood, Rebecca J. Leary, Markus Riester, John E. Levine, Muna Qayed, Stephan A. Grupp, Michael Boyer, Barbara De Moerloose, Eneida R. Nemecek, Henrique Bittencourt, Hidefumi Hiramatsu, Jochen Buechner, Stella M. Davies, Michael R. Verneris, Kevin Nguyen, Jennifer L. Brogdon, Hans Bitter, Michael Morrissey, Piotr Pierog, Serafino Pantano, Jeffrey A. Engelman, and Wendy Winckler. 2018. 'Genetic mechanisms of target antigen loss in CAR19 therapy of acute lymphoblastic leukemia', *Nat Med*, 24: 1504-06.

Pardoll, D. M. 2012. 'The blockade of immune checkpoints in cancer immunotherapy', *Nat Rev Cancer*, 12: 252-64.

Park, J. H., M. B. Geyer, and R. J. Brentjens. 2016. 'CD19-targeted CAR T-cell therapeutics for hematologic malignancies: interpreting clinical outcomes to date', *Blood*, 127: 3312-20.

Park, J. H., I. Riviere, M. Gonen, X. Wang, B. Senechal, K. J. Curran, C. Sauter, Y. Wang, B. Santomasso, E. Mead, M. Roshal, P. Maslak, M. Davila, R. J. Brentjens, and M. Sadelain. 2018. 'Long-Term Follow-up of CD19 CAR Therapy in Acute Lymphoblastic Leukemia', *N Engl J Med*, 378: 449-59.

Postow, M. A., J. Chesney, A. C. Pavlick, C. Robert, K. Grossmann, D. McDermott, G. P. Linette, N. Meyer, J. K. Giguere, S. S. Agarwala, M. Shaheen, M. S. Ernstoff, D. Minor, A. K. Salama, M. Taylor, P. A. Ott, L. M. Rollin, C. Horak, P. Gagnier, J. D. Wolchok, and F. S. Hodi. 2015. 'Nivolumab and ipilimumab versus ipilimumab in untreated melanoma', *N Engl J Med*, 372: 2006-17.

Powles, T., J. P. Eder, G. D. Fine, F. S. Braiteh, Y. Loriot, C. Cruz, J. Bellmunt, H. A. Burris, D. P. Petrylak, S. L. Teng, X. Shen, Z. Boyd, P. S. Hegde, D. S. Chen, and N. J. Vogelzang. 2014. 'MPDL3280A (anti-PD-L1) treatment leads to clinical activity in metastatic bladder cancer', *Nature*, 515: 558-62.

Robert, C., J. Schachter, G. V. Long, A. Arance, J. J. Grob, L. Mortier, A. Daud, M. S. Carlino, C. McNeil, M. Lotem, J. Larkin, P. Lorigan, B. Neyns, C. U. Blank, O. Hamid, C. Mateus, R. Shapira-Frommer, M. Kosh, H. Zhou, N. Ibrahim, S. Ebbinghaus, and A. Ribas. 2015. 'Pembrolizumab versus Ipilimumab in Advanced Melanoma', *N Engl J Med*, 372: 2521-32.

Ruella, Marco, Jun Xu, David M. Barrett, Joseph A. Fraietta, Tyler J. Reich, David E. Ambrose, Michael Klichinsky, Olga Shestova, Prachi R. Patel, Irina Kulikovskaya, Farzana Nazimuddin, Vijay G. Bhoj, Elena J. Orlando, Terry J. Fry, Hans Bitter, Shannon L. Maude, Bruce L. Levine, Christopher L. Nobles, Frederic D. Bushman, Regina M. Young, John Scholler, Saar I. Gill, Carl H. June, Stephan A. Grupp, Simon F. Lacey, and J. Joseph Melenhorst. 2018. 'Induction of resistance to chimeric antigen receptor T cell therapy by transduction of a single leukemic B cell', *Nat Med*, 24: 1499-503.

Rupp, L. J., K. Schumann, K. T. Roybal, R. E. Gate, C. J. Ye, W. A. Lim, and A. Marson. 2017. 'CRISPR/Cas9-mediated PD-1 disruption enhances anti-tumor efficacy of human chimeric antigen receptor T cells', *Sci Rep*, 7: 737.

Sadelain, M., R. Brentjens, and I. Riviere. 2013. 'The basic principles of chimeric antigen receptor design', *Cancer Discov*, 3: 388-98.

Schlenker, R., L. F. Olguin-Contreras, M. Leisegang, J. Schnappinger, A. Disovic, S. Ruhland, P. J. Nelson, H. Leonhardt, H. Harz, S. Wilde, D. J. Schendel, W. Uckert, G. Willimsky, and E. Noessner. 2017. 'Chimeric PD-1:28 Receptor Upgrades Low-Avidity T cells and Restores Effector Function of Tumor-Infiltrating Lymphocytes for Adoptive Cell Therapy', *Cancer Res*, 77: 3577-90.

Schrappe, M., S. P. Hunger, C. H. Pui, V. Saha, P. S. Gaynon, A. Baruchel, V. Conter, J. Otten, A. Ohara, A. B. Versluys, G. Escherich, M. Heyman, L. B. Silverman, K. Horibe, G. Mann, B. M. Camitta, J. Harbott, H. Riehm, S. Richards, M. Devidas, and M. Zimmermann. 2012.

'Outcomes after induction failure in childhood acute lymphoblastic leukemia', *N Engl J Med*, 366: 1371-81.

Shimabukuro-Vornhagen, A., P. Godel, M. Subklewe, H. J. Stemmler, H. A. Schlosser, M. Schlaak, M. Kochanek, B. Boll, and M. S. von Bergwelt-Baildon. 2018. 'Cytokine release syndrome', *J Immunother Cancer*, 6: 56.

Singh, B. P., and A. K. Salama. 2016. 'Updates in Therapy for Advanced Melanoma', *Cancers (Basel)*, 8.

Smith, M., D. Arthur, B. Camitta, A. J. Carroll, W. Crist, P. Gaynon, R. Gelber, N. Heerema, E. L. Korn, M. Link, S. Murphy, C. H. Pui, J. Pullen, G. Reamon, S. E. Sallan, H. Sather, J. Shuster, R. Simon, M. Trigg, D. Tubergen, F. Uckun, and R. Ungerleider. 1996. 'Uniform approach to risk classification and treatment assignment for children with acute lymphoblastic leukemia', *J Clin Oncol*, 14: 18-24.

Snyder, A., V. Makarov, T. Merghoub, J. Yuan, J. M. Zaretsky, A. Desrichard, L. A. Walsh, M. A. Postow, P. Wong, T. S. Ho, T. J. Hollmann, C. Bruggeman, K. Kannan, Y. Li, C. Elipenahli, C. Liu, C. T. Harbison, L. Wang, A. Ribas, J. D. Wolchok, and T. A. Chan. 2014. 'Genetic basis for clinical response to CTLA-4 blockade in melanoma', *N Engl J Med*, 371: 2189-99.

Stitz, J., C. J. Buchholz, M. Engelstadter, W. Uckert, U. Bloemer, I. Schmitt, and K. Cichutek. 2000. 'Lentiviral vectors pseudotyped with envelope glycoproteins derived from gibbon ape leukemia virus and murine leukemia virus 10A1', *Virology*, 273: 16-20.

Straathof, K. C., M. A. Pulè, P. Yotnda, G. Dotti, E. F. Vanin, M. K. Brenner, H. E. Heslop, D. M. Spencer, and C. M. Rooney. 2005. 'An inducible caspase 9 safety switch for T-cell therapy', *Blood*, 105: 4247-54.

Terwilliger, T., and M. Abdul-Hay. 2017. 'Acute lymphoblastic leukemia: a comprehensive review and 2017 update', *Blood Cancer J*, 7: e577.

Topalian, S. L., C. G. Drake, and D. M. Pardoll. 2015. 'Immune checkpoint blockade: a common denominator approach to cancer therapy', *Cancer Cell*, 27: 450-61.

Torre, Matthew, Isaac H. Solomon, Claire L. Sutherland, Sarah Nikiforow, Daniel J. DeAngelo, Richard M. Stone, Henrikas Vaitkevicius, Ilene A. Galinsky, Robert F. Padera, Nikolaus Trede, and Sandro Santagata. 2018. 'Neuropathology of a Case With Fatal CAR T-Cell-Associated Cerebral Edema', *Journal of Neuropathology & Experimental Neurology*: nly064-nly64.

Turtle, C. J., L. A. Hanafi, C. Berger, T. A. Gooley, S. Cherian, M. Hudecek, D. Sommermeyer, K. Melville, B. Pender, T. M. Budiarto, E. Robinson, N. N. Steevens, C. Chaney, L. Soma, X. Chen, C. Yeung, B. Wood, D. Li, J. Cao, S. Heimfeld, M. C. Jensen, S. R. Riddell, and D. G. Maloney. 2016. 'CD19 CAR-T cells of defined CD4+:CD8+ composition in adult B cell ALL patients', *J Clin Invest*, 126: 2123-38.

U.S. Food & Drug Administration. 2017. 'FDA approves tisagenlecleucel for B-cell ALL and tocilizumab for cytokine release syndrome', Accessed 2018/07/20. https://www.fda.gov/Drugs/InformationOnDrugs/ApprovedDrugs/ucm574154.htm.

von Stackelberg, A., F. Locatelli, G. Zugmaier, R. Handgretinger, T. M. Trippett, C. Rizzari, P. Bader, M. M. O'Brien, B. Brethon, D. Bhojwani, P. G. Schlegel, A. Borkhardt, S. R. Rheingold, T. M. Cooper, C. M. Zwaan, P. Barnette, C. Messina, G. Michel, S. G. DuBois, K. Hu, M. Zhu, J. A. Whitlock, and L. Gore. 2016. 'Phase I/Phase II Study of Blinatumomab in Pediatric Patients With Relapsed/Refractory Acute Lymphoblastic Leukemia', *J Clin Oncol*, 34: 4381-89.

Wang, X., L. L. Popplewell, J. R. Wagner, A. Naranjo, M. S. Blanchard, M. R. Mott, A. P. Norris, C. W. Wong, R. Z. Urak, W. C. Chang, S. K. Khaled, T. Siddiqi, L. E. Budde, J. Xu, B. Chang, N. Gidwaney, S. H. Thomas, L. J. Cooper, S. R. Riddell, C. E. Brown, M. C. Jensen, and S. J. Forman. 2016. 'Phase 1 studies of central memory-derived CD19 CAR T-cell therapy following autologous HSCT in patients with B-cell NHL', *Blood*, 127: 2980-90.

Wartewig, T., Z. Kurgyis, S. Keppler, K. Pechloff, E. Hameister, R. Ollinger, R. Maresch, T. Buch, K. Steiger, C. Winter, R. Rad, and J. Ruland. 2017. 'PD-1 is a haploinsufficient suppressor of T cell lymphomagenesis', *Nature*, 552: 121-25.

Zhang, L. N., Y. Song, and D. Liu. 2018. 'CD19 CAR-T cell therapy for relapsed/refractory acute lymphoblastic leukemia: factors affecting toxicities and long-term efficacies', *J Hematol Oncol*, 11: 41.

Supplements

Primer Sequences

CAR_ident_forw	GCCAAACATTATTACTACGGTGGTA
CAR_ident_rev	TATGGGAATAAATGGCGGTAAGATG

CAR Sequences

Sequence of 19_3z CAR

CAGCATCGTTCTGTGTTGTCTCTGTCTGACTGTGTTTCTGTATTTGTCTGAAAATTAGCTCGACAAAGTTA
AGTAATAGTCCCTCTCTCCAAGCTCACTTACAGGCGGCCGCGCCGCCACCATGCTTCTCCTGGTGACAA
GCCTTCTGCTCTGTGAGTTACCACACCCAGCATTCCTCCTGATCCCAGACATCCAGATGACACAGACTAC
ATCCTCCCTGTCTGCCTCTCTGGGAGACAGAGTCACCATCAGTTGCAGGGCAAGTCAGGACATTAGTAA
ATATTTAAATTGGTATCAGCAGAAACCAGATGGAACTGTTAAACTCCTGATCTACCATACATCAAGATTA
CACTCAGGAGTCCCATCAAGGTTCAGTGGCAGTGGGTCTGGAACAGATTATTCTCTCACCATTAGCAAC
CTGGAGCAAGAAGATATTGCCACTTACTTTTGCCAACAGGGTAATACGCTTCCGTACACGTTCGGAGGG
GGGACTAAGTTGGAAATAACAGGCTCCACCTCTGGATCCGGCAAGCCCGGATCTGGCGAGGGATCCAC
CAAGGGCGAGGTGAAACTGCAGGAGTCAGGACCTGGCCTGGTGGCGCCCTCACAGAGCCTGTCCGTC
ACATGCACTGTCTCAGGGGTCTCATTACCCGACTATGGTGTAAGCTGGATTCGCCAGCCTCCACGAAAG
GGTCTGGAGTGGCTGGGAGTAATATGGGGTAGTGAAACCACATACTATAATTCAGCTCTCAAATCCAG
ACTGACCATCATCAAGGACAACTCCAAGAGCCAAGTTTTCTTAAAAATGAACAGTCTGCAAACTGATGA
CACAGCCATTTACTACTGTGCCAAACATTATTACTACGGTGGTAGCTATGCTATGGACTACTGGGGTCA
AGGAACCTCAGTCACCGTCTCCTCAGAGCAAAAGCTCATTTCTGAAGAGGACTTGTTCGTGCCGGTCTT
CCTGCCAGCGAAGCCCACCACGACGCCAGCGCCGCGACCACCAACACCGGCGCCCACCATCGCGTCGC
AGCCCCTGTCCCTGCGCCCAGAGGCGTGCCGGCCAGCGGCGGGGGGCGCAGTGCACACGAGGGGGCT
GGACTTCGCCTGTGATATCTACATCTGGGCGCCCTTGGCCGGGACTTGTGGGGTCCTTCTCCTGTCACT
GGTTATCACCCTTTACTGCAACCACAGGAACAGAGTGAAGTTCAGCAGGAGCGCAGACGCCCCCGCGT
ACCAGCAGGGCCAGAACCAGCTCTATAACGAGCTCAATCTAGGACGAAGAGAGGAGTACGATGTTTTG
GACAAGAGACGTGGCCGGGACCCTGAGATGGGGGGAAAGCCGAGAAGGAAGAACCCTCAGGAAGGC
CTGTACAATGAACTGCAGAAAGATAAGATGGCGGAGGCCTACAGTGAGATTGGGATGAAAGGCGAGC

GCCGGAGGGGCAAGGGGCACGATGGCCTTTACCAGGGTCTCAGTACAGCCACCAAGGACACCTACGA
CGCCCTTCACATGCAGGCCCTGCCCCCTCGCTAAGAATTCGAGCATCTTACCGCCATTTATTCCCATATTT
GTTCTGTTTTTCTTGATTTGGGTATACATTTAAATGCATTTAAATGTATACCCAAATCAAGAAAAACAGA
ACAAATATGGGAATAAATGGCGGTAAGATGCTCGAATTCTTAGCGAGGGGGCAGGGCCTGCATGTGA
AGGGCGTCGTAGGTGTCCTTGGTGGCTGTACTGAGACCCTGGTAAAGGCCATCGTGCCCCTTGCCCCTC
CGGCGCTCGCCTTTCATCCCAATCTCACTGTAGGCCTCCGCCATCTTATCTTTCTGCAGTTCATTGTACAG
GCCTTCCTGAGGGTTCTTCCTTCTCGGCTTTCCCCCCATCTCAGGGTCCCGGCCACGTCTCTTGTCCAAAA
CATCGTACTCCTCTCTTCGTCCTAGATTGAGCTCGTTATAGAGCTGGTTCTGGCCCTGCTGGTACGCGGG
GGCGTCTGCGCTCCTGCTGAACTTCACTCTGTTCCTGTGGTTGCAGTAAAGGGTGATAACCAGTGACAG
GAGAAGGACCCCACAAGTCCCGGCCAAGGGCGCCCAGATGTAGATATCACAGGCGAAGTCCAGCCCC
CTCGTGTGCACTGCGCCCCCCGCCGCTGGCCGGCACGCCTCTGGGCGCAGGGACAGGGGCTGCGACG
CGATGGTGGGCGCCGGTGTTGGTGGTCGCGGCGCTGGCGTCGTGGTGGGCTTCGCTGGCAGGAAGAC
CGGCACGAACAAGTCCTCTTCAGAAATGAGCTTTTGCTCTGAGGAGACGGTGACTGAGGTTCCTTGACC
CCAGTAGTCCATAGCATAGCTACCACCGTAGTAATAATGTTTGGCACAGTAGTAAATGGCTGTGTCATC
AGTTTGCAGACTGTTCATTTTTAAGAAAACTTGGCTCTTGGAGTTGTCCTTGATGATGGTCAGTCTGGAT
TTGAGAGCTGAATTATAGTATGTGGTTTCACTACCCCATATTACTCCCAGCCACTCCAGACCCTTTCGTG
GAGGCTGGCGAATCCAGCTTACACCATAGTCGGGTAATGAGACCCCTGAGACAGTGCATGTGACGGAC
AGGCTCTGTGAGGGCGCCACCAGGCCAGGTCCTGACTCCTGCAGTTTCACCTCGCCCTTGGTGGATCCC
TCGCCAGATCCGGGCTTGCCGGATCCAGAGGTGGAGCCTGTTATTTCCAACTTAGTCCCCCCTCCGAAC
GTGTACGGAAGCGTATTACCCTGTTGGCAAAAGTAAGTGGCAATATCTTCTTGCTCCAGGTTGCTAATG
GTGAGAGAATAATCTGTTCCAGACCCACTGCCACTGAACCTTGATGGGACTCCTGAGTGTAATCTTGAT
GTATGGTAGATCAGGAGTTTAACAGTTCCATCTGGTTTCTGCTGATACCAATTTAAATATTTACTAATGT
CCTGACTTGCCCTGCAACTGATGGTGACTCTGTCTCCCAGAGAGGCAGACAGGGAGGATGTAGTCTGT
GTCATCTGGATGTCTGGGATCAGGAGGAATGCTGGGTGTGGTAACTCACAGAGCAGAAGGCTTGTCAC
CAGGAGAAGCATGGTGGCGGCGCGGCCGCCTGTAAGTGAGCTTGGAGAGAGGGACTATTACTTAACT
TTGTCGAGCTAATTTTCAGACAAATACAGAAACACAGTCAGACAGAGACAACACAGAACGATGCTG

Sequence of 19_BB_3z CAR

CAGCATCGTTCTGTGTTGTCTCTGTCTGACTGTGTTTCTGTATTTGTCTGAAAATTAGCTCGACAAAGTTA
AGTAATAGTCCCTCTCTCCAAGCTCACTTACAGGCGGCCGCGCCGCCACCATGCTTCTCCTGGTGACAA
GCCTTCTGCTCTGTGAGTTACCACACCCAGCATTCCTCCTGATCCCAGACATCCAGATGACACAGACTAC
ATCCTCCCTGTCTGCCTCTCTGGGAGACAGAGTCACCATCAGTTGCAGGGCAAGTCAGGACATTAGTAA

ATATTTAAATTGGTATCAGCAGAAACCAGATGGAACTGTTAAACTCCTGATCTACCATACATCAAGATTA
CACTCAGGAGTCCCATCAAGGTTCAGTGGCAGTGGGTCTGGAACAGATTATTCTCTCACCATTAGCAAC
CTGGAGCAAGAAGATATTGCCACTTACTTTTGCCAACAGGGTAATACGCTTCCGTACACGTTCGGAGGG
GGGACTAAGTTGGAAATAACAGGCTCCACCTCTGGATCCGGCAAGCCCGGATCTGGCGAGGGATCCAC
CAAGGGCGAGGTGAAACTGCAGGAGTCAGGACCTGGCCTGGTGGCGCCCTCACAGAGCCTGTCCGTC
ACATGCACTGTCTCAGGGGTCTCATTACCCGACTATGGTGTAAGCTGGATTCGCCAGCCTCCACGAAAG
GGTCTGGAGTGGCTGGGAGTAATATGGGGTAGTGAAACCACATACTATAATTCAGCTCTCAAATCCAG
ACTGACCATCATCAAGGACAACTCCAAGAGCCAAGTTTTCTTAAAAATGAACAGTCTGCAAACTGATGA
CACAGCCATTTACTACTGTGCCAAACATTATTACTACGGTGGTAGCTATGCTATGGACTACTGGGGTCA
AGGAACCTCAGTCACCGTCTCCTCAGAGCAAAAGCTCATTTCTGAAGAGGACTTGTTCGTGCCGGTCTT
CCTGCCAGCGAAGCCCACCACGACGCCAGCGCCGCGACCACCAACACCGGCGCCCACCATCGCGTCGC
AGCCCCTGTCCCTGCGCCCAGAGGCGTGCCGGCCAGCGGCGGGGGGCGCAGTGCACACGAGGGGGCT
GGACTTCGCCTGTGATATCTACATCTGGGCGCCCTTGGCCGGGACTTGTGGGGTCCTTCTCCTGTCACT
GGTTATCACCCTTTACTGCAACCACAGGAACAAACGGGGCAGAAAGAAACTCCTGTATATATTCAAACA
ACCATTTATGAGACCAGTACAAACTACTCAAGAGGAAGATGGCTGTAGCTGCCGATTTCCAGAAGAAG
AAGAAGGAGGATGTGAACTGAGAGTGAAGTTCAGCAGGAGCGCAGACGCCCCCGCGTACCAGCAGG
GCCAGAACCAGCTCTATAACGAGCTCAATCTAGGACGAAGAGAGGAGTACGATGTTTTGGACAAGAG
ACGTGGCCGGGACCCTGAGATGGGGGGAAAGCCGAGAAGGAAGAACCCTCAGGAAGGCCTGTACAA
TGAACTGCAGAAAGATAAGATGGCGGAGGCCTACAGTGAGATTGGGATGAAAGGCGAGCGCCGGAG
GGGCAAGGGGCACGATGGCCTTTACCAGGGTCTCAGTACAGCCACCAAGGACACCTACGACGCCCTTC
ACATGCAGGCCCTGCCCCCTCGCTAAGAATTCGAGCATCTTACCGCCATTTATTCCCATATTTGTTCTGTT
TTTCTTGATTTGGGTATACATTTAAATGCATTTAAATGTATACCCAAATCAAGAAAAACAGAACAAATAT
GGGAATAAATGGCGGTAAGATGCTCGAATTCTTAGCGAGGGGGCAGGGCCTGCATGTGAAGGGCGTC
GTAGGTGTCCTTGGTGGCTGTACTGAGACCCTGGTAAAGGCCATCGTGCCCCTTGCCCCTCCGGCGCTC
GCCTTTCATCCCAATCTCACTGTAGGCCTCCGCCATCTTATCTTTCTGCAGTTCATTGTACAGGCCTTCCT
GAGGGTTCTTCCTTCTCGGCTTTCCCCCCATCTCAGGGTCCCGGCCACGTCTCTTGTCCAAAACATCGTA
CTCCTCTCTTCGTCCTAGATTGAGCTCGTTATAGAGCTGGTTCTGGCCCTGCTGGTACGCGGGGGCGTC
TGCGCTCCTGCTGAACTTCACTCTCAGTTCACATCCTCCTTCTTCTTCTTCTGGAAATCGGCAGCTACAGC
CATCTTCCTCTTGAGTAGTTTGTACTGGTCTCATAAATGGTTGTTTGAATATATACAGGAGTTTCTTTCTG
CCCCGTTTGTTCCTGTGGTTGCAGTAAAGGGTGATAACCAGTGACAGGAGAAGGACCCCACAAGTCCC
GGCCAAGGGCGCCCAGATGTAGATATCACAGGCGAAGTCCAGCCCCCTCGTGTGCACTGCGCCCCCCG
CCGCTGGCCGGCACGCCTCTGGGCGCAGGGACAGGGGCTGCGACGCGATGGTGGGCGCCGGTGTTG
GTGGTCGCGGCGCTGGCGTCGTGGTGGGCTTCGCTGGCAGGAAGACCGGCACGAACAAGTCCTCTTC
AGAAATGAGCTTTTGCTCTGAGGAGACGGTGACTGAGGTTCCTTGACCCCAGTAGTCCATAGCATAGCT
ACCACCGTAGTAATAATGTTTGGCACAGTAGTAAATGGCTGTGTCATCAGTTTGCAGACTGTTCATTTTT

AAGAAAACTTGGCTCTTGGAGTTGTCCTTGATGATGGTCAGTCTGGATTTGAGAGCTGAATTATAGTAT
GTGGTTTCACTACCCCATATTACTCCCAGCCACTCCAGACCCTTTCGTGGAGGCTGGCGAATCCAGCTTA
CACCATAGTCGGGTAATGAGACCCCTGAGACAGTGCATGTGACGGACAGGCTCTGTGAGGGCGCCACC
AGGCCAGGTCCTGACTCCTGCAGTTTCACCTCGCCCTTGGTGGATCCCTCGCCAGATCCGGGCTTGCCG
GATCCAGAGGTGGAGCCTGTTATTTCCAACTTAGTCCCCCCTCCGAACGTGTACGGAAGCGTATTACCC
TGTTGGCAAAAGTAAGTGGCAATATCTTCTTGCTCCAGGTTGCTAATGGTGAGAGAATAATCTGTTCCA
GACCCACTGCCACTGAACCTTGATGGGACTCCTGAGTGTAATCTTGATGTATGGTAGATCAGGAGTTTA
ACAGTTCCATCTGGTTTCTGCTGATACCAATTTAAATATTTACTAATGTCCTGACTTGCCCTGCAACTGAT
GGTGACTCTGTCTCCCAGAGAGGCAGACAGGGAGGATGTAGTCTGTGTCATCTGGATGTCTGGGATCA
GGAGGAATGCTGGGTGTGGTAACTCACAGAGCAGAAGGCTTGTCACCAGGAGAAGCATGGTGGCGGC
GCGGCCGCCTGTAAGTGAGCTTGGAGAGAGGGACTATTACTTAACTTTGTCGAGCTAATTTTCAGACAA
ATACAGAAACACAGTCAGACAGAGACAACACAGAACGATGCTG

Sequence of 19_3z_PD-1_28 CAR

CAGCATCGTTCTGTGTTGTCTCTGTCTGACTGTGTTTCTGTATTTGTCTGAAAATTAGCTCGACAAAGTTA
AGTAATAGTCCCTCTCTCCAAGCTCACTTACAGGCGGCCGCGCCGCCACCATGCTTCTCCTGGTGACAA
GCCTTCTGCTCTGTGAGTTACCACACCCAGCATTCCTCCTGATCCCAGACATCCAGATGACACAGACTAC
ATCCTCCCTGTCTGCCTCTCTGGGAGACAGAGTCACCATCAGTTGCAGGGCAAGTCAGGACATTAGTAA
ATATTTAAATTGGTATCAGCAGAAACCAGATGGAACTGTTAAACTCCTGATCTACCATACATCAAGATTA
CACTCAGGAGTCCCATCAAGGTTCAGTGGCAGTGGGTCTGGAACAGATTATTCTCTCACCATTAGCAAC
CTGGAGCAAGAAGATATTGCCACTTACTTTTGCCAACAGGGTAATACGCTTCCGTACACGTTCGGAGGG
GGGACTAAGTTGGAAATAACAGGCTCCACCTCTGGATCCGGCAAGCCCGGATCTGGCGAGGGATCCAC
CAAGGGCGAGGTGAAACTGCAGGAGTCAGGACCTGGCCTGGTGGCGCCCTCACAGAGCCTGTCCGTC
ACATGCACTGTCTCAGGGGTCTCATTACCCGACTATGGTGTAAGCTGGATTCGCCAGCCTCCACGAAAG
GGTCTGGAGTGGCTGGGAGTAATATGGGGTAGTGAAACCACATACTATAATTCAGCTCTCAAATCCAG
ACTGACCATCATCAAGGACAACTCCAAGAGCCAAGTTTTCTTAAAAATGAACAGTCTGCAAACTGATGA
CACAGCCATTTACTACTGTGCCAAACATTATTACTACGGTGGTAGCTATGCTATGGACTACTGGGGTCA
AGGAACCTCAGTCACCGTCTCCTCAGAGCAAAAGCTCATTTCTGAAGAGGACTTGTTCGTGCCGGTCTT
CCTGCCAGCGAAGCCCACCACGACGCCAGCGCCGCGACCACCAACACCGGCGCCCACCATCGCGTCGC
AGCCCCTGTCCCTGCGCCCAGAGGCGTGCCGGCCAGCGGCGGGGGGCGCAGTGCACACGAGGGGGCT
GGACTTCGCCTGTGATATCTACATCTGGGCGCCCTTGGCCGGGACTTGTGGGGTCCTTCTCCTGTCACT
GGTTATCACCCTTTACTGCAACCACAGGAACAGAGTGAAGTTCAGCAGGAGCGCAGACGCCCCCGCGT

ACCAGCAGGGCCAGAACCAGCTCTATAACGAGCTCAATCTAGGACGAAGAGAGGAGTACGATGTTTTG
GACAAGAGACGTGGCCGGGACCCTGAGATGGGGGGAAAGCCGAGAAGGAAGAACCCTCAGGAAGGC
CTGTACAATGAACTGCAGAAAGATAAGATGGCGGAGGCCTACAGTGAGATTGGGATGAAAGGCGAGC
GCCGGAGGGGCAAGGGGCACGATGGCCTTTACCAGGGTCTCAGTACAGCCACCAAGGACACCTACGA
CGCCCTTCACATGCAGGCCCTGCCCCCTCGCGTGAAACAGACTTTGAATTTTGACCTTCTCAAGTTGGCG
GGAGACGTGGAGTCCAACCCAGGCCCGCAGATCCCACAGGCGCCCTGGCCAGTCGTCTGGGCGGTGC
TACAACTGGGCTGGCGGCCAGGATGGTTCTTAGACTCCCCAGACAGGCCCTGGAACCCCCCCACCTTCT
CCCCAGCCCTGCTCGTGGTGACCGAAGGGGACAACGCCACCTTCACCTGCAGCTTCTCCAACACATCGG
AGAGCTTCGTGCTAAACTGGTACCGCATGAGCCCCAGCAACCAGACGGACAAGCTGGCCGCCTTCCCC
GAGGACCGCAGCCAGCCCGGCCAGGACTGCCGCTTCCGTGTCACACAACTGCCCAACGGGCGTGACTT
CCACATGAGCGTGGTCAGGGCCCGGCGCAATGACAGCGGCACCTACCTCTGTGGGGCCATCTCCCTGG
CCCCCAAGGCGCAGATCAAAGAGAGCCTGCGGGCAGAGCTCAGGGTGACAGAGAGAAGGGCAGAAG
TGCCCACAGCCCACCCCAGCCCCTCACCCAGGCCAGCCGGCCAGTTCCAAACCCTGGTGGTTGGTGTCG
TGGGCGGCCTGCTGGGCAGCCTGGTGCTGCTAGTCTGGGTCCTGGCCGTCATCAGGAGTAAGAGGAG
CAGGCTCCTGCACAGTGACTACATGAACATGACTCCCCGCCGCCCCGGGCCCACCCGCAAGCATTACCA
GCCCTATGCCCCACCACGCGACTTCGCAGCCTATCGCTCCTGAGAATTCGAGCATCTTACCGCCATTTAT
TCCCATATTTGTTCTGTTTTTCTTGATTTGGGTATACATTTAAATGCATTTAAATGTATACCCAAATCAAG
AAAAACAGAACAAATATGGGAATAAATGGCGGTAAGATGCTCGAATTCTCAGGAGCGATAGGCTGCG
AAGTCGCGTGGTGGGGCATAGGGCTGGTAATGCTTGCGGGTGGGCCCGGGGCGGCGGGGAGTCATG
TTCATGTAGTCACTGTGCAGGAGCCTGCTCCTCTTACTCCTGATGACGGCCAGGACCCAGACTAGCAGC
ACCAGGCTGCCCAGCAGGCCGCCCACGACACCAACCACCAGGGTTTGGAACTGGCCGGCTGGCCTGG
GTGAGGGGCTGGGGTGGGCTGTGGGCACTTCTGCCCTTCTCTCTGTCACCCTGAGCTCTGCCCGCAGG
CTCTCTTTGATCTGCGCCTTGGGGGCCAGGGAGATGGCCCCACAGAGGTAGGTGCCGCTGTCATTGCG
CCGGGCCCTGACCACGCTCATGTGGAAGTCACGCCCGTTGGGCAGTTGTGTGACACGGAAGCGGCAGT
CCTGGCCGGGCTGGCTGCGGTCCTCGGGGAAGGCGGCCAGCTTGTCCGTCTGGTTGCTGGGGCTCATG
CGGTACCAGTTTAGCACGAAGCTCTCCGATGTGTTGGAGAAGCTGCAGGTGAAGGTGGCGTTGTCCCC
TTCGGTCACCACGAGCAGGGCTGGGGAGAAGGTGGGGGGGTTCCAGGGCCTGTCTGGGGAGTCTAA
GAACCATCCTGGCCGCCAGCCCAGTTGTAGCACCGCCCAGACGACTGGCCAGGGCGCCTGTGGGATCT
GCGGGCCTGGGTTGGACTCCACGTCTCCCGCCAACTTGAGAAGGTCAAAATTCAAAGTCTGTTTCACGC
GAGGGGGCAGGGCCTGCATGTGAAGGGCGTCGTAGGTGTCCTTGGTGGCTGTACTGAGACCCTGGTA
AAGGCCATCGTGCCCCTTGCCCCTCCGGCGCTCGCCTTTCATCCCAATCTCACTGTAGGCCTCCGCCATC
TTATCTTTCTGCAGTTCATTGTACAGGCCTTCCTGAGGGTTCTTCCTTCTCGGCTTTCCCCCCATCTCAGG
GTCCCGGCCACGTCTCTTGTCCAAAACATCGTACTCCTCTCTTCGTCCTAGATTGAGCTCGTTATAGAGC
TGGTTCTGGCCCTGCTGGTACGCGGGGGCGTCTGCGCTCCTGCTGAACTTCACTCTGTTCCTGTGGTTG
CAGTAAAGGGTGATAACCAGTGACAGGAGAAGGACCCCACAAGTCCCGGCCAAGGGCGCCCAGATGT

AGATATCACAGGCGAAGTCCAGCCCCCTCGTGTGCACTGCGCCCCCCGCCGCTGGCCGGCACGCCTCTG
GGCGCAGGGACAGGGGCTGCGACGCGATGGTGGGCGCCGGTGTTGGTGGTCGCGGCGCTGGCGTCG
TGGTGGGCTTCGCTGGCAGGAAGACCGGCACGAACAAGTCCTCTTCAGAAATGAGCTTTTGCTCTGAG
GAGACGGTGACTGAGGTTCCTTGACCCCAGTAGTCCATAGCATAGCTACCACCGTAGTAATAATGTTTG
GCACAGTAGTAAATGGCTGTGTCATCAGTTTGCAGACTGTTCATTTTTAAGAAAACTTGGCTCTTGGAG
TTGTCCTTGATGATGGTCAGTCTGGATTTGAGAGCTGAATTATAGTATGTGGTTTCACTACCCCATATTA
CTCCCAGCCACTCCAGACCCTTTCGTGGAGGCTGGCGAATCCAGCTTACACCATAGTCGGGTAATGAGA
CCCCTGAGACAGTGCATGTGACGGACAGGCTCTGTGAGGGCGCCACCAGGCCAGGTCCTGACTCCTGC
AGTTTCACCTCGCCCTTGGTGGATCCCTCGCCAGATCCGGGCTTGCCGGATCCAGAGGTGGAGCCTGTT
ATTTCCAACTTAGTCCCCCCTCCGAACGTGTACGGAAGCGTATTACCCTGTTGGCAAAAGTAAGTGGCA
ATATCTTCTTGCTCCAGGTTGCTAATGGTGAGAGAATAATCTGTTCCAGACCCACTGCCACTGAACCTTG
ATGGGACTCCTGAGTGTAATCTTGATGTATGGTAGATCAGGAGTTTAACAGTTCCATCTGGTTTCTGCT
GATACCAATTTAAATATTTACTAATGTCCTGACTTGCCCTGCAACTGATGGTGACTCTGTCTCCCAGAGA
GGCAGACAGGGAGGATGTAGTCTGTGTCATCTGGATGTCTGGGATCAGGAGGAATGCTGGGTGTGGT
AACTCACAGAGCAGAAGGCTTGTCACCAGGAGAAGCATGGTGGCGGCGCGGCCGCCTGTAAGTGAGC
TTGGAGAGAGGGACTATTACTTAACTTTGTCGAGCTAATTTTCAGACAAATACAGAAACACAGTCAGAC
AGAGACAACACAGAACGATGCTG

Sequence of 19_BB_3z_PD-1_28 CAR

CAGCATCGTTCTGTGTTGTCTCTGTCTGACTGTGTTTCTGTATTTGTCTGAAAATTAGCTCGACAAAGTTA
AGTAATAGTCCCTCTCTCCAAGCTCACTTACAGGCGGCCGCGCCGCCACCATGCTTCTCCTGGTGACAA
GCCTTCTGCTCTGTGAGTTACCACACCCAGCATTCCTCCTGATCCCAGACATCCAGATGACACAGACTAC
ATCCTCCCTGTCTGCCTCTCTGGGAGACAGAGTCACCATCAGTTGCAGGGCAAGTCAGGACATTAGTAA
ATATTTAAATTGGTATCAGCAGAAACCAGATGGAACTGTTAAACTCCTGATCTACCATACATCAAGATTA
CACTCAGGAGTCCCATCAAGGTTCAGTGGCAGTGGGTCTGGAACAGATTATTCTCTCACCATTAGCAAC
CTGGAGCAAGAAGATATTGCCACTTACTTTTGCCAACAGGGTAATACGCTTCCGTACACGTTCGGAGGG
GGGACTAAGTTGGAAATAACAGGCTCCACCTCTGGATCCGGCAAGCCCGGATCTGGCGAGGGATCCAC
CAAGGGCGAGGTGAAACTGCAGGAGTCAGGACCTGGCCTGGTGGCGCCCTCACAGAGCCTGTCCGTC
ACATGCACTGTCTCAGGGGTCTCATTACCCGACTATGGTGTAAGCTGGATTCGCCAGCCTCCACGAAAG
GGTCTGGAGTGGCTGGGAGTAATATGGGGTAGTGAAACCACATACTATAATTCAGCTCTCAAATCCAG
ACTGACCATCATCAAGGACAACTCCAAGAGCCAAGTTTTCTTAAAAATGAACAGTCTGCAAACTGATGA
CACAGCCATTTACTACTGTGCCAAACATTATTACTACGGTGGTAGCTATGCTATGGACTACTGGGGTCA

AGGAACCTCAGTCACCGTCTCCTCAGAGCAAAAGCTCATTTCTGAAGAGGACTTGTTCGTGCCGGTCTT
CCTGCCAGCGAAGCCCACCACGACGCCAGCGCCGCGACCACCAACACCGGCGCCCACCATCGCGTCGC
AGCCCCTGTCCCTGCGCCCAGAGGCGTGCCGGCCAGCGGCGGGGGGCGCAGTGCACACGAGGGGGCT
GGACTTCGCCTGTGATATCTACATCTGGGCGCCCTTGGCCGGGACTTGTGGGGTCCTTCTCCTGTCACT
GGTTATCACCCTTTACTGCAACCACAGGAACAAACGGGGCAGAAAGAAACTCCTGTATATATTCAAACA
ACCATTTATGAGACCAGTACAAACTACTCAAGAGGAAGATGGCTGTAGCTGCCGATTTCCAGAAGAAG
AAGAAGGAGGATGTGAACTGAGAGTGAAGTTCAGCAGGAGCGCAGACGCCCCCGCGTACCAGCAGG
GCCAGAACCAGCTCTATAACGAGCTCAATCTAGGACGAAGAGAGGAGTACGATGTTTTGGACAAGAG
ACGTGGCCGGGACCCTGAGATGGGGGGAAAGCCGAGAAGGAAGAACCCTCAGGAAGGCCTGTACAA
TGAACTGCAGAAAGATAAGATGGCGGAGGCCTACAGTGAGATTGGGATGAAAGGCGAGCGCCGGAG
GGGCAAGGGGCACGATGGCCTTTACCAGGGTCTCAGTACAGCCACCAAGGACACCTACGACGCCCTTC
ACATGCAGGCCCTGCCCCCTCGCGTGAAACAGACTTTGAATTTTGACCTTCTCAAGTTGGCGGGAGACG
TGGAGTCCAACCCAGGCCCGCAGATCCCACAGGCGCCCTGGCCAGTCGTCTGGGCGGTGCTACAACTG
GGCTGGCGGCCAGGATGGTTCTTAGACTCCCCAGACAGGCCCTGGAACCCCCCCACCTTCTCCCCAGCC
CTGCTCGTGGTGACCGAAGGGGACAACGCCACCTTCACCTGCAGCTTCTCCAACACATCGGAGAGCTTC
GTGCTAAACTGGTACCGCATGAGCCCCAGCAACCAGACGGACAAGCTGGCCGCCTTCCCCGAGGACCG
CAGCCAGCCCGGCCAGGACTGCCGCTTCCGTGTCACACAACTGCCCAACGGGCGTGACTTCCACATGA
GCGTGGTCAGGGCCCGGCGCAATGACAGCGGCACCTACCTCTGTGGGGCCATCTCCCTGGCCCCCAAG
GCGCAGATCAAAGAGAGCCTGCGGGCAGAGCTCAGGGTGACAGAGAGAAGGGCAGAAGTGCCCACA
GCCCACCCCAGCCCCTCACCCAGGCCAGCCGGCCAGTTCCAAACCCTGGTGGTTGGTGTCGTGGGCGG
CCTGCTGGGCAGCCTGGTGCTGCTAGTCTGGGTCCTGGCCGTCATCAGGAGTAAGAGGAGCAGGCTCC
TGCACAGTGACTACATGAACATGACTCCCCGCCGCCCCGGGCCCACCCGCAAGCATTACCAGCCCTATG
CCCCACCACGCGACTTCGCAGCCTATCGCTCCTGAGAATTCGAGCATCTTACCGCCATTTATTCCCATATT
TGTTCTGTTTTTCTTGATTTGGGTATACATTTAAATGCATTTAAATGTATACCCAAATCAAGAAAAACAG
AACAAATATGGGAATAAATGGCGGTAAGATGCTCGAATTCTCAGGAGCGATAGGCTGCGAAGTCGCG
TGGTGGGGCATAGGGCTGGTAATGCTTGCGGGTGGGCCCGGGGCGGCGGGGAGTCATGTTCATGTAG
TCACTGTGCAGGAGCCTGCTCCTCTTACTCCTGATGACGGCCAGGACCCAGACTAGCAGCACCAGGCTG
CCCAGCAGGCCGCCCACGACACCAACCACCAGGGTTTGGAACTGGCCGGCTGGCCTGGGTGAGGGGC
TGGGGTGGGCTGTGGGCACTTCTGCCCTTCTCTCTGTCACCCTGAGCTCTGCCCGCAGGCTCTCTTTGAT
CTGCGCCTTGGGGGCCAGGGAGATGGCCCCACAGAGGTAGGTGCCGCTGTCATTGCGCCGGGCCCTG
ACCACGCTCATGTGGAAGTCACGCCCGTTGGGCAGTTGTGTGACACGGAAGCGGCAGTCCTGGCCGG
GCTGGCTGCGGTCCTCGGGGAAGGCGGCCAGCTTGTCCGTCTGGTTGCTGGGGCTCATGCGGTACCAG
TTTAGCACGAAGCTCTCCGATGTGTTGGAGAAGCTGCAGGTGAAGGTGGCGTTGTCCCCTTCGGTCAC
CACGAGCAGGGCTGGGGAGAAGGTGGGGGGGTTCCAGGGCCTGTCTGGGGAGTCTAAGAACCATCCT
GGCCGCCAGCCCAGTTGTAGCACCGCCCAGACGACTGGCCAGGGCGCCTGTGGGATCTGCGGGCCTG

GGTTGGACTCCACGTCTCCCGCCAACTTGAGAAGGTCAAAATTCAAAGTCTGTTTCACGCGAGGGGGC
AGGGCCTGCATGTGAAGGGCGTCGTAGGTGTCCTTGGTGGCTGTACTGAGACCCTGGTAAAGGCCATC
GTGCCCCTTGCCCCTCCGGCGCTCGCCTTTCATCCCAATCTCACTGTAGGCCTCCGCCATCTTATCTTTCT
GCAGTTCATTGTACAGGCCTTCCTGAGGGTTCTTCCTTCTCGGCTTTCCCCCCATCTCAGGGTCCCGGCC
ACGTCTCTTGTCCAAAACATCGTACTCCTCTCTTCGTCCTAGATTGAGCTCGTTATAGAGCTGGTTCTGG
CCCTGCTGGTACGCGGGGGCGTCTGCGCTCCTGCTGAACTTCACTCTCAGTTCACATCCTCCTTCTTCTTC
TTCTGGAAATCGGCAGCTACAGCCATCTTCCTCTTGAGTAGTTTGTACTGGTCTCATAAATGGTTGTTTG
AATATATACAGGAGTTTCTTTCTGCCCCGTTTGTTCCTGTGGTTGCAGTAAAGGGTGATAACCAGTGAC
AGGAGAAGGACCCCACAAGTCCCGGCCAAGGGCGCCCAGATGTAGATATCACAGGCGAAGTCCAGCC
CCCTCGTGTGCACTGCGCCCCCCGCCGCTGGCCGGCACGCCTCTGGGCGCAGGGACAGGGGCTGCGAC
GCGATGGTGGGCGCCGGTGTTGGTGGTCGCGGCGCTGGCGTCGTGGTGGGCTTCGCTGGCAGGAAGA
CCGGCACGAACAAGTCCTCTTCAGAAATGAGCTTTTGCTCTGAGGAGACGGTGACTGAGGTTCCTTGAC
CCCAGTAGTCCATAGCATAGCTACCACCGTAGTAATAATGTTTGGCACAGTAGTAAATGGCTGTGTCAT
CAGTTTGCAGACTGTTCATTTTTAAGAAAACTTGGCTCTTGGAGTTGTCCTTGATGATGGTCAGTCTGGA
TTTGAGAGCTGAATTATAGTATGTGGTTTCACTACCCCATATTACTCCCAGCCACTCCAGACCCTTTCGT
GGAGGCTGGCGAATCCAGCTTACACCATAGTCGGGTAATGAGACCCCTGAGACAGTGCATGTGACGG
ACAGGCTCTGTGAGGGCGCCACCAGGCCAGGTCCTGACTCCTGCAGTTTCACCTCGCCCTTGGTGGATC
CCTCGCCAGATCCGGGCTTGCCGGATCCAGAGGTGGAGCCTGTTATTTCCAACTTAGTCCCCCCTCCGA
ACGTGTACGGAAGCGTATTACCCTGTTGGCAAAAGTAAGTGGCAATATCTTCTTGCTCCAGGTTGCTAA
TGGTGAGAGAATAATCTGTTCCAGACCCACTGCCACTGAACCTTGATGGGACTCCTGAGTGTAATCTTG
ATGTATGGTAGATCAGGAGTTTAACAGTTCCATCTGGTTTCTGCTGATACCAATTTAAATATTTACTAAT
GTCCTGACTTGCCCTGCAACTGATGGTGACTCTGTCTCCCAGAGAGGCAGACAGGGAGGATGTAGTCT
GTGTCATCTGGATGTCTGGGATCAGGAGGAATGCTGGGTGTGGTAACTCACAGAGCAGAAGGCTTGTC
ACCAGGAGAAGCATGGTGGCGGCGCGGCCGCCTGTAAGTGAGCTTGGAGAGAGGGACTATTACTTAA
CTTTGTCGAGCTAATTTTCAGACAAATACAGAAACACAGTCAGACAGAGACAACACAGAACGATGCTG

Sequence of 19t CAR

CAGCATCGTTCTGTGTTGTCTCTGTCTGACTGTGTTTCTGTATTTGTCTGAAAATTAGCTCGACAAAGTTA
AGTAATAGTCCCTCTCTCCAAGCTCACTTACAGGCGGCCGCGCCGCCACCATGCTTCTCCTGGTGACAA
GCCTTCTGCTCTGTGAGTTACCACACCCAGCATTCCTCCTGATCCCAGACATCCAGATGACACAGACTAC
ATCCTCCCTGTCTGCCTCTCTGGGAGACAGAGTCACCATCAGTTGCAGGGCAAGTCAGGACATTAGTAA
ATATTTAAATTGGTATCAGCAGAAACCAGATGGAACTGTTAAACTCCTGATCTACCATACATCAAGATTA

CACTCAGGAGTCCCATCAAGGTTCAGTGGCAGTGGGTCTGGAACAGATTATTCTCTCACCATTAGCAAC
CTGGAGCAAGAAGATATTGCCACTTACTTTTGCCAACAGGGTAATACGCTTCCGTACACGTTCGGAGGG
GGGACTAAGTTGGAAATAACAGGCTCCACCTCTGGATCCGGCAAGCCCGGATCTGGCGAGGGATCCAC
CAAGGGCGAGGTGAAACTGCAGGAGTCAGGACCTGGCCTGGTGGCGCCCTCACAGAGCCTGTCCGTC
ACATGCACTGTCTCAGGGGTCTCATTACCCGACTATGGTGTAAGCTGGATTCGCCAGCCTCCACGAAAG
GGTCTGGAGTGGCTGGGAGTAATATGGGGTAGTGAAACCACATACTATAATTCAGCTCTCAAATCCAG
ACTGACCATCATCAAGGACAACTCCAAGAGCCAAGTTTTCTTAAAAATGAACAGTCTGCAAACTGATGA
CACAGCCATTTACTACTGTGCCAAACATTATTACTACGGTGGTAGCTATGCTATGGACTACTGGGGTCA
AGGAACCTCAGTCACCGTCTCCTCAGAGCAAAAGCTCATTTCTGAAGAGGACTTGTTCGTGCCGGTCTT
CCTGCCAGCGAAGCCCACCACGACGCCAGCGCCGCGACCACCAACACCGGCGCCCACCATCGCGTCGC
AGCCCCTGTCCCTGCGCCCAGAGGCGTGCCGGCCAGCGGCGGGGGGCGCAGTGCACACGAGGGGGCT
GGACTTCGCCTGTGATATCTACATCTGGGCGCCCTTGGCCGGGACTTGTGGGGTCCTTCTCCTGTCACT
GGTTATCACCCTTTACTGCAACCACAGGAACTGAGAATTCGAGCATCTTACCGCCATTTATTCCCATATT
TGTTCTGTTTTTCTTGATTTGGGTATACATTTAAATGCATTTAAATGTATACCCAAATCAAGAAAAACAG
AACAAATATGGGAATAAATGGCGGTAAGATGCTCGAATTCTCAGTTCCTGTGGTTGCAGTAAAGGGTG
ATAACCAGTGACAGGAGAAGGACCCCACAAGTCCCGGCCAAGGGCGCCCAGATGTAGATATCACAGG
CGAAGTCCAGCCCCCTCGTGTGCACTGCGCCCCCCGCCGCTGGCCGGCACGCCTCTGGGCGCAGGGAC
AGGGGCTGCGACGCGATGGTGGGCGCCGGTGTTGGTGGTCGCGGCGCTGGCGTCGTGGTGGGCTTCG
CTGGCAGGAAGACCGGCACGAACAAGTCCTCTTCAGAAATGAGCTTTTGCTCTGAGGAGACGGTGACT
GAGGTTCCTTGACCCCAGTAGTCCATAGCATAGCTACCACCGTAGTAATAATGTTTGGCACAGTAGTAA
ATGGCTGTGTCATCAGTTTGCAGACTGTTCATTTTTAAGAAAACTTGGCTCTTGGAGTTGTCCTTGATGA
TGGTCAGTCTGGATTTGAGAGCTGAATTATAGTATGTGGTTTCACTACCCCATATTACTCCCAGCCACTC
CAGACCCTTTCGTGGAGGCTGGCGAATCCAGCTTACACCATAGTCGGGTAATGAGACCCCTGAGACAG
TGCATGTGACGGACAGGCTCTGTGAGGGCGCCACCAGGCCAGGTCCTGACTCCTGCAGTTTCACCTCG
CCCTTGGTGGATCCCTCGCCAGATCCGGGCTTGCCGGATCCAGAGGTGGAGCCTGTTATTTCCAACTTA
GTCCCCCCTCCGAACGTGTACGGAAGCGTATTACCCTGTTGGCAAAAGTAAGTGGCAATATCTTCTTGC
TCCAGGTTGCTAATGGTGAGAGAATAATCTGTTCCAGACCCACTGCCACTGAACCTTGATGGGACTCCT
GAGTGTAATCTTGATGTATGGTAGATCAGGAGTTTAACAGTTCCATCTGGTTTCTGCTGATACCAATTTA
AATATTTACTAATGTCCTGACTTGCCCTGCAACTGATGGTGACTCTGTCTCCCAGAGAGGCAGACAGGG
AGGATGTAGTCTGTGTCATCTGGATGTCTGGGATCAGGAGGAATGCTGGGTGTGGTAACTCACAGAGC
AGAAGGCTTGTCACCAGGAGAAGCATGGTGGCGGCGCGGCCGCCTGTAAGTGAGCTTGGAGAGAGG
GACTATTACTTAACTTTGTCGAGCTAATTTTCAGACAAATACAGAAACACAGTCAGACAGAGACAACAC
AGAACGATGCTG

CAR identification by PCR

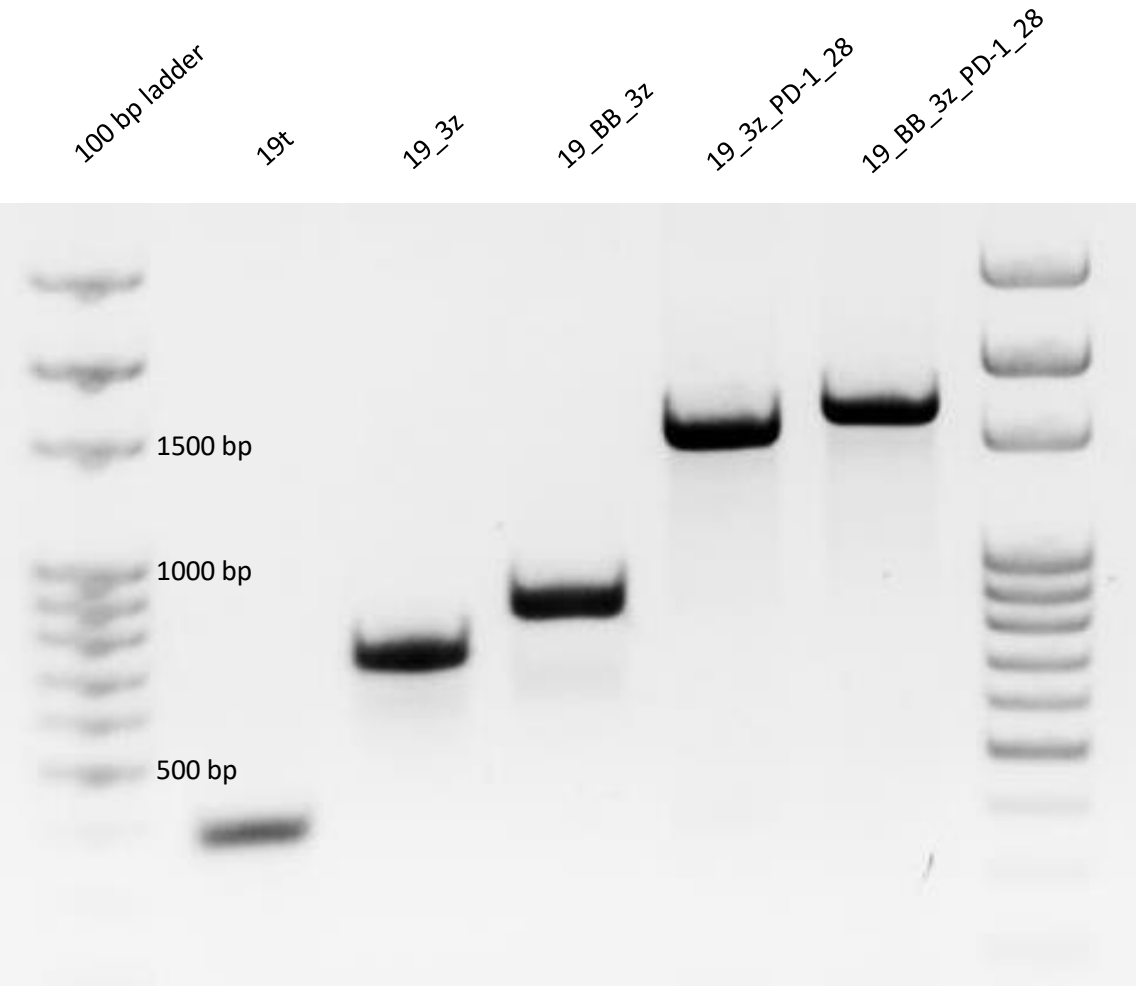

CAR construct	Insert length in bp
19t	494
19_3z	830
19_BB_3z	956
19_3z_PD-1_28	1589
19_BB_3z_PD-1_28	1715

Vector maps

Vector map of pMP71

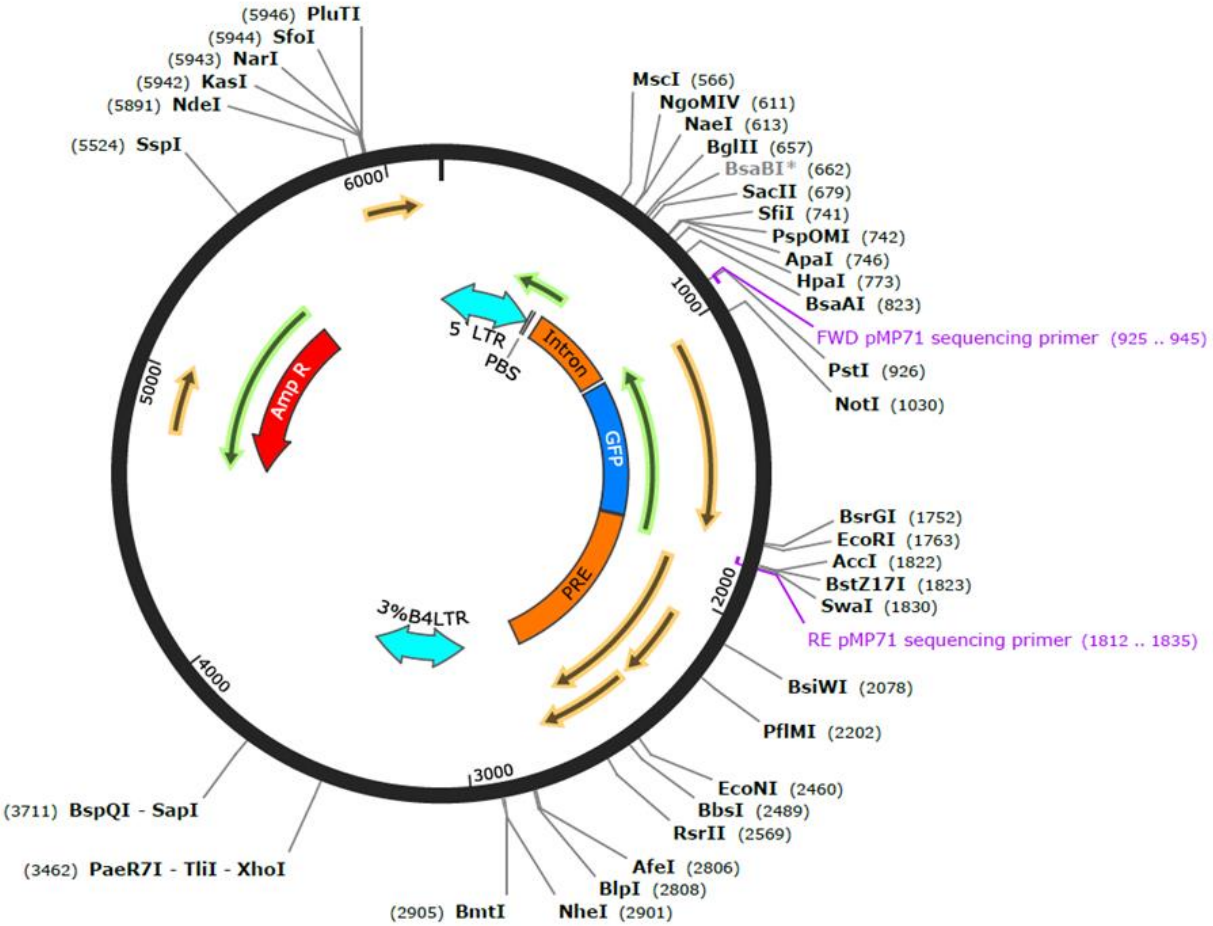

CAR constructs were inserted instead of GFP.

Vector map of gag/pol (pcDNA3.1-MLV-g/p)

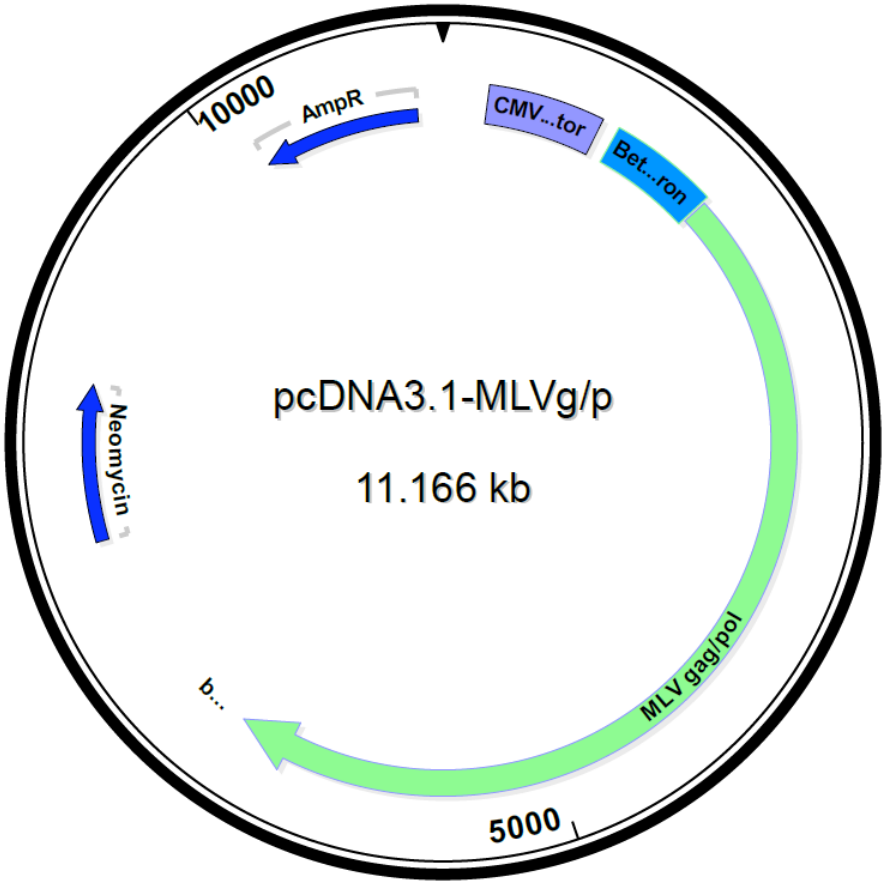

Quantile-Quantile Plots

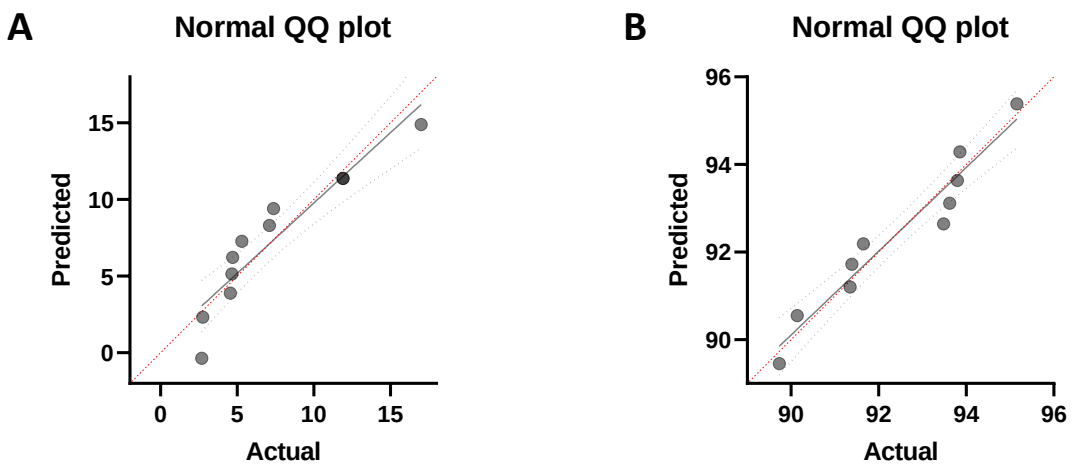

Quantile-Quantile Plots.
(A) To show that results of intracellular cytokine stain assays are distributed normally IFN-γ secretion of 19_BB_3z CAR after co-culture with Daudi cells was used as example. It was tested for normality using Shapiro-Wilk test (p=0.0655). For graphical assessment of normality Quantile-Quantile plot was used. In the QQ plot the 95% confidence bands of the best-fit line are included (n=11). **(B)** Killing efficacy of 19_BB_3z CAR after co-culture with $CD19^+$ K562 cells in a 1:1 ratio is used exemplary for testing normal distribution of cytotoxicity assays. It was tested for normality using Shapiro-Wilk test (p=0.4174). Quantile-Quantile plot is shown above for graphical assessment of normality. In the QQ plot the 95% confidence bands of the best-fit line are included (n=10). IFN-γ: interferon gamma, QQ plot: Quantile-Quantile plot.

Acknowledgements

I would like to thank Tobias Feuchtinger for the possibility to do my doctoral thesis in his laboratory and all the trust and support throughout that process.

A special thanks to Franziska Blaeschke for all the guidance, patience and great advice. I could not have asked for a better supervisor. Thank you not just for the scientific input but even more for cheering me up when experiments failed and all the laughter during and after work.

Also a great thank you to Dana Stenger, who had the task to teach me all the laboratory basics, methods and lab rules. I cannot appreciate enough that I could always come to you with my questions and had someone to turn to with my problems.

I thank Tanja Weißer, Nadine Stoll and Nicola Habjan for all the technical assistance that was needed to realize my project. Thank you for helping me out whenever needed.

Especially to those above, the other doctoral candidates and the whole Feuchtinger Lab a huge thank you for making my time in the laboratory such an instructive experience and amazing time. Despite all the hard work and huge effort from everyone there was always room for joy and fun.

I thank the Bettina-Bräu-Stiftung for the scholarship while working on my doctoral thesis. Their generous support helped me to focus on my laboratory work.

Last but not least I would like to thank all my friends and family for their constant support throughout my work in the lab but also seven years of medical studies. Thank you Anna and Felix for joining me on the journey from my first day as a (little bit overwhelmed) medical student until finally becoming a doctor seven years later. Thank you Lucia, Anna and Laura for being the best inspiration growing up. And I thank my parents for always believing in me and supporting me throughout my way.

Affidavit

LMU LUDWIG-MAXIMILIANS-UNIVERSITÄT MÜNCHEN | Promotionsbüro Medizinische Fakultät | MMRS

Eidesstattliche Versicherung

Apfelbeck Antonia

Name, Vorname

Ich erkläre hiermit an Eides statt, dass ich die vorliegende Dissertation mit dem Titel:

Generation and Characterization of CD19 CAR T Cells with PD-1_CD28 Fusion Receptor

selbständig verfasst, mich außer der angegebenen keiner weiteren Hilfsmittel bedient und alle Erkenntnisse, die aus dem Schrifttum ganz oder annähernd übernommen sind, als solche kenntlich gemacht und nach ihrer Herkunft unter Bezeichnung der Fundstelle einzeln nachgewiesen habe.

Ich erkläre des Weiteren, dass die hier vorgelegte Dissertation nicht in gleicher oder in ähnlicher Form bei einer anderen Stelle zur Erlangung eines akademischen Grades eingereicht wurde.

Wörth/Do, den 22.02.2022	Antonia Apfelbeck
Ort, Datum	Unterschrift Doktorandin bzw. Doktorand